

**Analysis and Design of Shear Wall Coupling Beams in Mid- to High-rise  
Timber Buildings**

by

Katherine J Augustine

A Thesis Submitted to the Faculty of the  
Milwaukee School of Engineering  
in Partial Fulfillment of the  
Requirements for the Degree of  
Master of Science in Architectural Engineering

Milwaukee, Wisconsin

August 2022

## Abstract

The purpose of this research project was to design a coupling beam connection to be utilized in mid- to high-rise mass timber framed buildings. Coupling beams connect two shear walls together and transfer shear forces between the two, forcing them to work together as one composite member, allowing the structure to resist higher lateral loads. The connections analyzed during this project include an I-shape connection, and two knife plate connections. The goal of the analysis was to create a steel connection that would yield and exhibit ductile behavior prior to any other connection elements, in this case CLT and bolts, yielding. After analyzing the I-shape model, the connection was able to withstand a shear force greater than that of the CLT member. The knife plate iterations had different results. Preliminary calculations were conducted, and the conclusion was that a shear force of 30 kip applied to either knife plate configuration would result in a ductile failure of the steel plate, prior to any yielding of the CLT member or bolts. Table 7 summarizes the data values from the analysis. Figure 45 and Figure 63 show that both connections were able to transition from the elastic region to the plastic on the nonlinear force versus displacement graph. The maximum deformation for the knife plate connection at yield point is (KP) 0.224 inches at a load of 36 kip. For the knife plate with reduced cross section (KPRC) connection, the maximum deformation is 0.123 inches with a 15.6 kip load applied. The maximum stresses at yield point for KP and KPRC are 47 ksi and 38 ksi, respectively. Additional future work would involve creating more connection iterations and putting together a design guide for the connections to implement these designs in mass timber construction projects.

*Keywords:* hybrid structures, shear wall coupling beams, tall mass timber buildings, cross laminated timber (CLT), shear wall

## **Acknowledgments**

I have learned a lot during this year of research and testing my capstone project. Although technological difficulties and outside life events became unexpected hurdles, the overall process of performing this capstone was a wonderful experience. Reflecting on this year makes me realize how much I can accomplish with the right support and people in my corner encouraging me.

I would like to thank the faculty members at the Milwaukee School of Engineering (MSOE) who were instrumental in helping me with this project. Not only for the education prior to beginning my research but also the guidance during my three quarters of work. A special thanks to Dr. Pouria Bahmani, Ph. D., for being my research advisor throughout this period and offering me countless hours of help this year. In addition, I would like to thank Dr. Chris Raebel, Ph D., and Dr. Todd Davis, Ph. D., for being my committee members and providing helpful feedback each quarter to make this project as successful as possible. I would also like to thank the Mechanical Engineering department at MSOE for working with me on this project to gain access to the Harley Lab, allowing for higher computing power during the simulation phase of this project.

Lastly, I would like to thank my friends and family for listening and trying to understand what I have done for this project. I know it is not always as exciting to them, but they offered constant support and encouragement throughout the entirety of my education.

## Table of Contents

List of Figures .....	7
List of Tables .....	11
Nomenclature .....	12
Chapter 1: Introduction .....	13
Chapter 2: Literature Review .....	18
2.1 Cross-Laminated Timber Shear Wall Connections for Seismic Applications .....	18
2.2 Ductile Coupled Reinforced Concrete Shear Walls and Coupled Composite Steel Plate Shear Walls as Distinct Seismic Force-Resisting Systems in ASCE 7 .....	19
2.3 Full-Scale Shake Table Test of a Two-Story Mass-Timber Building with Resilient Rocking Walls (Pei et al., 2018) .....	21
2.4 Seismically Resilient Self-Centering Cross-Laminated Rocking Walls with Coupling Beams .....	22
2.5 Coupling Beam Types, Practical Reinforced Concrete Building Design .....	23
Chapter 3: Calculations and Modeling .....	25
3.1 Finite Element Analysis of Coupling Connections in ANSYS ® .....	25
3.2 The 3D Model .....	26
3.2.1 Modeling in SpaceClaim .....	26
3.2.2 ANSYS ® Workbench Models .....	33
3.3 Materials .....	34
3.3.1 Nonlinear Structural Steel .....	36
3.3.2 Mass Timber (CLT or Glulam) .....	37

3.4	Finite Element Mesh .....	38
3.5	Boundary Conditions.....	42
3.6	Contact Elements.....	45
3.7	Loading.....	47
Chapter 4: Finite Element Analysis Results .....		49
4.1	I-Shape Connection .....	50
4.2	Knife Plate Connection .....	52
4.2.1	Von Mises Stresses – Equivalent Stress .....	52
4.2.2	Total and Directional Deformation.....	56
4.2.3	Normal Stress and Strain .....	61
4.2.4	Force Reaction.....	64
4.2.5	Analysis .....	66
4.3	Knife Plate Connection with Reduced Cross Section (KPRC) .....	69
4.3.1	Von Mises Stresses – Equivalent Stress .....	70
4.3.2	Total and Directional Deformation.....	73
4.3.3	Normal Stress and Strain .....	77
4.3.4	Force Reaction.....	80
4.3.5	Analysis .....	81
4.4	Accuracy.....	84
Chapter 5: Conclusions and Recommendations .....		86
5.1	Summary Values .....	86
5.2	Conclusion.....	86
5.3	Future Research.....	88

References .....	89
Appendix A: Reference Tables .....	90
Appendix B: Calculations and ANSYS ® Reports.....	93

## List of Figures

Figure 1: Uncoupled versus Coupled Shear Walls: (a) Uncoupled Shear Wall System; (b) Coupled Shear Wall System .....	14
Figure 2: 3-ply and 5-ply CLT Panels .....	16
Figure 3: Shear Wall System Reacting Under Lateral Load Conditions (from Ghosh, 2019) .....	21
Figure 4: SAP2000 Pushover of SC-CLT Wall with CLT Coupling Beams .....	22
Figure 5: SAP2000 Pushover of SC-CLT Wall with Ductile Steel Coupling Beams .....	23
Figure 6: Five Conventional Coupling Beam Types .....	24
Figure 7: Built Up I-Shape Component Modeled in SpaceClaim; (a) Without Horizontal Bolts (b) With Horizontal Bolts.....	27
Figure 8: Mass Timber Component Modeled in SpaceClaim .....	28
Figure 9: Knife Plate Steel Component Modeled in SpaceClaim: (a) Without Horizontal Bolts and (b) With Horizontal Bolts .....	29
Figure 10: Knife Plate CLT Component Modeled in SpaceClaim .....	30
Figure 11: KPRC Steel Component Modeled in SpaceClaim (a) Without Horizontal Bolts and (b) With Horizontal Bolts.....	31
Figure 12: Complete I-Shape Connection Modeled in ANSYS ® Workbench .....	32
Figure 13: Complete Knife Plate Connection Modeled in ANSYS ® Workbench.....	32
Figure 14: Complete KPRC Connection Modeled in ANSYS ® Workbench .....	33
Figure 15: Outline of Schematic A2: Engineering Data Tab.....	35
Figure 16: Nonlinear Stress versus Strain Curve .....	36

Figure 17: I-Shape Mesh: (a) Both CLT and Steel Components and (b) Steel Component.....	40
Figure 18: Higher Mesh Concentration Near Bolts Holes.....	40
Figure 19: I-Shape Mesh: (a) Both CLT and Steel Components and (b) Steel Component.....	41
Figure 20: I-Shape Mesh: Higher Mesh Concentration Near Bolts Holes .....	41
Figure 21: Fixed Boundary Condition on the Knife Plate Connection.....	43
Figure 22: Roller Boundary Condition on the Knife Plate Connection.....	44
Figure 23: Details of “Displacement” Boundary Conditions .....	45
Figure 24: Knife Plate to CLT Contact Assignment.....	46
Figure 25: Applied Downward Shear Force at the Center of the Coupling Beam .....	48
Figure 26: Mesh Refinement Example .....	50
Figure 27: I-Shape Half Model Isometric.....	51
Figure 28: Convergence Criteria from Knife Plate Connection Analysis .....	53
Figure 29: Knife Plate von Mises Stress Isometric View, Entire Configuration at 50 kip .....	54
Figure 30: Knife Plate von Mises Stress Isometric View, Steel Component at 50 kip ....	55
Figure 31: Knife Plate Maximum Stress at Bolt Holes.....	55
Figure 32: Knife Plate Minimum Stress at Plate Edge .....	56
Figure 33: Knife Plate Total Deformation Isometric at 50 kip.....	57
Figure 34: Knife Plate Maximum Total Deformation at CLT Face .....	58
Figure 35: Knife Plate Minimum Total Deformation at Plate Edge .....	58
Figure 36: Knife Plate Directional Deformation Isometric View at 50 kip.....	59



Figure 37: Knife Plate Maximum Directional Deformation at CLT Beam Edge .....	60
Figure 38: Knife Plate Minimum Directional Deformation at CLT Beam Edge .....	60
Figure 39: Stress Strain Curve .....	61
Figure 40: Knife Plate Normal Stress Concentration Isometric View at 50 kip.....	62
Figure 41: Knife Plate Steel Component Maximum and Minimum Normal Stress Concentration .....	63
Figure 42: Knife Plate Strain Concentration Isometric View at 50 kip .....	63
Figure 43: Knife Plate Steel Component Maximum and Minimum Strain Concentration .....	64
Figure 44: Knife Plate Force Reaction and Applied Mesh .....	64
Figure 45: Force versus Displacement Plot for Knife Plate Connection .....	68
Figure 46: Stress Strain Curve Knife Plate Connection.....	69
Figure 47: Convergence Criteria from KPRC Connection Analysis .....	70
Figure 48: KPRC von Mises Stress Isometric View, Entire Configuration at 30 kip .....	71
Figure 49: KPRC von Mises Stress Isometric View, Steel Component at 30 kip .....	72
Figure 50: KPRC Maximum Stress at Lowest Cross Section.....	72
Figure 51: KPRC Minimum Stress at Largest Cross Section .....	73
Figure 52: KPRC Total Deformation Isometric at 30 kip.....	73
Figure 53: KPRC Maximum Total Deformation at CLT Face .....	74
Figure 54: KPRC Minimum Total Deformation at Plate Edge.....	75
Figure 55: KPRC Directional Deformation Isometric View at 30 kip .....	76
Figure 56: KPRC Maximum Directional Deformation at CLT Beam Edge .....	76
Figure 57: KPRC Minimum Directional Deformation at CLT Beam Edge .....	77

Figure 58: KPRC Normal Stress Concentration Isometric View at 30 kip .....	78
Figure 59: KPRC Steel Component Maximum and Minimum Normal Stress Concentration .....	78
Figure 60: KPRC Strain Concentration Isometric View at 30 kip.....	79
Figure 61: KPRC Steel Component Maximum and Minimum Strain Concentration .....	79
Figure 62: Force Reaction and Applied Mesh for KPRC Connection.....	80
Figure 63: Force versus Displacement Plot for KPRC Connection.....	83
Figure 64: Stress Strain Curve KPRC Connection .....	83
Figure 65: Force Convergence Plot for I-Shape .....	85
Figure 66: Force Convergence Plot for Knife Plate.....	85

## List of Tables

Table 1: Nonlinear Structural Steel Values for Bolts .....	37
Table 2: Engineered Lumber Reference Values for CLT .....	38
Table 3: Force Reaction Results from ANSYS ® Run for the Knife Plate Connection Configuration .....	66
Table 4: Results from ANSYS ® Run for the Knife Plate Connection Configuration up to 10 Seconds .....	67
Table 5: Force Reaction Results from ANSYS ® Run for the KPRC Connection Configuration .....	81
Table 6: Results from ANSYS ® Run for the KPRC Connection Configuration up to 10 Seconds .....	82
Table 7: Summary Values from ANSYS ® Runs for Both Knife Plate Connection Configurations.....	86

## Nomenclature

### *Symbols*

C = compressive force

d = distance between the tensile and compressive forces

lbf = pounds force

M<sub>-1</sub> = bending force in shear wall 1

M<sub>-2</sub> = bending force in shear wall 2

T = tensile force

### *Abbreviations*

ACI            American Concrete Institute

AISC          American Institute of Steel Construction

CLT           Cross-Laminated Timber

FEA           Finite Element Analysis

KPRC        Knife plate with reduced cross section

LFRS         Lateral Force Resisting System

NDS           National Design Specification for Wood Construction

NHERI        Natural Hazards Engineering Research Infrastructure

RC            Reinforced concrete

SC-CLT       Self centering cross laminated timber

## Chapter 1: Introduction

Shear walls are members that resist lateral loads, transferring those loads through shear and bending to the foundation. In mid- to high-rise construction, wind and seismic loads govern the design of shear walls. Shear walls can be grouped in two major systems: uncoupled shear walls and coupled shear walls. Several isolated shear walls can be coupled over the height of the building by means of coupling beams to achieve a higher level of resistance against lateral loads. The coupling beams, therefore, should be designed to transfer the shear between the two shear walls, forcing them to work as one composite member. Without coupling beams to connect the two shear walls together, the isolated walls behave independently of each other, which leads to significant reduction in the overall stiffness and strength of the lateral load resisting system.

Figure 1 represents the behavior of uncoupled and coupled shear wall systems. The two separate walls must overcome bending moments and shear forces, identified in Figure 1(a) with the uncoupled shear walls,  $M_1$ , and  $M_2$ . As shown, Wall 1 resists lateral loads independently from the reaction at Wall 2, and vice versa. When the walls are coupled by means of coupling beams, the two walls begin to work together in resisting the lateral forces which changes the load path and how the loads are transferred to the foundation. As seen in Figure 1(b) with the coupled shear walls, in addition to the bending moments, accompanying overall tensile and compressive forces are introduced into the system. The shear forces in coupling beams along the height of the building create tensile force ( $T$ ) and compressive force ( $C$ ) at the base of the shear walls. These forces create a couple with a moment arm equal to the distance between the tensile and compressive forces (i.e.,  $d$ ) induced in the shear walls (i.e.,  $M = (T \text{ or } C) \times d$ ). This

means that higher lateral stiffness and strength can be achieved, and more lateral loads can be resisted by a coupled shear wall system compared to an uncoupled shear wall system; hence the design is more efficient.

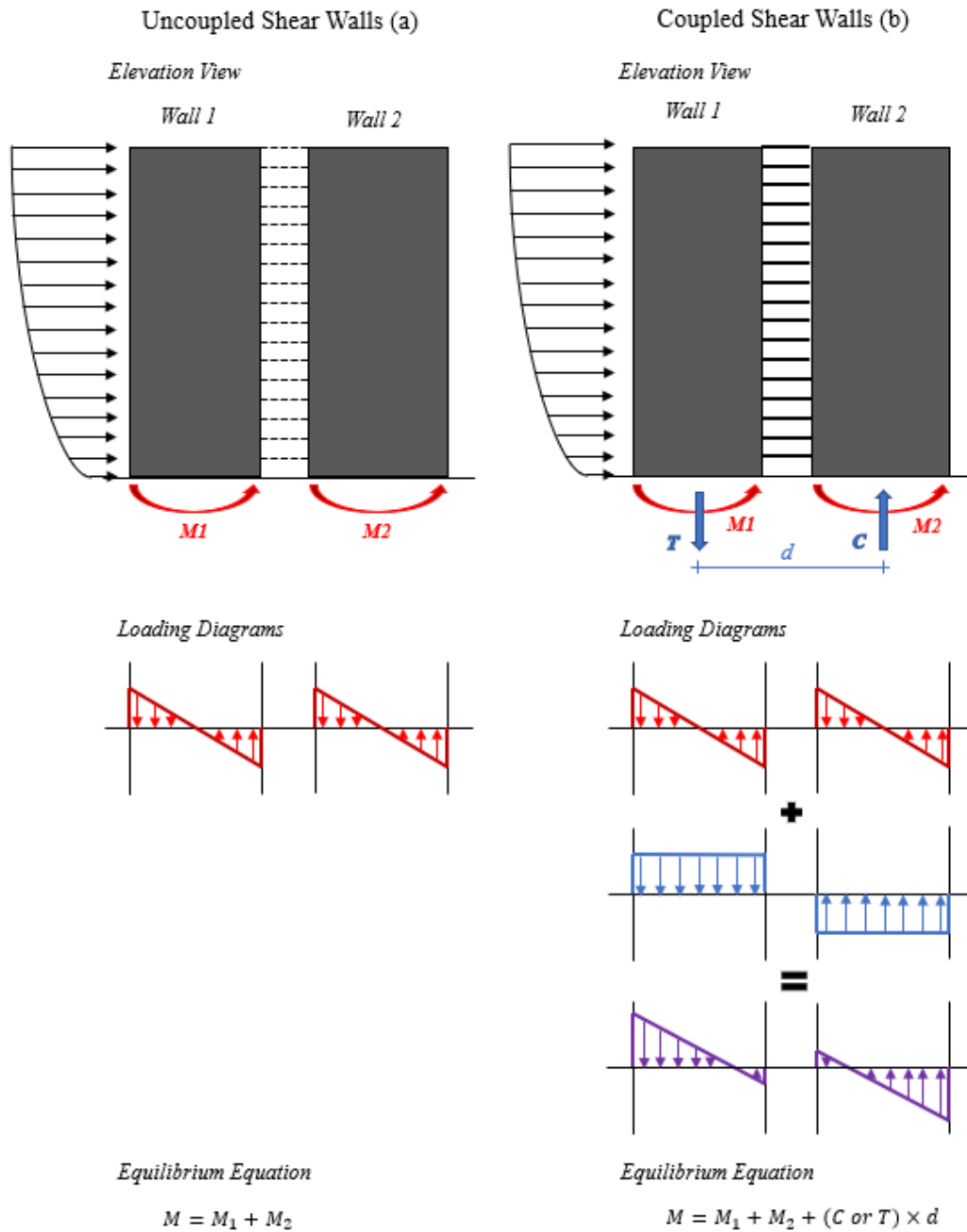


**Figure 1: Uncoupled versus Coupled Shear Walls: (a) Uncoupled Shear Wall System; (b) Coupled Shear Wall System.**

It is quite common, and more widely accepted, to use steel and reinforced concrete coupling beams. There are ample research and design guides available on how to design steel and reinforced concrete coupling beams: AISC 341, ACI 318, Tassios, Moretti, and Bezas (1996), Park & Yun (2005), etc. Because of this, they are seen more often in mid- to high-rise construction. When designing coupling beams, it is important to ensure an efficient design by increasing the ductility of members which leads to higher energy dissipation of the overall lateral load resisting system. Typically, these beams are designed to yield after design-level loading events to dissipate more energy, and hence post event member repair is common. Therefore, constructability during the initial construction phase and ease of access post construction for inspection and repair are both aspects in design that need to remain in focus.

Current design practices in high rise construction are starting to see a rise in mass timber buildings. The purpose of this study is to introduce the design of coupling beams built out of mass timber members, e.g., cross laminated timber (CLT). CLT is one of the many types of solid engineered lumber prefabricated into wood panels. It is a lightweight material that has a high strength to weight ratio and superior acoustic, fire, seismic, and thermal performance in comparison to other material types typical for building construction. CLT members are created by bonding several kiln-dried layers of lumber boards alternating in direction with structural adhesives and pressed to form the rectangular panels. Typically, CLT panels are 3-ply or 5ply, as shown in Figure 2.

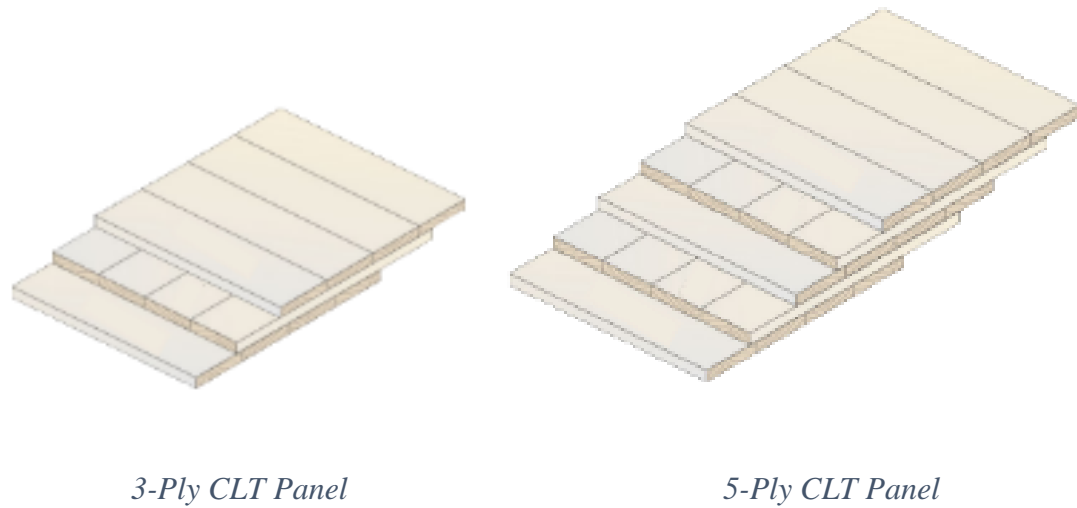


**Figure 2: 3-ply and 5-ply CLT Panels.**

After extensive review of literature, not much research or guidance in design of coupling beams for mass timber construction is available. The goal of this project was to address that research gap by modeling and analyzing various design configurations of coupling beams in tall mass timber buildings. The connection between the coupling member and shear wall requires a design that optimizes energy dissipation in extreme loading conditions and maintains efficient levels of ductility for minimal amounts of structural damage after high loading events, such as earthquakes.

The remaining portions of this paper go into several additional chapters. The next chapter summarizes the literature review conducted prior to any design work. It reviews five diverse sources deemed to be relevant to the need for this research and testing to be done. Chapter 3 moves on to address the calculations and modeling phase of this project. The AISC manual, NDS, and various papers were used to determine the capacities of the connections modeled and tested in an analysis software called ANSYS ®. The entire modeling phase in ANSYS ® is outlined in Chapter 3 as it walks through the geometry of



each configuration modeled as well as how it was constrained and loaded. Chapter 4 then discusses the test results and analyzes what those results mean. Lastly, Chapter 5 discusses the conclusions and recommendations decided upon after analyzing the results and research described in the prior chapters. This also includes future research opportunities for students relating to this project.

## **Chapter 2: Literature Review**

To better understand the design procedures and standards associated with shear wall coupling beams and their connections, extensive research was conducted via the Milwaukee School of Engineering (MSOE) databases and Google Scholar. At the time of writing this report, there is ample documentation and design suggestions for shear wall coupling beams for steel and concrete coupling beams; however, there is very minimal research conducted at the time this paper was written to understand the behavior of shear wall systems in mass timber construction and no research was found to address the design of shear wall coupling beams in this type of construction. The latest trend of mass-timber high rises prompts inquiry into coupling beams made of mass timber such as CLT. The current research suggests that mass timber shear walls with coupling beams is not as practical as other building materials because of their rigid behavior and low ductility. This brings in the opportunity for connection design to create a more ductile wall with higher energy dissipation using mass timber elements.

### **2.1 Cross-Laminated Timber Shear Wall Connections for Seismic Applications**

Falk (2020) investigated seismic design parameters for CLT walls because they have not been established in code as much as other building materials. CLT walls are very stiff and stronger than traditional wood construction. This allows CLT to compete with other materials such as steel and concrete in construction of mid- to high-rise buildings. While their near rigid behavior under in-plane loading may seem like a positive characteristic, it proves to be less than desirable in seismic applications because ductility and energy dissipation are difficult to achieve by the panels alone. This means

that the connections in design are even more vital to the functionality of CLT shear walls in high lateral load conditions. Case studies of full-scale buildings were tested under seismic activity, and they indicated the CLT connections and shear walls can withstand seismic loading. The two experimental studies on CLT shear wall buildings investigated in this report are the SOFIE and NHERI projects. The SOFIE project included testing of a seven-story tall CLT building with shear walls using a full-scale shake table test. The goal of the project was to gain a better understanding of how the CLT buildings react to seismic behavior. The conclusions on the SOFIE project showed a structural response of high accelerations, which called for more ductility and energy dissipation to be introduced into the system. Overall, the CLT building was determined feasible to build in a high seismic region. The Natural Hazards Engineering Research Infrastructure (NHERI) project consisted of a two-story mass timber shake table test. It was conducted to determine the lateral force resisting system (LFRS) capabilities of different CLT shear wall configurations. The conclusions of this project showed the various configurations tested were able to perform in mid- to low-rise structures. More testing is required to understand the configuration's ability to perform within higher buildings.

## **2.2 Ductile Coupled Reinforced Concrete Shear Walls and Coupled Composite Steel Plate Shear Walls as Distinct Seismic Force-Resisting Systems in ASCE 7**

Ghosh (2019) introduced the efficiency with coupled shear walls when reducing lateral loads subjected on a building. They differ from uncoupled walls because the uncoupled walls behave independently from each other, not as a system, where loads and stresses are not transferred between walls. When two shear walls are coupled, a beam of

some materials is connected between them, referred to as a coupling beam, through one of many types of connections. Shear walls and coupling beams constructed out of steel and reinforced concrete are more practical than other building materials. Because mass timber is not typically very ductile, it has not been a strong choice for a coupling beam material. Having a LFRS that is ductile and efficiently dissipates energy is recognized by ASCE 7 as a practical design choice. After being subject to lateral loads, from wind or seismic activity, shear walls will transfer forces at the end of the coupling beams as tensile forces in one wall pier and as compressive in the other, as shown in Figure 3. This coupling action due to the tensile and compressive forces help resist overturning moment induced at the base of the wall due to lateral loads. The key design feature of this system is that energy dissipation occurs within the coupling beam to reduce the forces being transferred by the walls themselves.

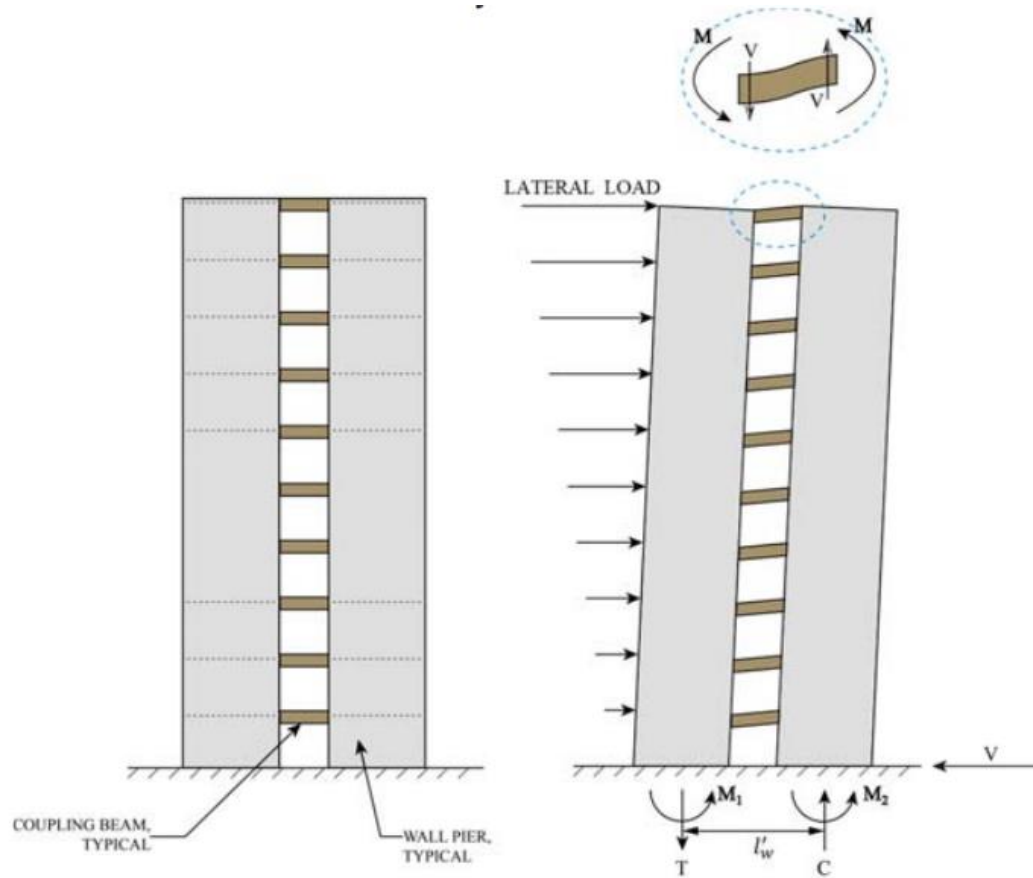


Figure 3: Shear Wall System Reacting Under Lateral Load Conditions (Ghosh, 2019).

### 2.3 Full-Scale Shake Table Test of a Two-Story Mass-Timber Building with Resilient Rocking Walls (Pei et al., 2018)

The NHERI TallWood project was designed to test a full-scale two-story mass timber building at the largest shake table in the United States. The building was comprised of two coupled two-story tall post-tensioned CLT rocking walls surrounded by mass timber gravity frames. During testing, over 350 sensors were installed to monitor the movement, strains, and load the building was experiencing. The conclusion of the test was positive. The lateral responses showed there was less damage during acceleration amplification, despite having a longer natural periods and showing a 5% total drift over the building height. The rocking wall remained elastic during the tests with minor

damage to the wall panels. Overall, the damage inspection did not produce many, or significant, results. A key conclusion was one viable way to design the connection detail between diaphragm and rocking wall is to use a slotted shear key detail to allow the rocking movement of the wall.

## 2.4 Seismically Resilient Self-Centering Cross-Laminated Rocking Walls with Coupling Beams

Dowden and Tatar (2019) conducted research relating to self-centering cross laminated timber (SC-CLT) in comparison to steel coupling beams at large wall openings. Through testing, as seen in Figure 4, the SC-CLT members had high concentrations of stress located near wall openings that could lead to beam fracture at the connection points.

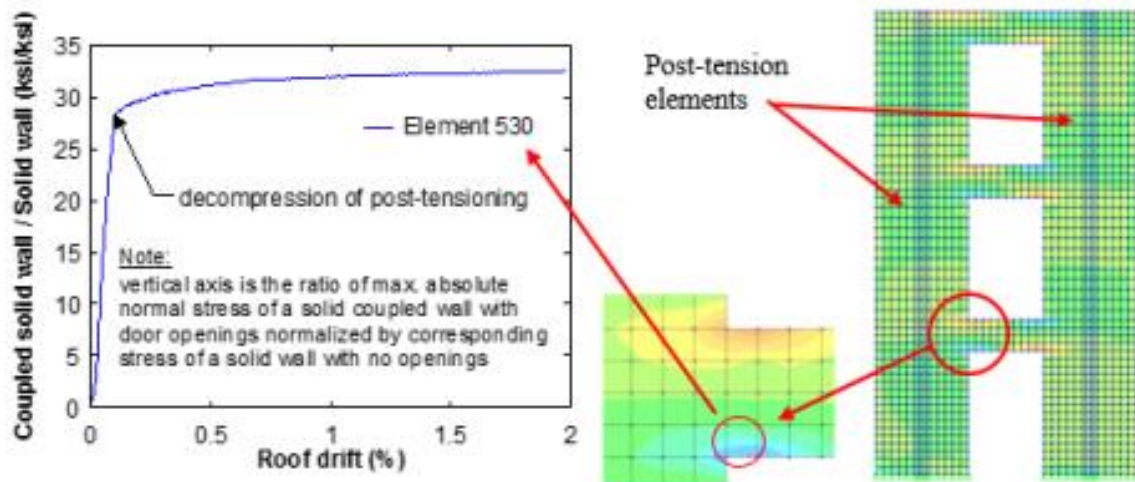
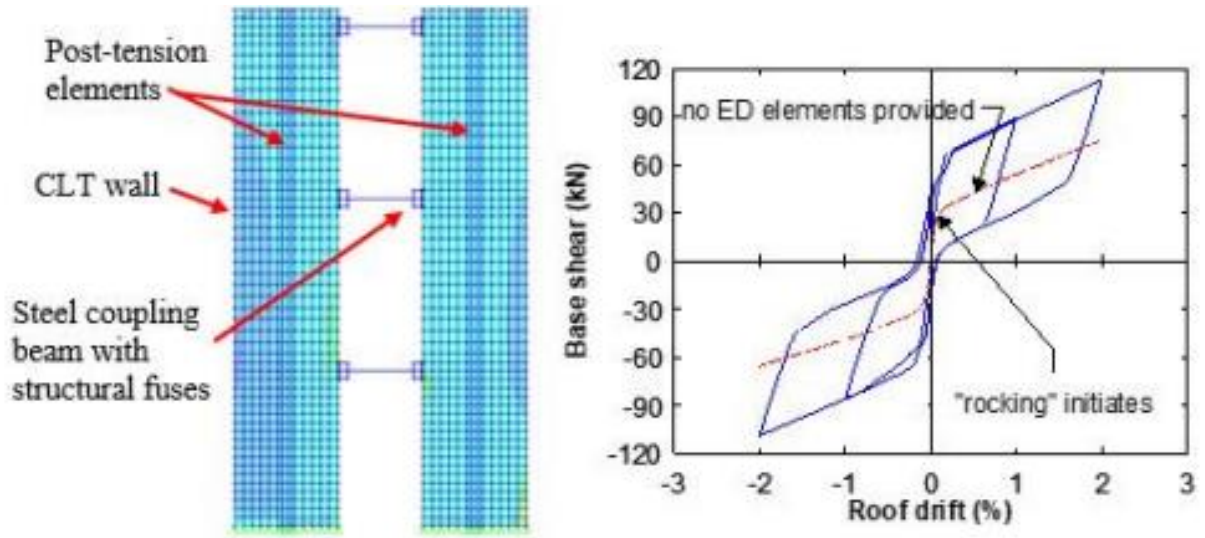


Figure 4: SAP2000 Pushover of SC-CLT Wall with CLT Coupling Beams (Dowden and Tatar, 2019).

Monolithic CLT beams and jointed CLT beams with metal connections are proving difficult to repair after large earthquakes. Testing results such as these indicate that it might be more economical and practical to use steel coupling beams instead.

Figure 5 shows that the steel coupling beams present a much lower stress concentration.



**Figure 5: SAP2000 Pushover of SC-CLT Wall with Ductile Steel Coupling Beams (Dowden and Tatar, 2019).**

There is a lot of potential to address the short comings of SC-CLT member and a significant desire to include seismic resilient and eco-friendly construction practices in the design of building structures. Utilizing mass timber framing members would be one of the options to design more sustainable structures.

## **2.5 Coupling Beam Types, Practical Reinforced Concrete Building Design**

Liao and Pimentel (2019) stated that not one single type of coupling beam is universally applicable. The five types covered in this paper show that each can be used in different building types, applications, etc. The five types discussed were conventional reinforced concrete (RC) coupling beams, diagonally reinforced concrete coupling beams, steel coupling beams, encased steel composite coupling beams, and embedded steel plate composite coupling beams (Figure 6). RC shear walls are the typical lateral force resisting system for RC buildings and adjacent shear wall piers are typically connected with coupling beams above openings (i.e., doors and corridors) at floor levels.

The coupling beams reduce flexural moments in shear wall piers, provide energy dissipation, and improve shear wall efficiency.

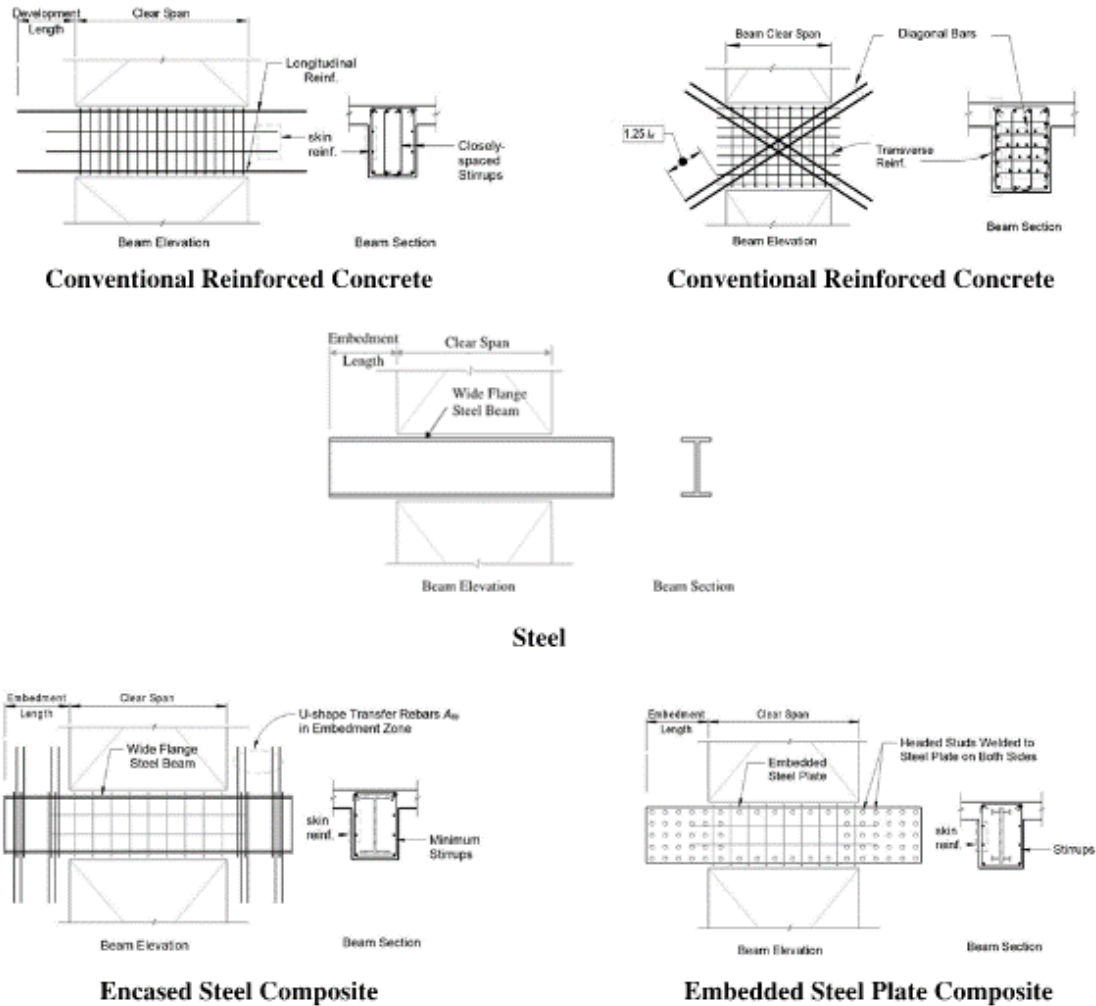


Figure 6: Five Conventional Coupling Beam Types (Liao and Pimentel, 2019).



## Chapter 3: Calculations and Modeling

### 3.1 Finite Element Analysis of Coupling Connections in ANSYS ®

Finite Element Analysis (FEA) was used to analyze the connections of coupling beams. FEA helps users to not only understand the effects of real conditions that could be present on a certain part or assembly but also quantify those results by using mathematical models. The purpose of FEA in this case was to investigate the behavior and solve the structural performance issues of the connections (e.g., steel built up I-shape embedded in the CLT beam).

ANSYS ® is a software that can conduct a nonlinear finite element analysis. It uses finite element modeling to investigate the behavior of the members and connections in different loading conditions. ANSYS ® supplies an ample number of resources for a user to quickly learn how to create a model in SpaceClaim, import it into Workbench, create an appropriate mesh, and set up proper boundary and loading conditions. There are many analysis tools in the software for postprocessing the analysis data. One of the tools that an ANSYS ® user needs to understand is to generate a mesh. To solve a FEA problem in ANSYS ®, a mesh is applied to divide the modeled structure into several miniscule elements and nodes (potentially millions of them). Nodes are the points where multiple mesh elements intersect. Similar to how integrals are taking infinitesimally small areas and adding them all together, the mesh simulation takes the individual results of each element and node then combines and integrates them over a specific domain to determine a result (e.g., reactions at supports or deformation at nodes). Each node or element within the mesh can be selected, analyzed, and used to apply multiple kinds of boundary conditions.

## 3.2 The 3D Model

A 2D model was first created for this project and used in calculating the strength of the connection. After understanding the various capacities of the connection, a 3D model was created in Revit ® for viewing purposes. The connection design was then modeled in ANSYS ® to run a nonlinear pushover analysis which will be discussed in §Section 3.6. There were several steps involved with modeling the connection in ANSYS ®: creating the geometric shapes in SpaceClaim, creating a static structural analysis system in Workbench using the geometry created in SpaceClaim, meshing the domain, and applying the proper boundary and loading conditions.

### 3.2.1 *Modeling in SpaceClaim*

**3.2.1.1 Connection with I-shape Steel Member.** To start the ANSYS ® modeling process, each component was drafted in SpaceClaim. This software allows users to sketch a variety of shapes using different line types on the x, y, or z-axis, extrude pieces to give them their depth, and move them around to manipulate their faces or edges. As a preliminary design, the built up I-shape, as seen in Figure 7, was created by drawing the outline of the cross section of an I-shape member to give it the overall flange width of 12 inches, height of 18 inches, and web thickness of ½-inch. Then it was extruded using the pull feature to give it a depth of 12 inches. The bolt holes were cut into the I-shape by sketching ¾ inch circles on the faces of the I-shape in the locations the bolts were to be placed and pulling those wholes through the thickness of the modeled plate.

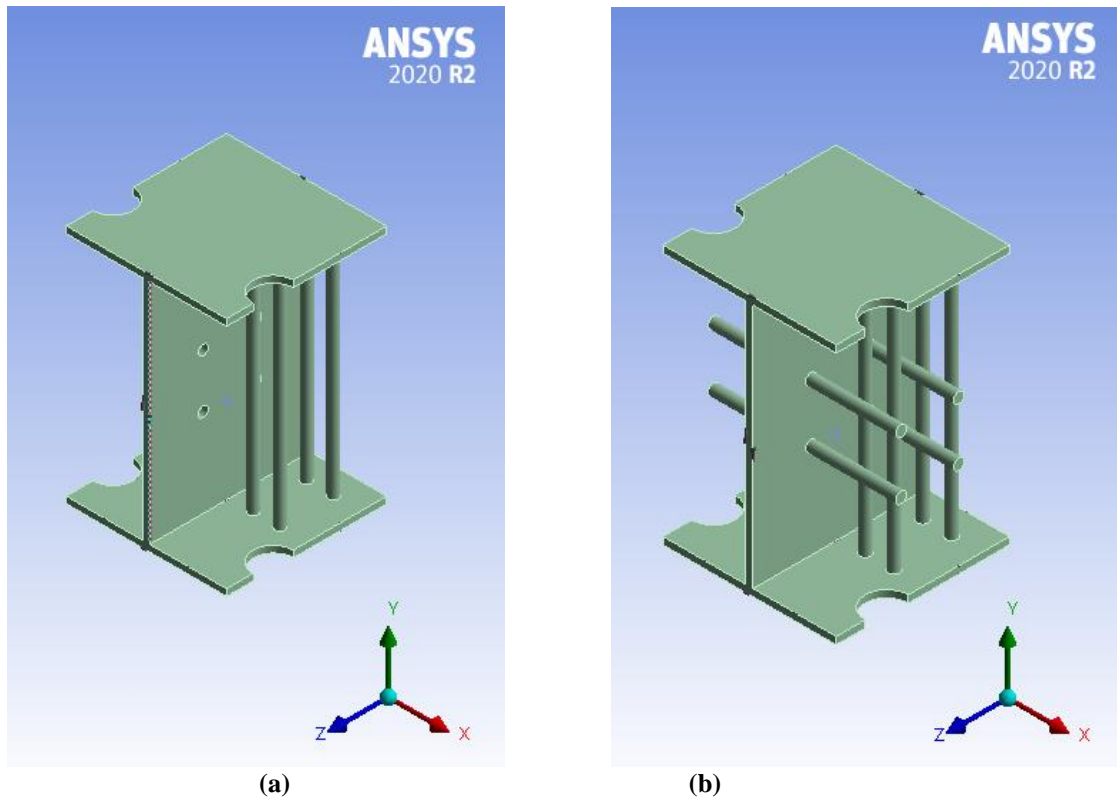


**Figure 7: Built Up I-Shape Component Modeled in SpaceClaim; (a) Without Horizontal Bolts (b) With Horizontal Bolts.**

The mass timber component, either CLT or glulam, as shown in Figure 8, was modeled by drawing a rectangle. The height and width of the member is 18 inches and 12 inches, respectively. This is like the I-shape dimensions, as the mass timber member fits within the boundaries of the I-shape. A rectangular section  $\frac{1}{2}$  inch wide by 18 inches tall of the member was cut out at the midpoint of the XY-face. Because the I-shape is imbedded 12 inches into the mass timber member, this rectangular section was extruded 12 inches into the member in the z-direction to give space to allow the I-shape to fit within it. Holes were cut into the mass timber member in the same locations as with the built up I-shape to accommodate the bolts.

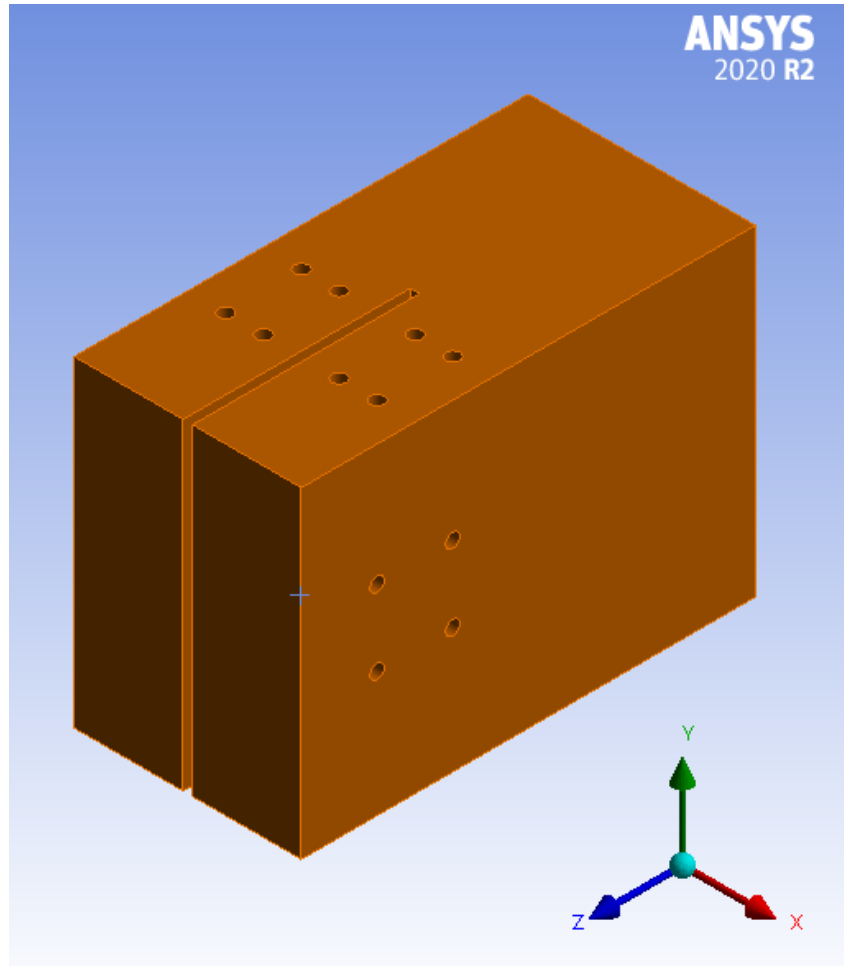


**Figure 8: Mass Timber Component Modeled in SpaceClaim.**

The bolts were initially modeled to look exactly like a typical A325 standard  $\frac{3}{4}$ -inch steel bolt. However, since the bolt heads are more complex to model and result in a longer run time in the analysis portion without increasing the accuracy of the analysis, simpler cylindrical shapes with the bolt material property were used instead. As shown in Figure 9(b), the bolts that filled the spaces cut into the built up I-shape and mass timber members were  $\frac{3}{4}$ -inch cylinders, extruded to fit within the holes.

**3.2.1.2 Connection with Knife Steel Plate.** The knife plate was an additional configuration modeled during the analysis portion of this project. It was constructed in SpaceClaim by removing the top and bottom plates of the I-shape model. This also

removed the vertical bolts as well. So, the remaining portion of the steel connection piece was a plate 17 inches tall, 12 inches long, and  $\frac{1}{4}$  inch thick. To connect it to the CLT member, 4 bolt holes are punched through the plate in the same locations as discussed in the preceding connection configuration. The steel portion of the knife plate model is shown in Figure 9.

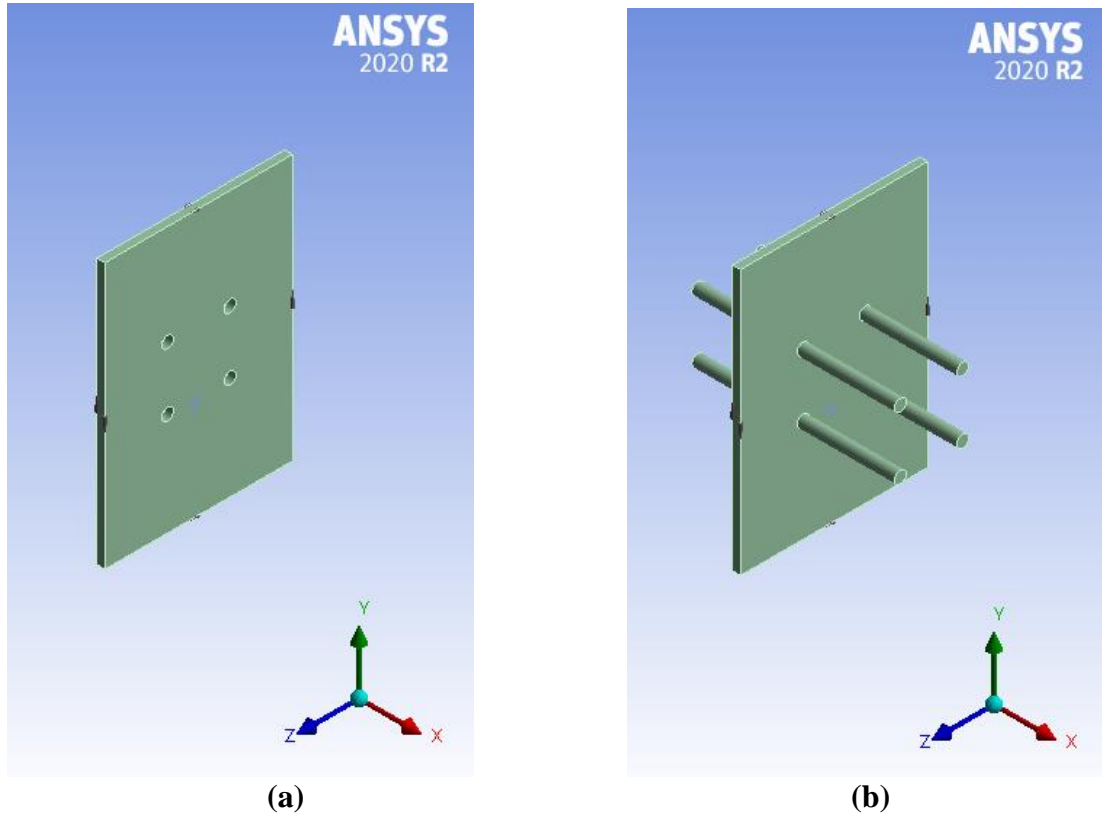


**Figure 9: Knife Plate Steel Component Modeled in SpaceClaim: (a) Without Horizontal Bolts and (b) With Horizontal Bolts.**

The CLT component of the knife plate connection was modeled in a similar fashion as the I-shape mentioned above. The vertical bolt holes were removed from the connection and therefore removed from the CLT member. Aside from that, the CLT member remains the same and is shown below in Figure 10.

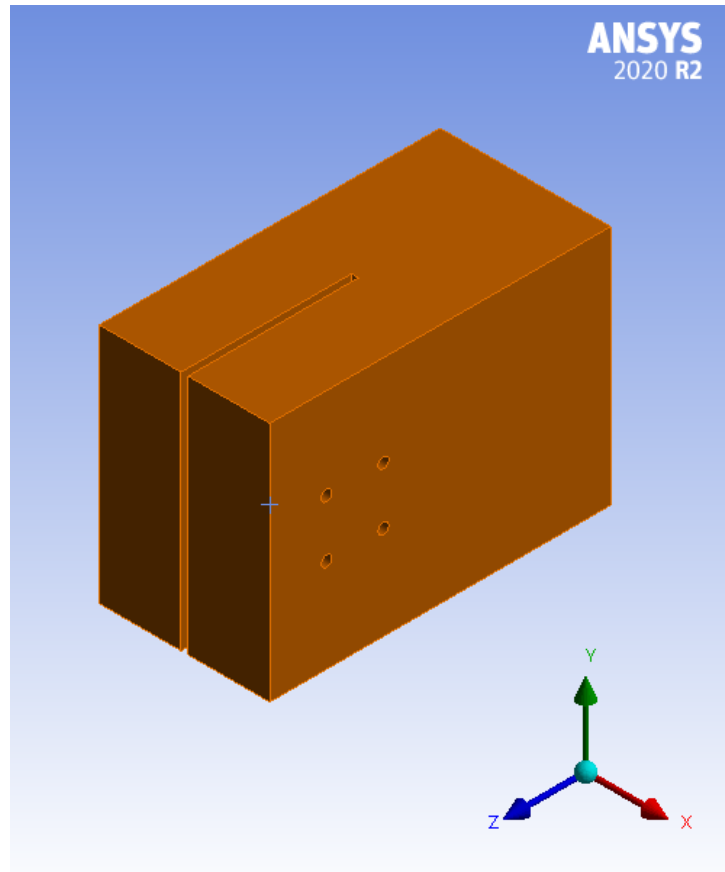


**Figure 10: Knife Plate CLT Component Modeled in SpaceClaim.**

**3.2.1.3 Connection with Knife Steel Plate with Reduced Cross Section.** The knife plate was further adjusted to reduce the cross section at the face of the plate closest to the shear wall. This resulted in a plate that on one end was 8 inches tall and a  $\frac{1}{2}$ -inch wide. As the length of the plate increases, the height of it increases to be 17 inches tall. Figure 11 shows the steel plate with the reduced cross section. The CLT member was not altered from the original knife plate connection, except that it had a  $\frac{1}{2}$  inch slot through it instead of a  $\frac{1}{4}$ -inch slot.

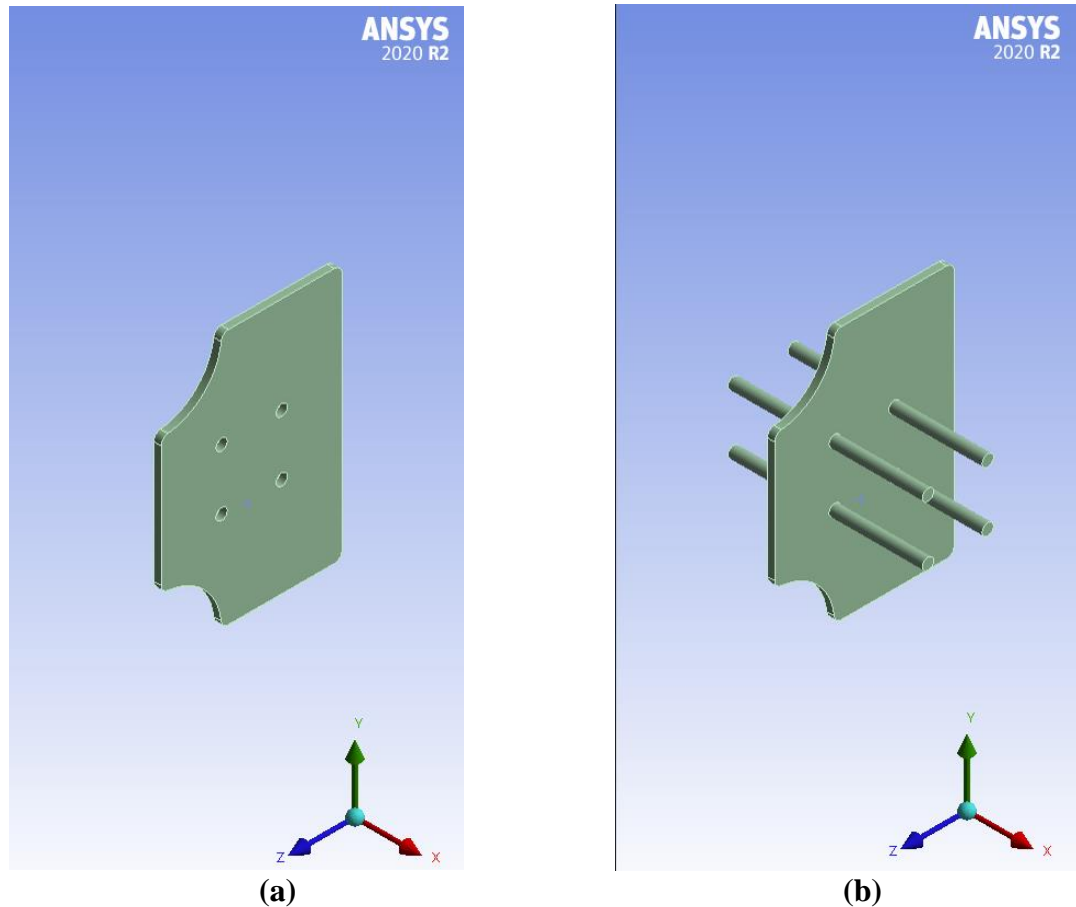


**Figure 11: KPRC Steel Component Modeled in SpaceClaim (a) Without Horizontal Bolts and (b) With Horizontal Bolts.**

After modeling each individual component, the assembly tool was used to bring all of them together. If drawn using the same local coordinate systems, the components should be imported to fit exactly where they should be. If not, the align tool can be used to make sure the correct faces are flush against the different components. Multiple imports were needed for the 2 different bolt types since there are 8 vertical and 4 horizontal bolts. The following three figures (Figure 12, Figure 13, and Figure 14) show the results of modeling the entirety of the components together in ANSYS ® Mechanical system.

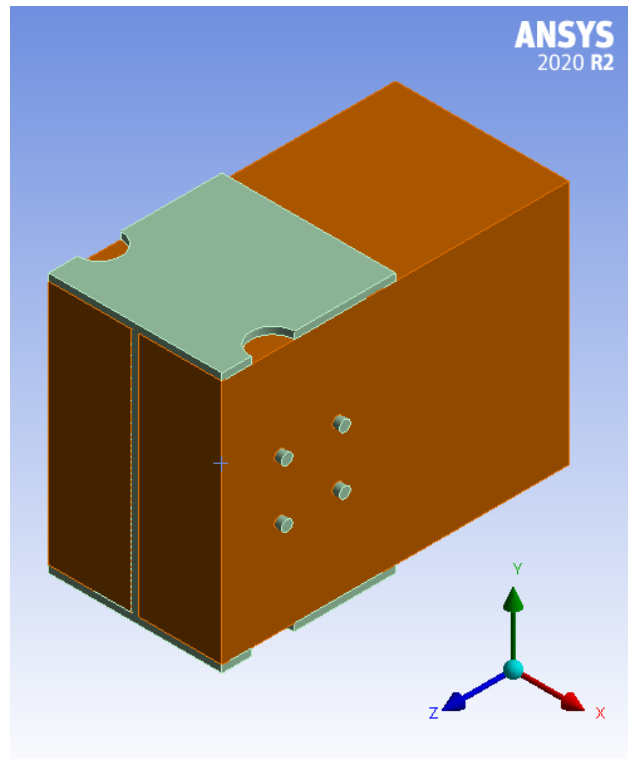


**Figure 12: Complete I-Shape Connection Modeled in ANSYS ® Workbench.**

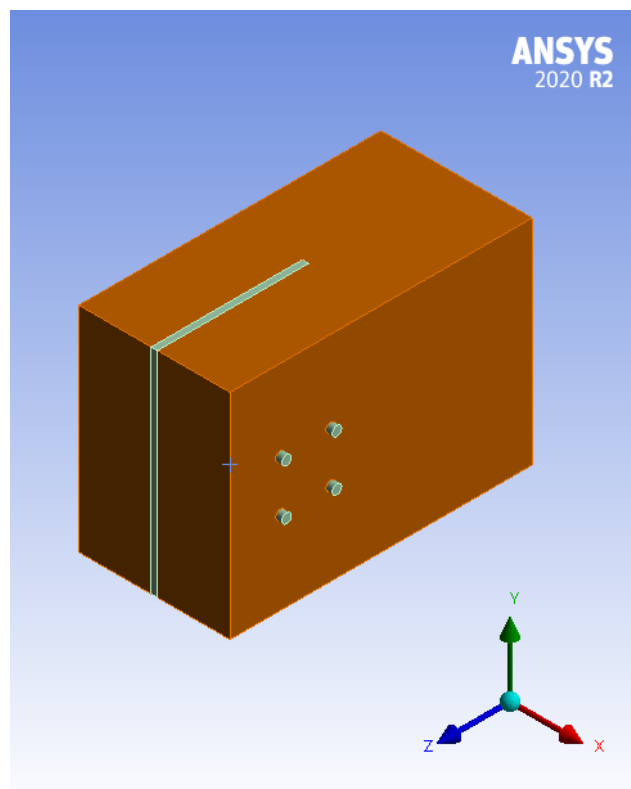


**Figure 13: Complete Knife Plate Connection Modeled in ANSYS ® Workbench.**



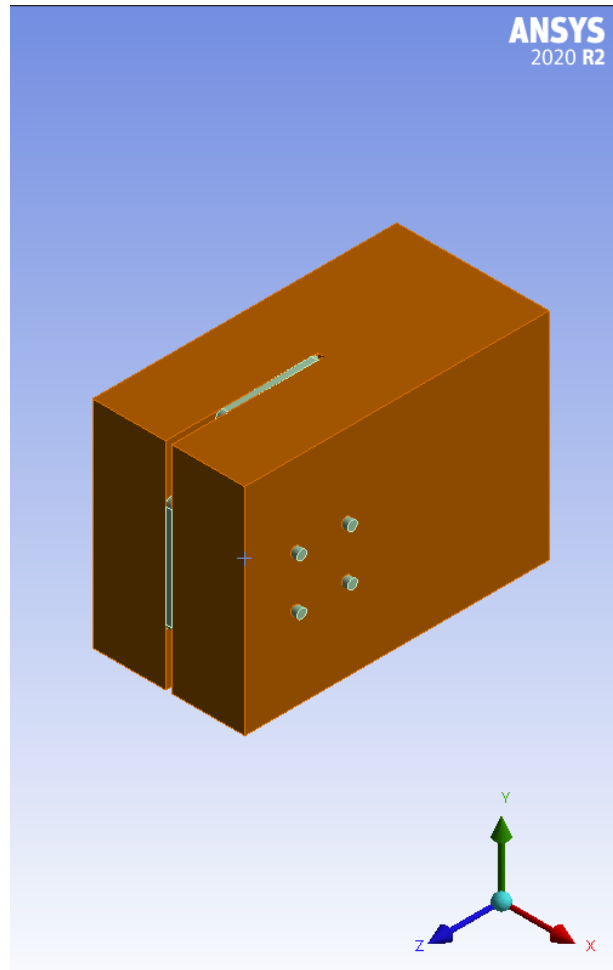


**Figure 14: Complete KPRC Connection Modeled in ANSYS ® Workbench.**

### **3.2.2 ANSYS ® Workbench Models**

When opening Workbench, in ANSYS ®, the first step is to select the type of analysis system being used for the project. For this connection analysis, the “static structural” module for the analysis system was used. Each part needed to have its own material assignment. ANSYS ® has preloaded materials that can be assigned to the geometry, or there is another option to create a new material. The nonlinear structural steel used to model the built up I-shape, steel knife plate, and bolts is already loaded in ANSYS ®, but the mass timber material type was not available. Bilinear stress-strain relationship is then assigned to the nonlinear structural steel. For the mechanical

properties of CLT and glulam, extensive research in literature was conducted and proper material properties were assigned to these elements. The material properties are discussed in more detail in §Section 3.3 of this thesis. After this, the geometry was imported from SpaceClaim, and the model was ready to be analyzed in ANSYS ® Mechanical system.

Once the model has successfully been imported into Workbench, the mechanical system can be opened. This is where the mesh is generated, loading and boundary conditions are applied to the geometry, and the results from the analysis are displayed on the 3D figure. As discussed previously, applying the mesh is a unique process to FEA that allows for each of the thousands of elements and nodes to have their own properties be analyzed by ANSYS ® and added together to give overall stresses, deformations, etc. for the model. Loading and boundary conditions were also applied to the model to simulate real world conditions, which are discussed in more detail in §Section 3.4 and §Section 3.6.

### **3.3 Materials**

The connection modeled for this research project was designed using two materials: nonlinear structural steel and engineered lumber. The two types of engineered lumber created in ANSYS ® is CLT and Glulam. The final connection model utilized the data provided by the CLT material type. ANSY has several different preset materials available to use during modeling, but any mass timber material is not included in that. So, those two lumber types were researched, and the data gathered was put into the custom material and assigned to the engineered lumber component of the connections modeled. The “Engineering Data” tab on the main ANSYS ® Workbench page contains information on the materials loaded into the project. After double-clicking on that tab,

several small screens will populate. The screen labeled: Outline of Schematic A2:

Engineering Data, shown in Figure 15, is the one containing all the loaded material types available to apply to the model.

	A	B	C	D	E
	Contents of Engineering Data				Source
	Material				Description
3	CLT			GRU	Fir (abies lasiocarpa), longitudinal direction (L) Data compiled by the Granta Design team at ANSYS, incorporating various sources including JAHM and MagWeb. ANSYS Inc. provides no warranty for this data.
4	Glulam			GRU	Fir (abies lasiocarpa), longitudinal direction (L) Data compiled by the Granta Design team at ANSYS, incorporating various sources including JAHM and MagWeb. ANSYS Inc. provides no warranty for this data.
5	Structural Steel			Gen	Fatigue Data at zero mean stress comes from 1998 ASME BPV Code, Section 8, Div 2, Table 5-110.1
6	Structural Steel NL - Bolts			Gen	Fatigue Data at zero mean stress comes from 1998 ASME BPV Code, Section 8, Div 2, Table 5-110.1
7	Structural Steel NL - I-Shape			Gen	Fatigue Data at zero mean stress comes from 1998 ASME BPV Code, Section 8, Div 2, Table 5-110.1
*	Click here to add a new material				

**Figure 15: Outline of Schematic A2: Engineering Data Tab.**

There is an option to add a new material at the bottom of the material list. This is an option to start a completely new material with no baseline/default values to start.

Adapting an existing material is also available as an option by right-clicking on a similar material and copying it then adjusting the given values to fit the material you are trying to create. For this project, the wood material was copied and adjusted to fit the engineered lumber values calculated through research.

As previously mentioned, materials need to be assigned to components after modeling them in SpaceClaim and uploading the geometry into ANSYS ® Mechanical. Within the ANSYS ® Mechanical interface, there is a materials tab. This is where every material that has been loaded into the project will be displayed. Right-clicking on one of these materials will give the option to create a material assignment. From there, the material can be selected and applied to the individual component that it belongs to.

### 3.3.1 Nonlinear Structural Steel

All real-life structures exhibit nonlinear behavior and hence require a nonlinear FEA to investigate its true behavior. Nonlinear materials are the types that hold a relationship between applied forces and displacements that do not maintain an elastic, or linear, relationship. A typical linear analysis utilizes linear elastic materials and small deformations after a load is applied, whereas a nonlinear analysis considers larger displacements and understands that the structure's stiffness changes as the loading is applied. The loading imposed on the model for this project was applied in segments over time, also known as a pushover analysis; see §Section 3.6 for a more thorough description. This allowed for a force vs. displacement graph to be plotted to show the nonlinear relationship of the structural steel used. Most nonlinear analyses illustrate their nonlinear behavior by using stress vs. strain curves. A force versus displacement graph can be adapted to convert the two axes into stress and strain, respectively. Figure 16 illustrates a typical nonlinear stress versus strain curve.

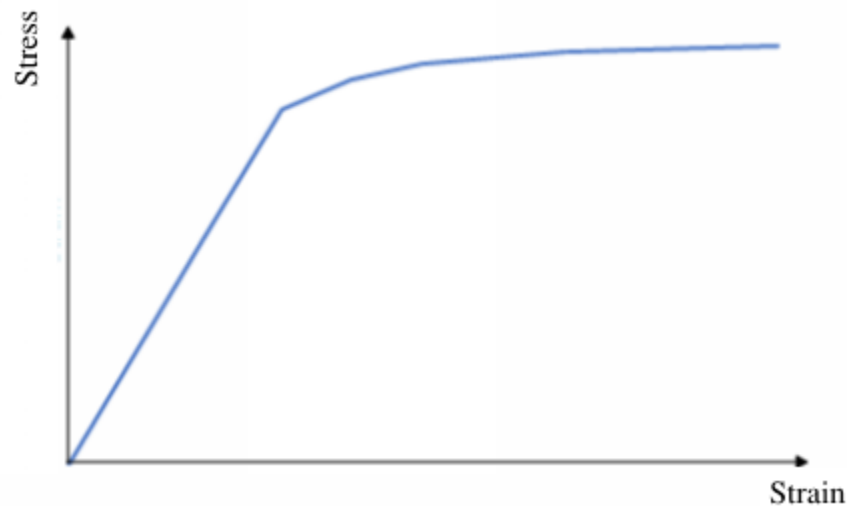


**Figure 16: Nonlinear Stress versus Strain Curve.**

The connection configurations modeled utilized nonlinear structural steel for the I-shape, knife plate, and bolts. The I-shape and knife plate components had the structural steel assigned to them without making any modifications. The bolts, however, required slight adjustments to the material data in the ANSYS ® program based on research values gathered. Table 1 shows the final values used in the material assignment for the bolts. The sources used to create Table 1 are referenced in Appendix A.

**Table 1: Nonlinear Structural Steel Values for Bolts.**

<b>Property</b>	<b>Value</b>	<b>Units</b>
Modulus of Elasticity	29,000	ksi
Tensile Yield Strength	92,000	ksi
Tensile Ultimate Strength	120,000	ksi

*Note.* This table shows the different reference values obtained from a combination of outside sources (shown in Appendix A), averaged, and utilized in adapting the nonlinear structural steel bolt material type in ANSYS ®.

### **3.3.2 Mass Timber (CLT or Glulam)**

As discussed in the introduction to this report, CLT is a lightweight material that has a high strength to weight ratio and superior acoustic, fire, seismic, and thermal performance in comparison to other material types typical for building construction. A CLT panel is made by using a kiln-drying process after bonding several layers of lumber boards together laid in alternating directions. They are pressed and typically layered in 3-ply or 5ply rectangular panels, see Figure 2 for a 3D view of the panels. The mass timber portion of the connection modeled in ANSYS ® has the CLT material properties assigned to it. After a thorough search using several different engineered lumber manufacturers' websites, design values for various material properties were recorded and utilized after creating the CLT material type in ANSYS ®. Table 2 has the final reference

values used to create their respective material types in ANSYS ®. The sources used to create Table 2 are referenced in Appendix A.

**Table 2: Engineered Lumber Reference Values for CLT.**

<b>Property</b>	<b>Value</b>	<b>Unit</b>
Density	0.0191	lb./in <sup>3</sup>
Thermal Expansion	1.47	R-value/in
Modulus of Elasticity	1,508,320	psi
Tensile Yield Strength	2,445	psi
Tensile Ultimate Strength	2,445	psi

*Note.* This table shows the different reference values obtained from a combination of outside sources (shown in Appendix A), averaged, and utilized in creating the CLT material type in ANSYS ®.

### **3.4 Finite Element Mesh**

Meshing objects in ANSYS ® gives the software the ability to turn one solid component or domain into pieces, known as elements, with nodes in between them. This allows for the FEA software to be able to solve the problem, generate test values, and converge. Convergence will be discussed later in Chapter 4. Mesh refinement is a process that helps validate the results of the model's analysis. Typically, the initial mesh applied to the geometry will be rough and coarse, meaning the size of the elements will be large and few elements or nodes will comprise the components. This type of mesh will require less computing power; however, the solution will be less accurate compared to a more refined mesh. Coarse meshes are used to verify the solution makes sense and the applied loads and constraints are functioning the way they should be. After that initial run-through, the mesh refining process begins. Mesh refinement applies more fine conditions to the geometry resulting in a higher number of elements and nodes. Finer meshes take longer to run and more computing power. For the connections modeled for this research project, a virtual computer was required to run each model and reach convergence. This

will be discussed in more detail in §Section 3.5. Several “runs” of the model are required to get the model to converge with a finer mesh, but the resulting data reported are more accurate. How fine or coarse of a mesh used in analysis is up to the designer and how precise of results they are looking for.

For the connections modeled during the testing phase of this project, a fine mesh was used. The computing power available to run the substantial number of elements involved with a finer mesh was not available at the time of testing. So, there had to be some give and take with how fine of a mesh that could be applied to the model. The built up I-shape connection configuration had a total element count of 209,743 and node count of 321,254. Figure 17 shows the meshing applied to the entire connection, and Figure 18 shows the element concentration being higher around the bolts. The bolts and bolt holes are expected to have higher stress concentrations; therefore, it is important to have higher mesh refinement near their intersection with the I-shape member to ensure accurate results.

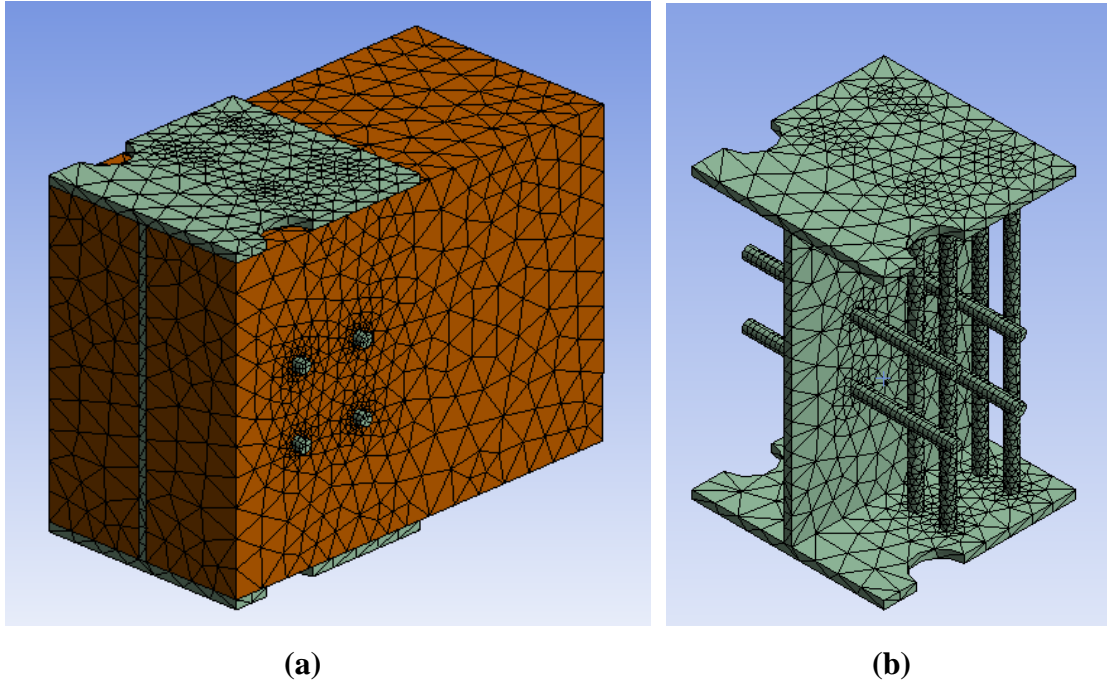


**Figure 17: I-Shape Mesh: (a) Both CLT and Steel Components and (b) Steel Component.**

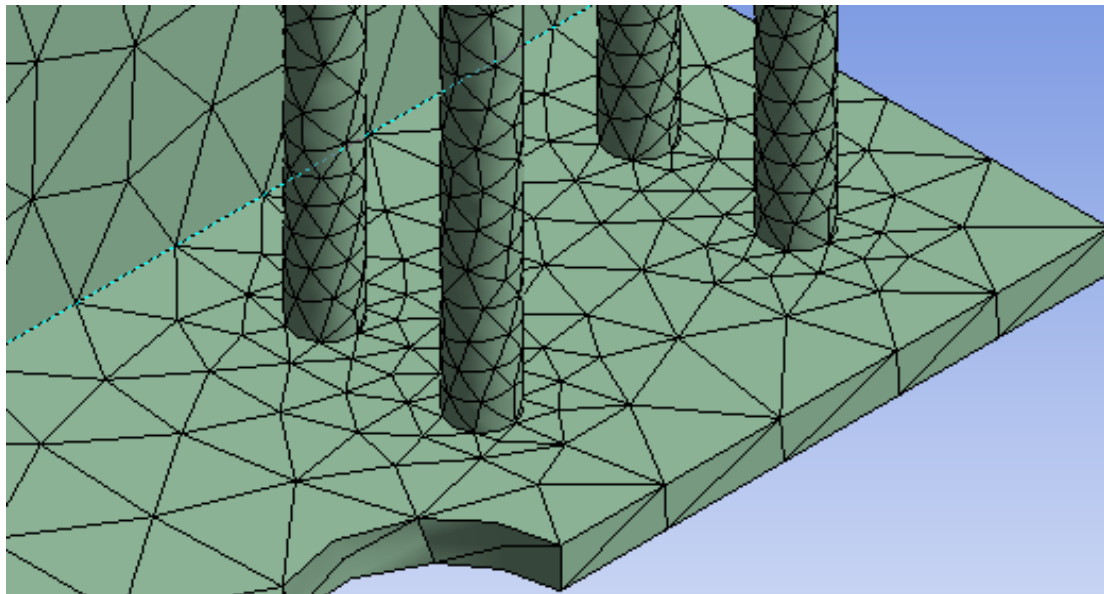


**Figure 18: Higher Mesh Concentration Near Bolts Holes.**

The knife plate model ran much faster and took less time to converge because of the lower number of elements. This is not due to the mesh being sized any differently but because the top and bottom plates in addition to the vertical bolts were no longer involved in the analysis. The knife plate connection configuration had a total element



count of 76,251 and node count of 118,373. In comparison to the I-shape model, the knife plate had less than half the elements and a fifth of the number of nodes to run through.

Figure 19 shows the meshing applied to the connection, and Figure 20 shows the concentration at the bolt holes.

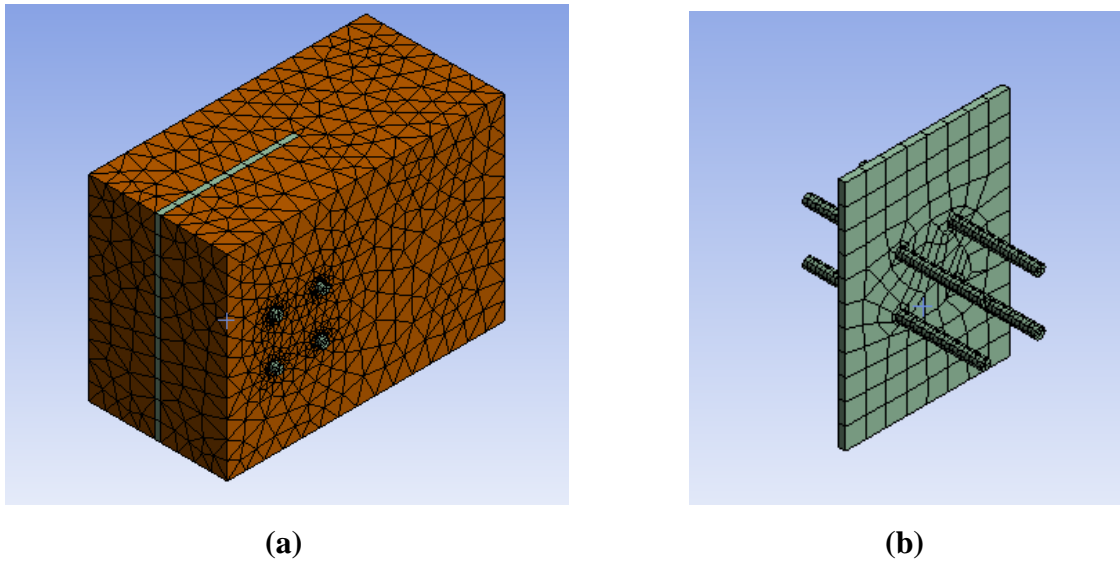


**Figure 19: I-Shape Mesh: (a) Both CLT and Steel Components and (b) Steel Component.**

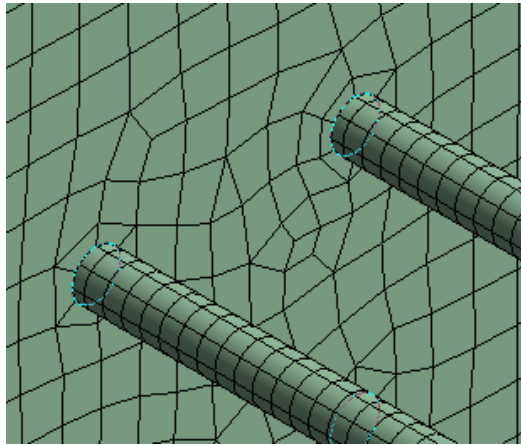


**Figure 20: I-Shape Mesh: Higher Mesh Concentration Near Bolts Holes.**

Both the knife plate configuration and KPRC connection had the same mesh properties applied to the models in ANSYS ®. The KPRC connection configuration had a total element count of 72,919 and node count of 113,281. This is slightly less than the

knife plate connection because there is a smaller cross section on the KPRC model, taking away from both the element and nodal quantities. The run times for this configuration took longer than the rectangular knife plate connection, however. This is due to the curved edges on the KPRC model which takes ANSYS ® longer to analyze.

### 3.5 Boundary Conditions

In addition to applying a mesh to the model, boundary conditions also need to be applied to simulate realistic testing conditions. These conditions are applied to the face connecting to the shear wall and the cut cross section halfway into the coupling beam – 2 feet along the z-axis. The entire coupling beam connection is symmetrical along the z-axis. This symmetry is not only geometric, but in the reactions and internal forces as well. Figure 1 illustrates the symmetry for both the shear and moment forces within the coupling beam. Because of this symmetry, the model was able to be a cut in half version of the whole design. As discussed previously, a virtual computer was utilized to perform the analysis on this connection. Despite having only half the model being analyzed, the computing power required was too large for the university computers available for testing both in terms of computing power and available memory on the device. Even after introducing the virtual computer, provided by MSOE's Harley Lab which had much larger computing power and memory available, the I-shape model had to be cut in half again along the x-axis to obtain any viable results. This was not an ideal or preferred method of testing, because the internal forces are not necessarily symmetrical along the x-axis like they are along the z-axis.

There are two boundary conditions applied to all three connection configurations. The face that connects to the shear wall, farthest in the negative z-direction, has a fixed

connection on the face of the steel. Figure 21 shows the modeled fixed support in ANSYS ® Mechanical for the knife plate connection. The I-shape also has the fixed support in the same location applied to all three plates (top, bottom, and embedded within the CLT). This fixed support restricts movement in all directions and rotations. It is the most rigid type of support.

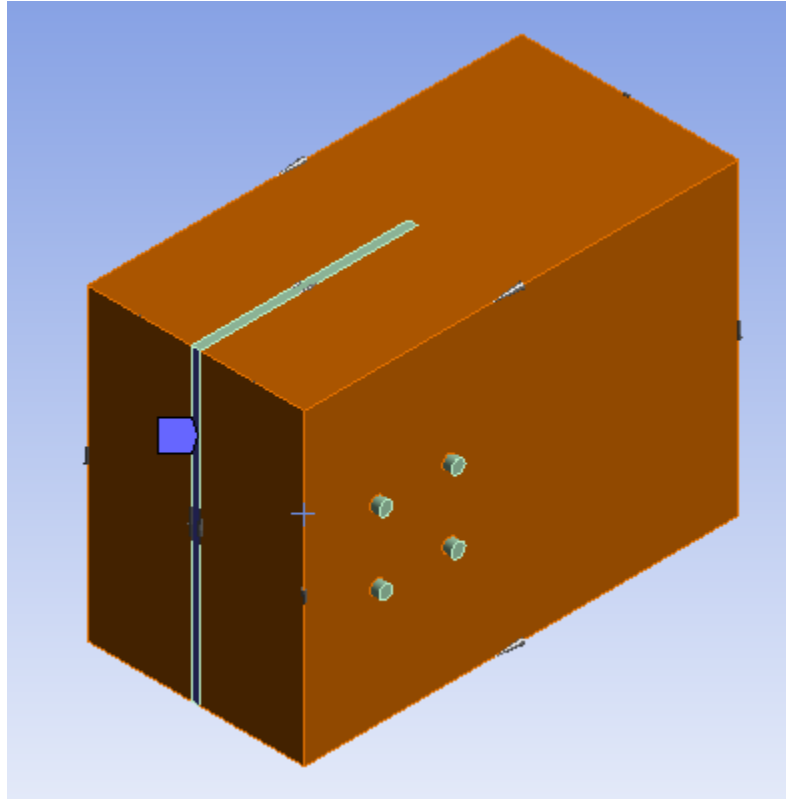


**Figure 21: Fixed Boundary Condition on the Knife Plate Connection.**

The other boundary condition applied to the model is a roller along the face of the horizontal bolts. A roller support, which is less rigid than the fixed support, restricts movement in one or two perpendicular directions. The I-shape and knife plate connections, when construction in a building, will not have significant movement in the x-direction due to both ends being fixed to shear walls. This boundary condition is required because the model is only half of the actual coupling beam (i.e., 2 feet instead of

4 feet long), so the movement needs to be restricted to give the most realistic simulation. The roller support is applied to the faces at either end of the horizontal bolts, as shown in Figure 22 by the yellow highlighted bolt faces. ANSYS ® calls this type of boundary condition a “displacement” because the user can apply a displacement value in any direction along a face, edge, or point. For this analysis, the x-component of the support had zero displacement and the y- and z-components were free to move. Figure 23 shows the different displacement values and other details of the support condition.

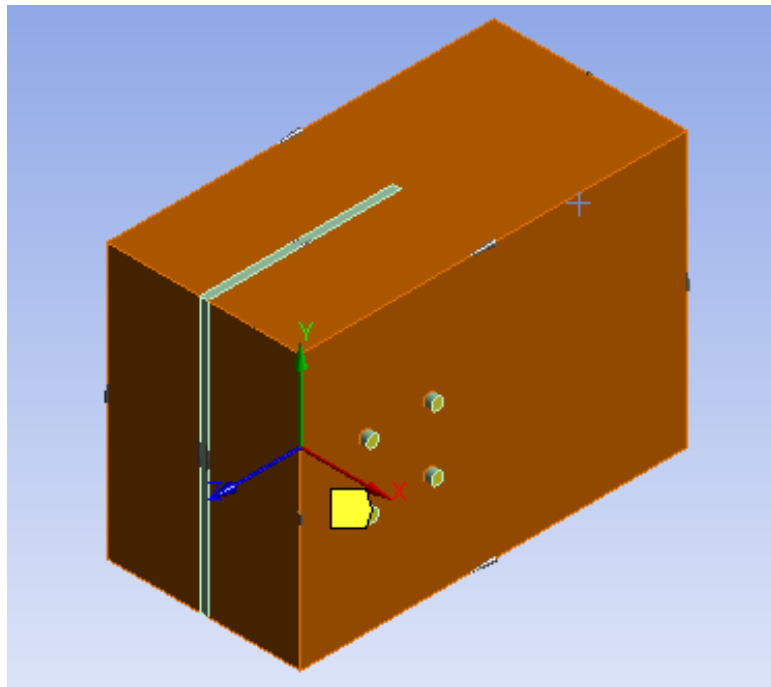


**Figure 22: Roller Boundary Condition on the Knife Plate Connection.**

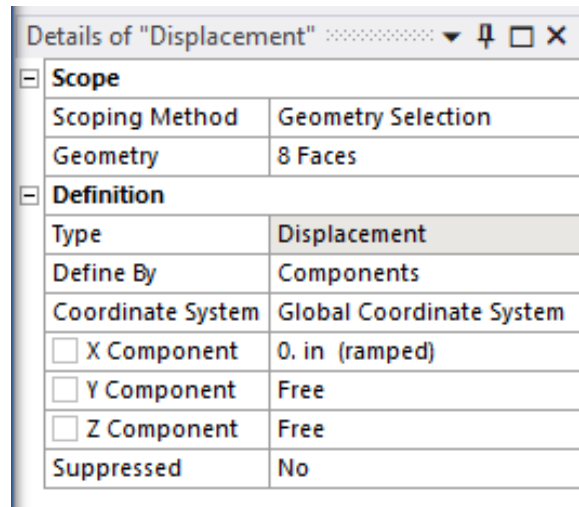


Figure 23: Details of “Displacement” Boundary Conditions.

### 3.6 Contact Elements

A key component of modeling multiple components in ANSYS ® is to address how they interact with one another. Two bodies that do not share a common node will not transfer forces between the two without assigning contact and target element to establish interactions. Because the connections modeled for testing have multiple components, it is imperative that the contact elements are addressed to interact with the target elements in a realistic way. Contact elements have contact detection points, or nodes, which do not pass through the target element. The finer the mesh, the more likely the contact element will penetrate through the target element. Target elements, however, can penetrate through the contact surface.

There are different criteria that are used to determine which component is the contact element and which is the target element. The one most applicable to this project, is the 3D internal contact case. This is where there is an inner member and an outer member. The inner member should be considered the contact surface. If the inner member is much stiffer than the outer member, then the inner member can be the target

surface. Each element that has contact with another element within the connections modeled have a contact region defined, where one element is assigned as a contact body and the other is the target body. Figure 24 gives an example of one of the contact assignments used for the knife plate connection. The knife plate connections have a total of nine contact regions, and the I-shape connection has a total of five contact regions and four frictional contacts. The I-shape was designed with the vertical bolts within the same component as the plates for the purpose of decreasing the amount of contact elements needing to be addressed within the ANSYS ® model.

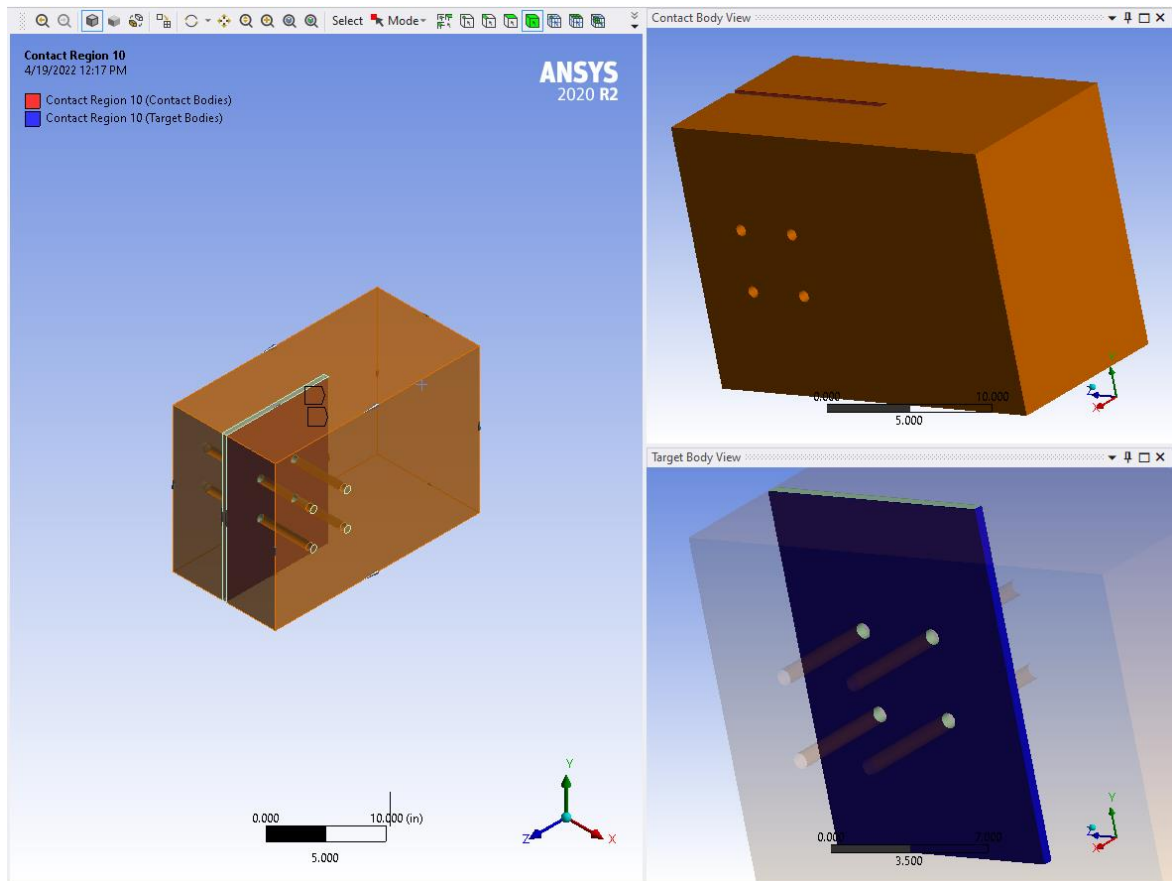


**Figure 24: Knife Plate to CLT Contact Assignment.**

### 3.7 Loading

The steel plates embedded within the engineered lumber component in all three connection configurations can be considered structural fuses. These fuses are utilized during nonlinear analysis because they are the sacrificial element to aid in energy dissipation during a loading event. When these fuses reach their yielding point, it is much more feasible to identify and replace without compromising the structural integrity of the entire system. So, this allows for the timber member, in this case the CLT coupling beam, to maintain its ability to transfer bending and shear forces.

The loading applied to the connections designed for this project can be described as that used in a nonlinear pushover analysis. A pushover analysis is a loading process where a fraction of the overall force is applied at incrementally increasing magnitudes. For the case of this analysis, the sub steps began at 200 lbs. each over a time interval until the force reached its maximum value. Calculations were done prior to loading to determine a rough estimate of where the maximum load could be expected. During the initial load application in ANSYS®, the resulting force after applying all sub steps was 1,000 lbs. Once the model was debugged and resulted in a convergence, the results were analyzed. After the analysis, the model was then run through increased loads up until convergence. The results of these analyses are presented in Chapter 4. The importance of running this type of analysis is that as the magnitude of load increases, weak links and failure modes are found within the structure. As certain portions of the system yield, the forces are shifted to other components that have not reached yielding. Identifying these weak points in the connection allow for adjustment to the design to create a coupling beam system that can with stand real loading seen in mid- to high-rise structures. Not

only is the loading process important, but where the load is applied is also key in obtaining realistic results. Because the internal moment within the coupling beam is zero at the midpoint, as previously discussed in the introduction of this paper, the load is applied as a shear force along the face of the connection at that location, as shown in Figure 25. These loading conditions are identical between all three of the I-shape and knife plate connection configurations.

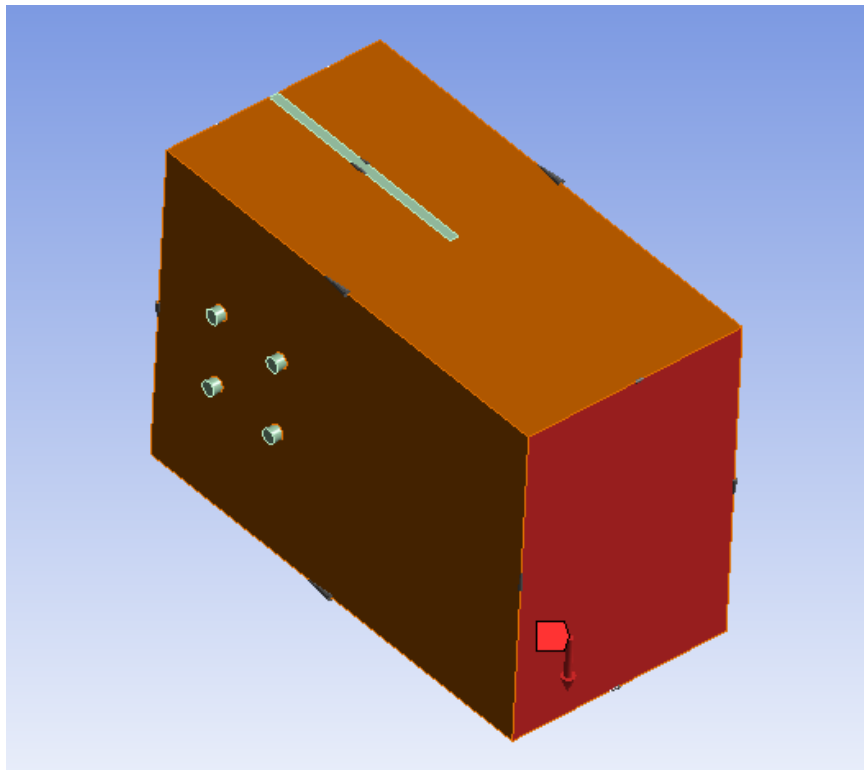


**Figure 25: Applied Downward Shear Force at the Center of the Coupling Beam.**



## Chapter 4: Finite Element Analysis Results

Each model was initially analyzed using a 1000 lbs. shear force at the end of the CLT member until convergence. This was done for the purpose of debugging the models and setting up the appropriate conditions to get realistic data. More information about the debugging process is discussed in preceding sections below. After that process was completed, each model then had an increasingly larger force applied to it. Increasing the force after each run resulted in data that can be used to find the strength of the connection. To determine the ultimate strength and the nonlinear behavior of the coupling beam connections, shear force vs. deflection in the Y-direction was plotted for each case. If the force applied is not large enough, the connection remains in the elastic region which leads to a linear force-deformation relationship. So, increasing the force after each convergence, per connection configuration, helped investigate the nonlinear behavior and, the strength of the coupling beam connection.

All three configurations varied how long they took to run and how many trials were required to make the model converge. The full I-Shape connection with 8 total bolts required longer run times, as expected, which were typically around 4 hours per run. This is because there are several more components within the connection that add to the number of elements and nodes being analyzed. The term “run” describes each cycle of analysis that ANSYS ® performs on the model. There are multiple of these analyses required to get the model to converge and increases in the time taken as the number of runs increases. Mesh refinement occurs after each run, up until convergence, as well. This means that the number of nodes and elements increases after every run time, as

shown in Figure 26, which also results in increased time required for each run. The knife plate connections did not take as long to run and took less run times to reach convergence.

	Equivalent Stress (psi)	Change (%)	Nodes	Elements
1	51502		98813	61954
2	54759	6.1302	118747	76424
3	61119	10.977	178799	116676
4	85271	32.998	445658	303074
5	1.997e+005	80.31	957054	667436

**Figure 26: Mesh Refinement Example.**

It is important to note that the figure presented above, Figure 26, shows an example of how the quantity of nodes and elements increases after each run is conducted. The equivalent stress and change percentage values are not relevant to this portion of the discussion.

#### **4.1 I-Shape Connection**

The I-Shape connection configuration was able to converge after being loaded at 1,000 lbs. Once the force was increased, the model required more memory than available with the computers used for this project. To continue with the analysis for this connection, the model was cut in half along the XZ axis to reduce the computing power required for each run in ANSYS ®. Figure 27 shows the geometry tested. The bolt heads were initially removed to reduce the run time and computing power needed to make the models converge, as discussed earlier. Because the I-shape model had to be cut in half, those bolt heads were added back into the configuration because it is slightly more accurate to include them in the model.

The half I-shape model started with a 1,000 lb. force to make sure it was able to converge. After, the loading was increased to 2,000 lbs. applied every second until the

maximum load was applied. Several trials of this model were run under increasingly larger loading conditions. As mentioned earlier, the I-shape model was designed with a fissure in the top plate to reduce its strength capacity. Despite this feature, the model began reaching ultimate strength values that would not be applicable in an actual loading event because the CLT member would yield prior to that of the I-shape connection. Due to time constraints while testing the model, in addition to having two other configurations that still required analysis, this configuration's data will not be included in the report. So, the conclusion of this connection configuration is that it was unable to move from the elastic phase into a plastic phase prior to the CLT member yielding. This is, however, still a viable configuration. It requires manipulation of its height and thicknesses to reduce its strength to be less than that of the CLT member. After coming to this conclusion, the knife plate configurations were tested in a comparable manner to determine their stresses and displacements. See Appendix B for the calculations that show the strength of the I-shape and both knife plate configurations.

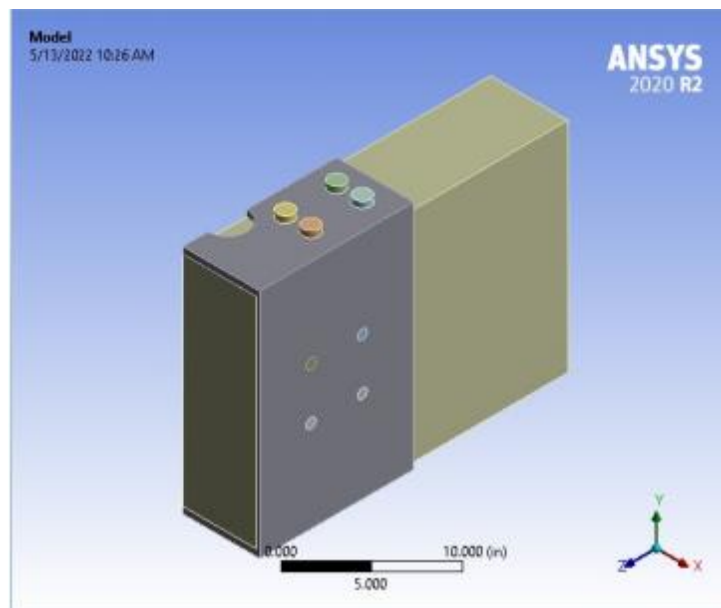


**Figure 27: I-Shape Half Model Isometric.**

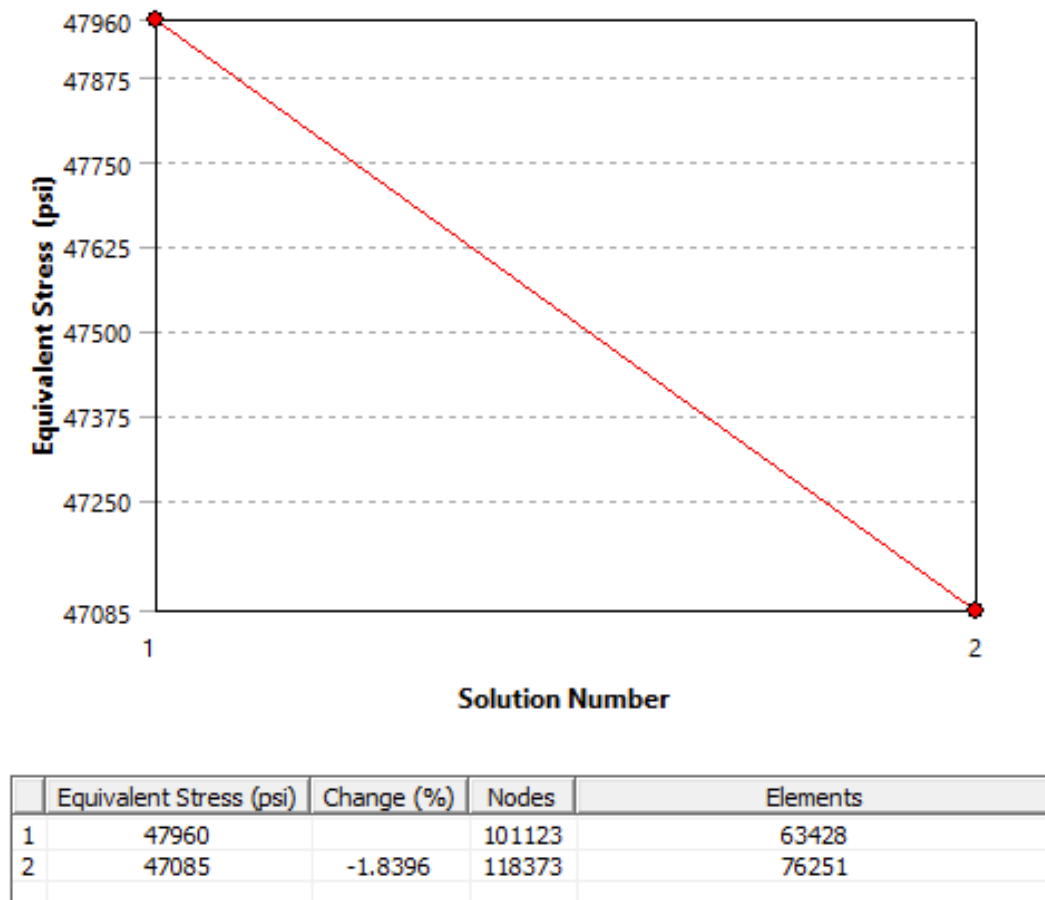
## 4.2 Knife Plate Connection

The knife plate connection configuration ran through multiple iterations before coming to a load that resulted in a nonlinear force versus displacement graph. As performed on the I-shape connection discussed above, the loading started at 1,000 lbs. to help debug and verify initial results. The final force used on this model was 50,000 lbs., or 50 kips to develop an appropriate nonlinear curve. Unlike the I-shape model, the knife plate connection was able to be analyzed without cutting it in half along the XZ plane. There are several different data categories that can be gathered while using ANSYS ® to run an analysis. Only a few were used during this research: von Mises stresses, total deformation, directional deformation, normal stress, normal elastic strain, and force reaction. In the following sections, these various parameters are presented from the final analysis run report. See Appendix B for the full report from ANSYS ® on the knife plate connections.

### 4.2.1 Von Mises Stresses – Equivalent Stress

Von Mises, or equivalent, stresses are a theoretical measure of stress utilized in ductile materials under complex loading. It is a commonly used variable in fatigue strength calculations and is used to estimate yield failure criteria. Simply put, the equivalent stress function is ANSYS's ® way of combining the three principal stresses into one value. The equivalent stress is compared to the yield stress of the material to judge how and when the material will yield. These stresses were recorded from the ANSYS ® report after running the connection to convergence. ANSYS ® offers a “probe” feature in its software that allows the user to point out maximum and minimum locations on the model for the various outputs. The von Mises stresses for this connection

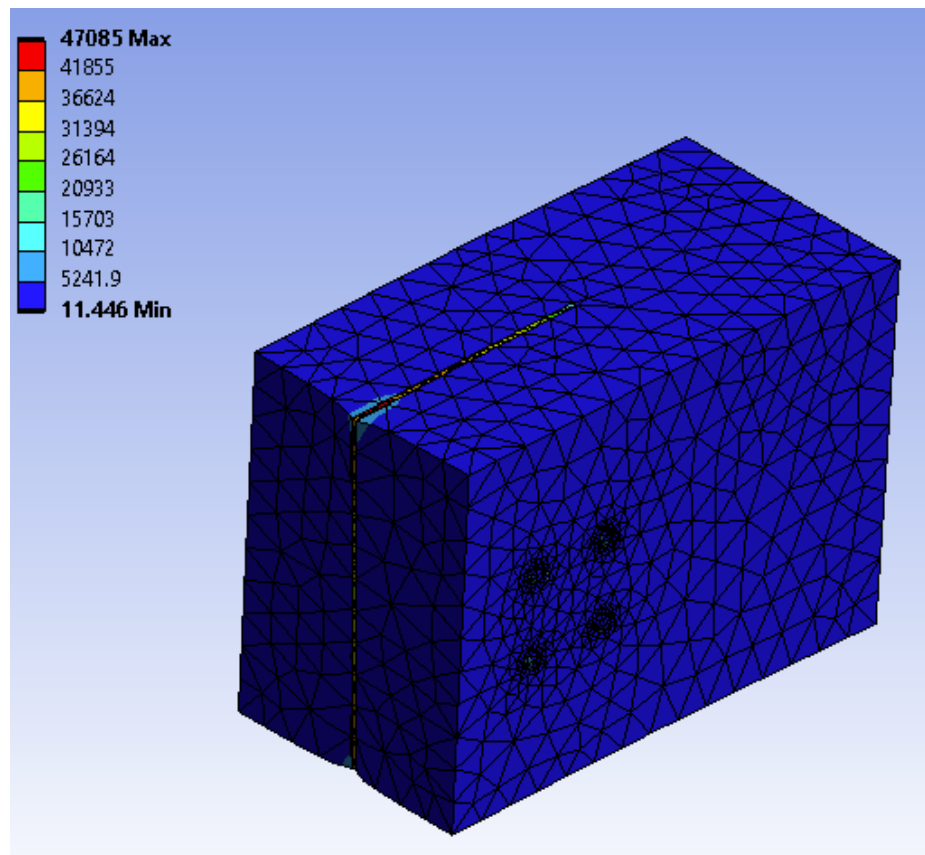
were concentrated within the steel plate resulting in minimal stresses being present in the CLT member. Below are several figures illustrating the spread of stresses on the geometric body. The von Mises stress category also shows convergence criteria. When a model converges, there is an output graph and table that show the percent change, stresses, nodal and elemental quantities after each run. Figure 28 shows the convergence graph and table after the analysis was completed.



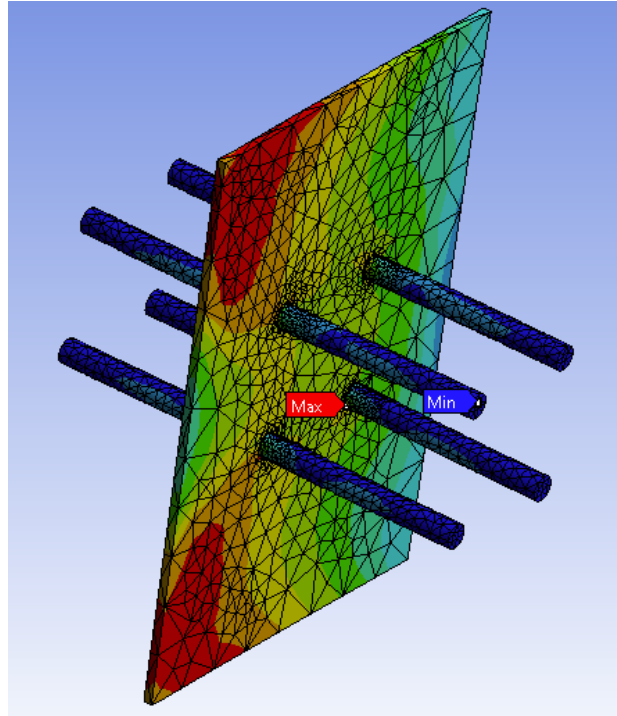
**Figure 28: Convergence Criteria from Knife Plate Connection Analysis.**

Figure 29 shows an overall isometric view of the whole connection. The probe feature was used when creating these figures to show where the maximum and minimum stresses are. Figure 30 shows just the steel knife plate, without the CLT beam, to show

where the maximum and minimum stresses are located. Figure 31 shows a zoomed view of the maximum stress of 47,085 psi, located within the bolt holes. Figure 32 shows the minimum stress concentration of 11.4 psi, located at the edge of the plate. Results like these were expected for this concentration, which is the primary reason for increasing the mesh around the bolt holes to get a more accurate depiction of what is occurring in that location. It is important to note that a substantial portion of the red coloring indicating high stress values are located at the two corners of the knife plate that are near the fixed boundary condition.



**Figure 29: Knife Plate von Mises Stress Isometric View, Entire Configuration at 50 kip.**



**Figure 30: Knife Plate von Mises Stress Isometric View, Steel Component at 50 kip.**

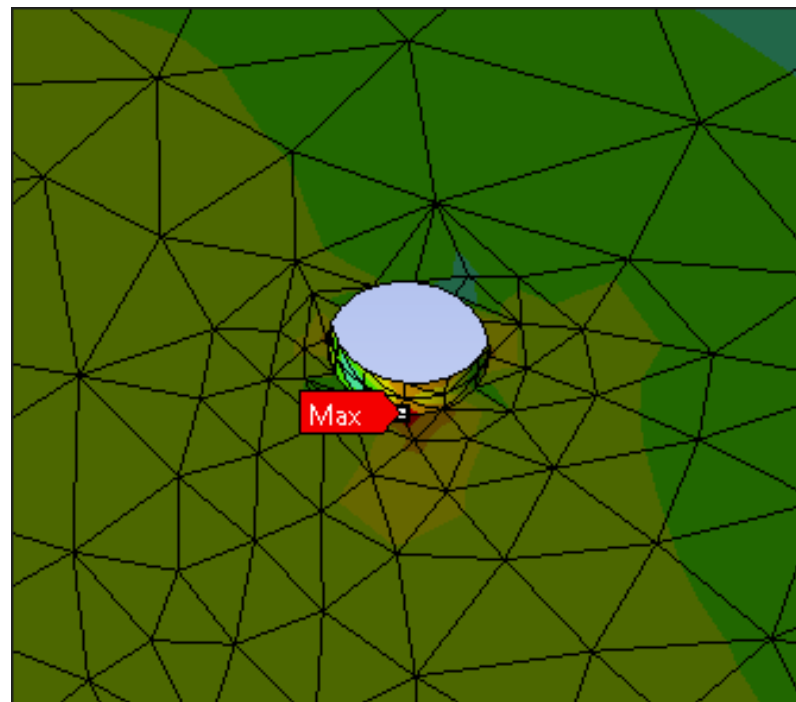


**Figure 31: Knife Plate Maximum Stress at Bolt Holes.**

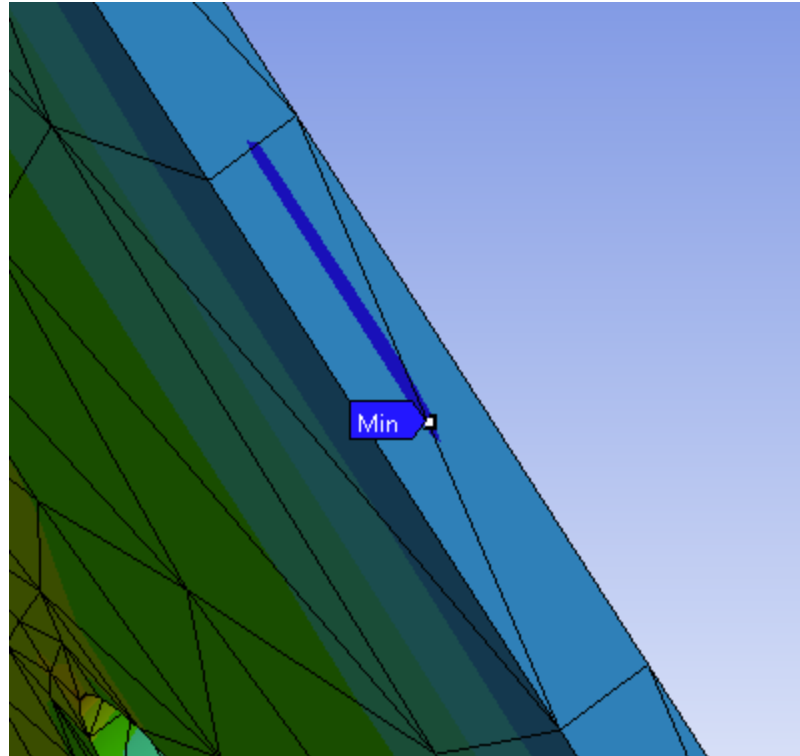


**Figure 32: Knife Plate Minimum Stress at Plate Edge.**

#### ***4.2.2 Total and Directional Deformation***

In addition to the stresses analyzed during the simulation phase of this project, deformation, or displacement, was also recorded. Deformation is the amount of change that occurs during bending, twisting, pulling, etc. in the structural components after experiencing a certain load. There were two types of deformation recorded in the ANSYS® report for all connection configurations – total and directional. Total deformation shows the deformation in all three coordinates (X, Y, and Z). ANSYS® allows the user to select a single coordinate system and view its deformation in that direction. For this report, the Y-Direction was used to show the deformation in the system. The total deformation across the entire configuration is shown in Figure 33 below. Like the stress figures, maximum and minimum probes were placed on the figure as well. To better illustrate where those maximum and minimum values are, Figure 34 and Figure 35 show



a zoomed-in view on the model. The maximum deformation for this configuration with a load of 50 kip applied is approximately 0.586 inch and is located on the face of the CLT member where the shear force was applied. The minimum deformation of 0 inches is located on the opposite face of the CLT member, farthest away from where the loading was applied. This is also the location where the fixed support is. These results are as expected for a loading condition such as the one utilized for the model with the boundary conditions applied.

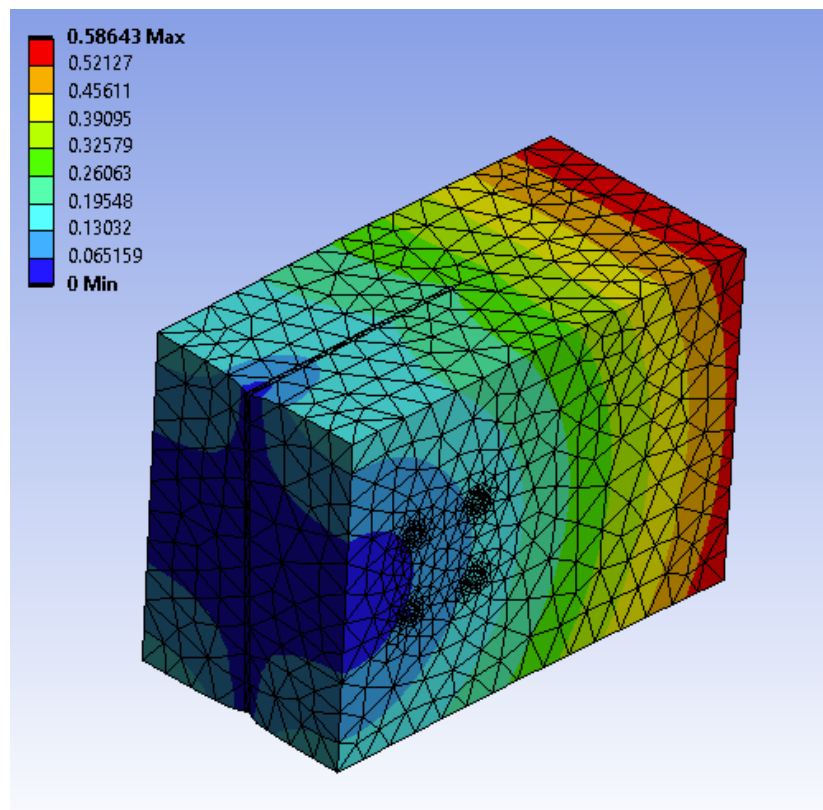


**Figure 33: Knife Plate Total Deformation Isometric at 50 kip.**

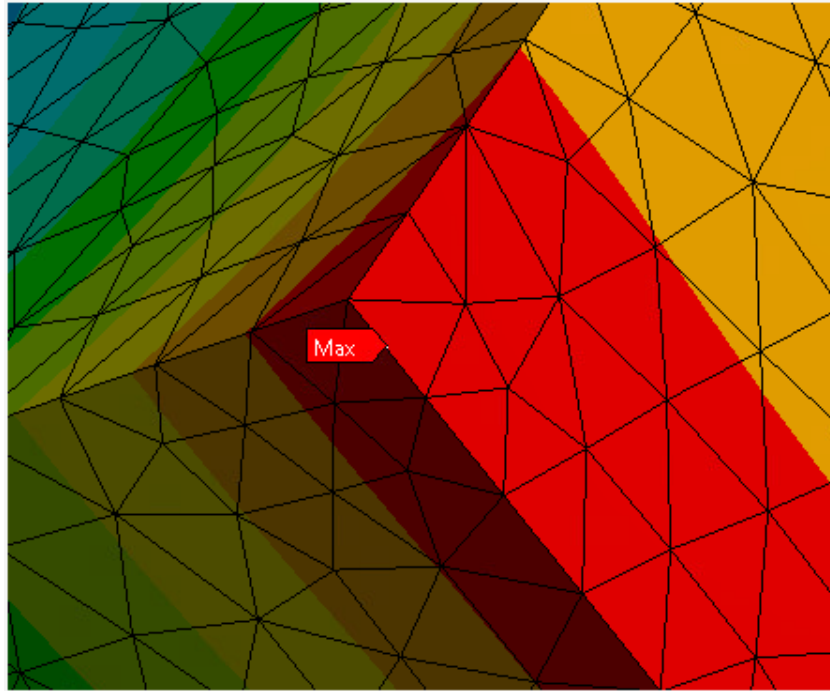


**Figure 34: Knife Plate Maximum Total Deformation at CLT Face.**

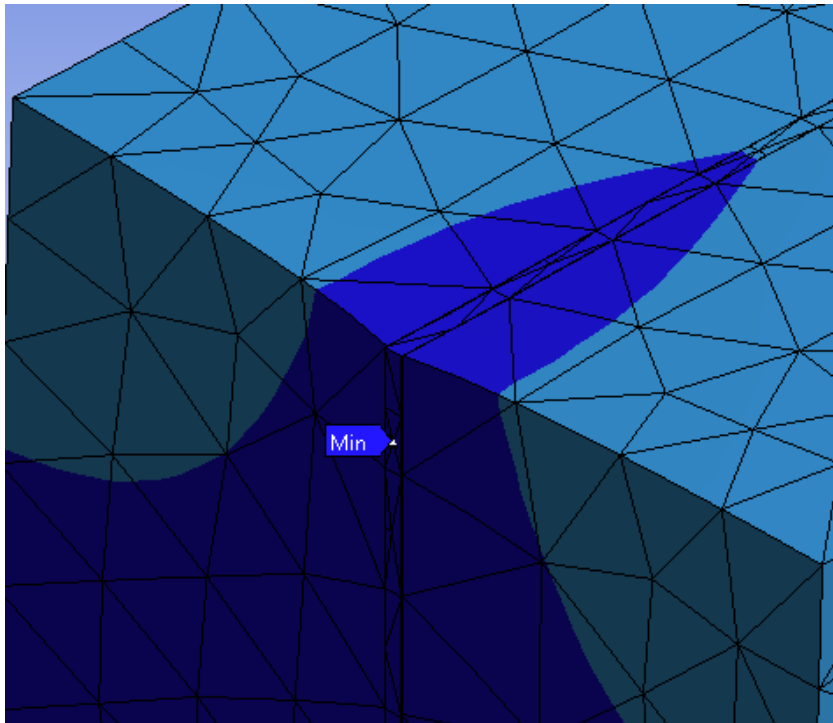


**Figure 35: Knife Plate Minimum Total Deformation at Plate Edge.**

Directional deformation was measured in the Y-direction. The faces of the CLT member see the largest values of deformation. Figure 36 shows the overall isometric view of the entire connection. The face of the CLT member where the load applied sees the local minimum. ANSYS labeled this value at -0.540 inches, meaning it is being pulled down due to the applied shear load at the face of the CLT. A zoomed in view of this is in Figure 38. Conversely, the maximum displacement in the Y-direction is located at the opposing face of the CLT beam where the fixed support is. This means that the edge is being slightly pushed upward due to the applied load, which is expected. Figure 37 shows a zoomed in location of where the maximum value of 0.0110 inches is located.

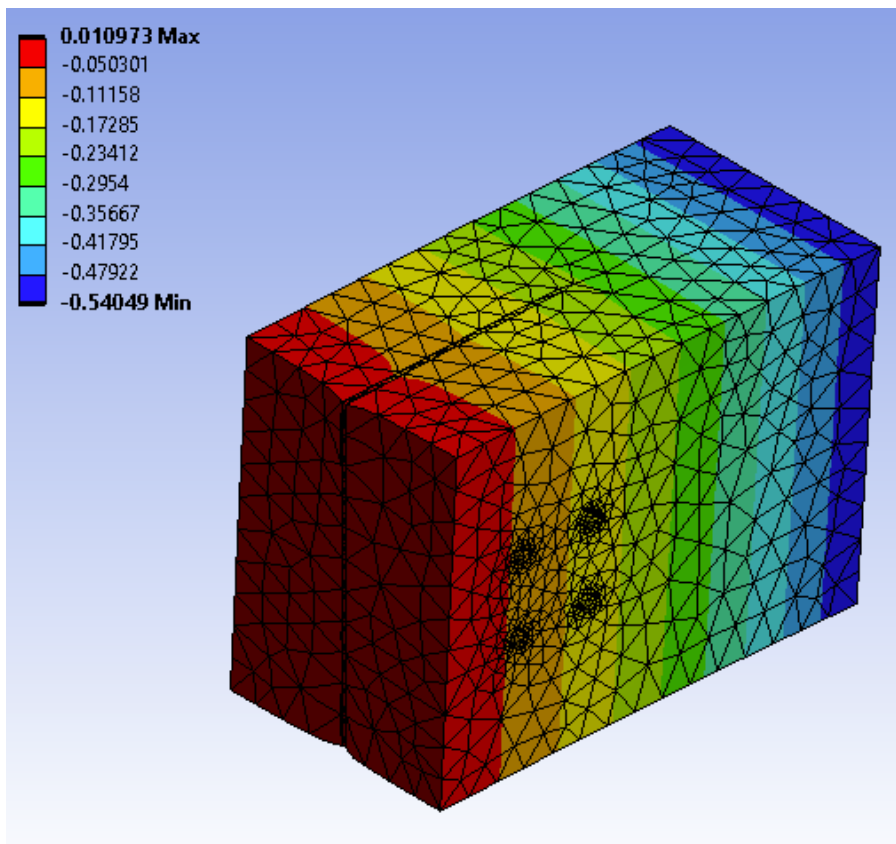


**Figure 36: Knife Plate Directional Deformation Isometric View at 50 kip.**

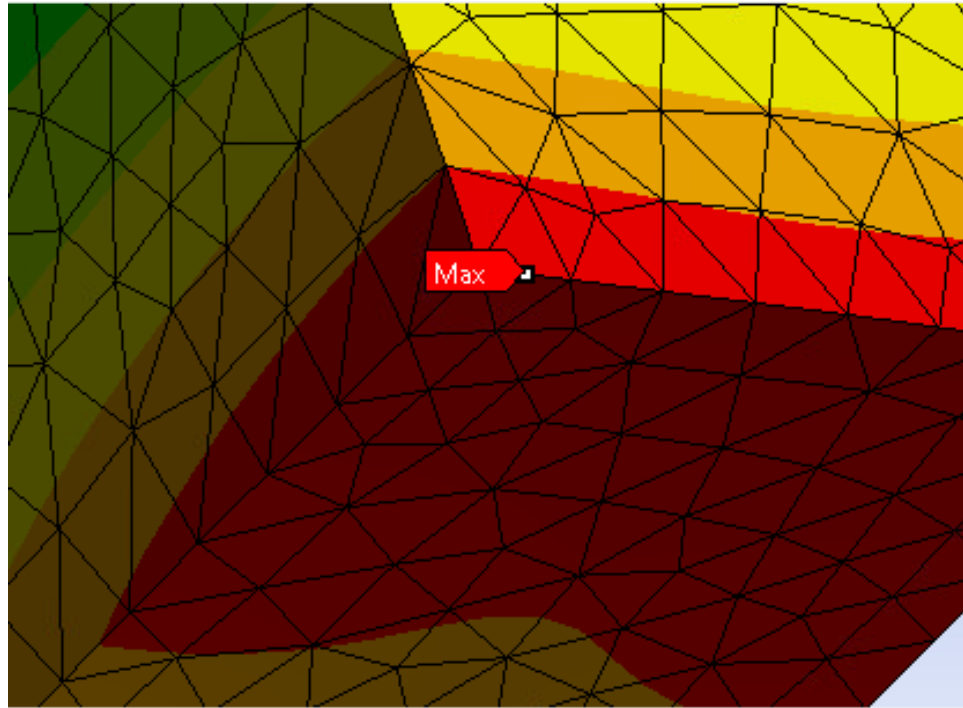


**Figure 37: Knife Plate Maximum Directional Deformation at CLT Beam Edge.**

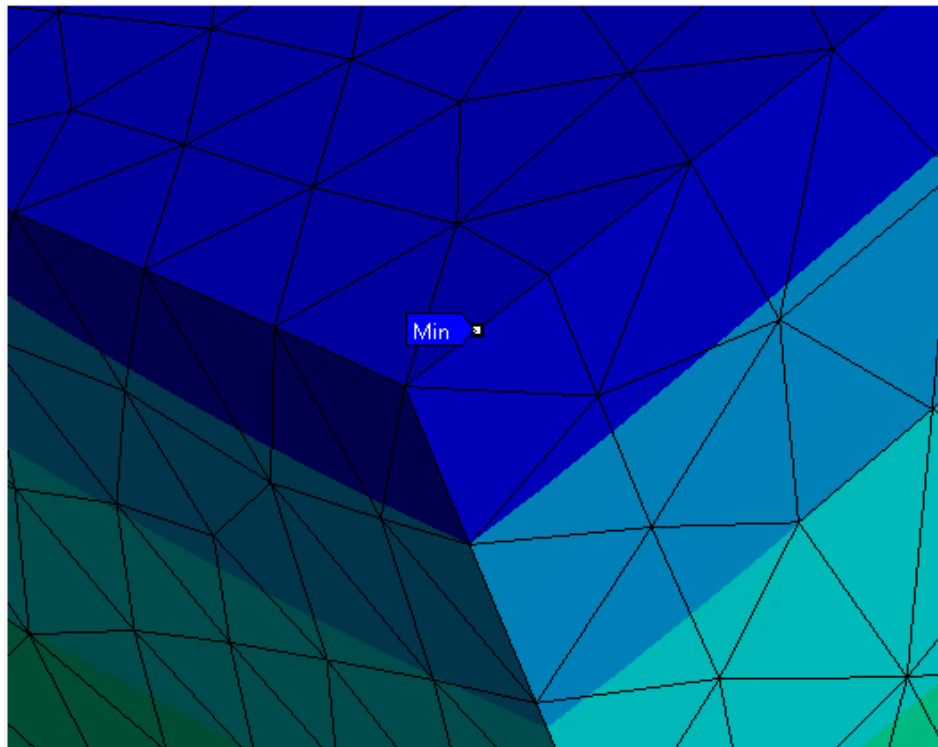


**Figure 38: Knife Plate Minimum Directional Deformation at CLT Beam Edge.**

### 4.2.3 Normal Stress and Strain

Normal stress is the stress that acts perpendicular to the surface of an object. It is the perpendicular force divided by the cross-sectional area. It can be either tensile or compressive, depending on how the load is applied. This, in conjunction with shear stress, can be used when designing sections to find those that have the proper cross-sectional area and material properties. Strain is a unitless property that takes the deformation, or amount of elongation divided by the original length of the member. Strain is often used to figure out the durability of a material because it shows how much it will deform under load. Stress and strain can also be used to determine the modulus of elasticity of a certain material. The stress-strain graph, shown in Figure 39, can help determine the elastic limit, yield point, ultimate stress, and fracture point of a certain test subject.

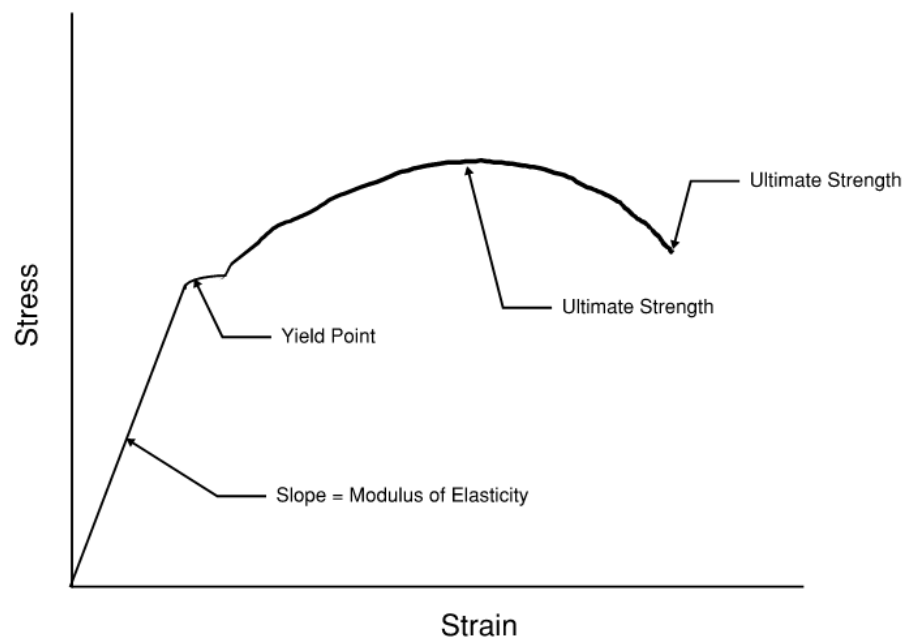


**Figure 39: Stress Strain Curve.**

The normal stress and strain were recorded during the analysis portion of this project for the knife plate configurations. Several figures below show the various locations of the data points. Figure 40 and Figure 41 show the different concentrations of the normal stress on the model as a whole and just the steel component, respectively. The maximum normal stress is 65,405 psi and the minimum is -56,667 psi. Figure 42 and Figure 43 show the different concentration of the elastic strain on the connection. The maximum elastic strain is 0.00166 and minimum is -0.00206.

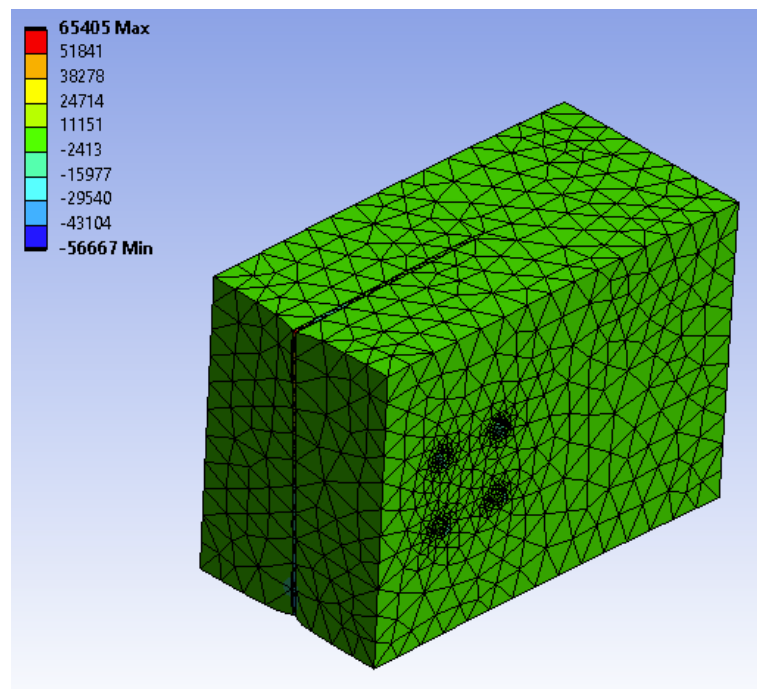


**Figure 40: Knife Plate Normal Stress Concentration Isometric View at 50 kip.**

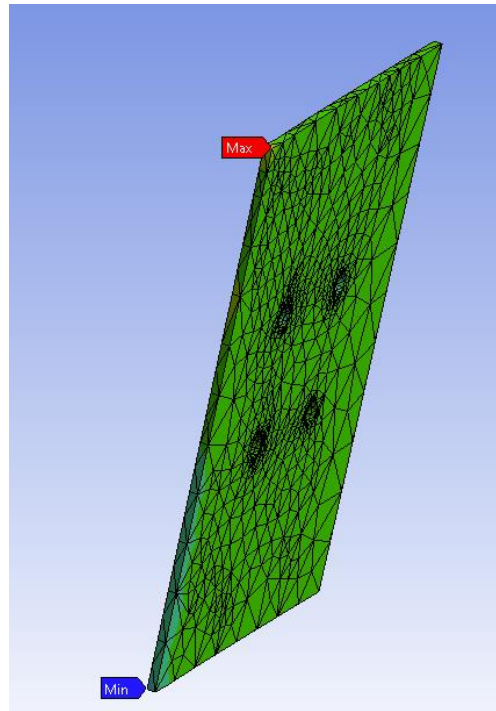


**Figure 41: Knife Plate Steel Component Maximum and Minimum Normal Stress Concentration.**

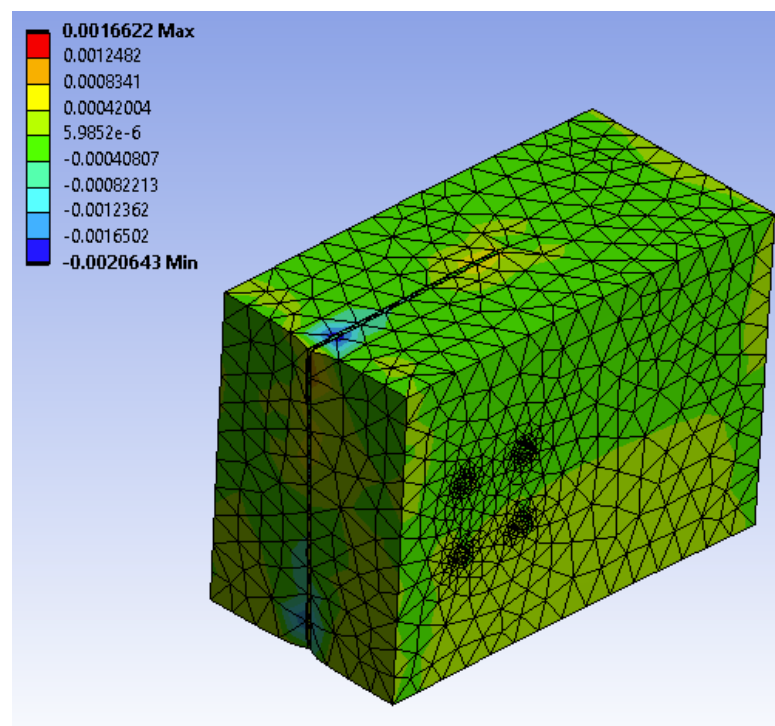


**Figure 42: Knife Plate Strain Concentration Isometric View at 50 kip.**

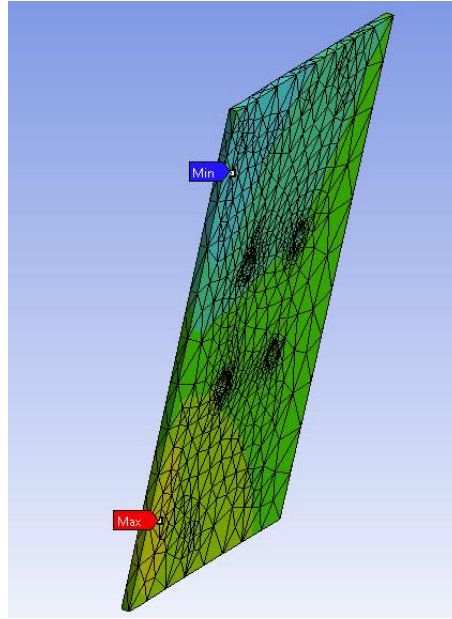


**Figure 43: Knife Plate Steel Component Maximum and Minimum Strain Concentration.**

#### **4.2.4 Force Reaction**

Force reaction was the final category recorded during the run using ANSYS ®.

The force reaction occurs at the location farthest in the Z-direction, at the point where the fixed boundary condition is applied. In addition to the location of the force reaction,

Figure 44 shows the applied mesh and direction of the force reaction.

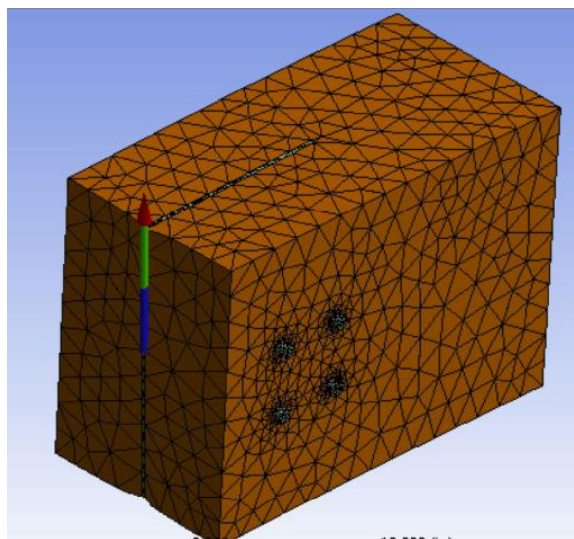


**Figure 44: Knife Plate Force Reaction and Applied Mesh.**



The results for force reaction portion of this connection are shown in Table 3, which show exactly how much force was present at the fixed boundary condition at different time intervals. As mentioned in preceding sections, the fixed boundary condition was placed at the interface between the shear wall and connection, shown in Figure 21 above. ANSYS ® records the values in all three directions. These data will be used to create the force versus displacement graph that shows the connection changing from an elastic state to a plastic state.

**Table 3: Force Reaction Results from ANSYS ® Run for the Knife Plate Connection Configuration.**

Time [sec]	Force Reaction [lbf]			
	X-Dir.	Y-Dir.	Z-Dir.	Total
1	1.71	5000	0	5000
2	3.41	10000	0	10000
3	5.56	15000	0.104	15000
4	9.58	20000	2.18	20000
5	21.3	25001	0.690	25001
5.2	22.9	26000	-0.390	26000
5.4	24.3	27000	-0.331	27000
5.7	28.1	28500	0	28500
6	37.8	30000	-0.429	30000
6.2	41.4	30998	-7.54	30998
6.4	40.9	32000	-0.499	32000
6.7	57.8	33498	-1.70	33498
7	69.1	35000	0	35000
7.2	81.0	35994	-3.37	35994
7.4	92.7	37000	0	37000
7.7	110	38500	0	38500
8	127	40000	0	40000
8.2	139	40998	0.810	40998
8.4	152	41997	-1.320	41998
8.7	171	43500	0	43500
9	188	44994	0.171	44994
9.2	200	45998	0.511	45999
9.4	211	46999	0	47000
9.7	227	48497	0	48498
10	243	49997	0	49998

*Note.* This table shows force reaction values in the X, Y, and Z-Dir. in pounds force (lbf). The values were recorded for the entirety of the run, seconds 1 through 10, for the knife plate connection configuration with a 50-kip force applied.

#### **4.2.5 Analysis**

The knife plate connection was analyzed in the same way as the I-shape connection prior to concluding that the results not applicable to the goal of the project. Besides their construction, the difference between the models was primarily the amount of load applied. Because this is a pushover analysis, the load is applied increasing rates

over time. The time intervals for this model start at 1 second apart, but after 5 seconds decrease to 0.2 seconds per step. The force is increased by 5,000 lbs. every second. Table 4 shows a portion of the data gathered at each time step for force reaction, deformation, stress, and strain for the full 10 seconds of run time.

**Table 4: Results from ANSYS ® Run for the Knife Plate Connection Configuration up to 10 Seconds.**

<b>Time [sec]</b>	<b>Force Reaction [lbf] Y-Dir.</b>	<b>Displacement [in] Y-Dir.</b>	<b>Normal Stress [psi]</b>	<b>Elastic Strain</b>
1	5000	0.0219	6886	0.000200
2	10000	0.0438	13772	0.000400
3	15000	0.0657	20659	0.000600
4	20000	0.0881	27620	0.000802
5	25001	0.113	34890	0.00101
5.2	26000	0.118	36402	0.00105
5.4	27000	0.124	37407	0.00106
5.7	28500	0.134	39764	0.00113
6	30000	0.144	42067	0.00113
6.2	30998	0.152	43927	0.00116
6.4	32000	0.162	45430	0.00119
6.7	33498	0.181	45848	0.00120
7	35000	0.206	46279	0.00123
7.2	35994	0.224	46891	0.00125
7.4	37000	0.243	45811	0.00123
7.7	38500	0.274	44328	0.00122
8	40000	0.306	43982	0.00120
8.2	40998	0.327	42849	0.00119
8.4	41997	0.350	43536	0.00121
8.7	43500	0.384	45933	0.00121
9	44994	0.420	50495	0.00128
9.2	45998	0.443	53517	0.00135
9.4	46999	0.467	56519	0.00143
9.7	48497	0.504	60980	0.00154
10	49997	0.540	65405	0.00166

*Note.* This table shows deformation, force, stress, and strain values for seconds 1 through 10 from the ANSYS analysis report for the knife plate configuration with a 50-kip force applied.

The data from Table 4 were used in plotted the force versus displacement graph in Figure 45 and the stress strain curve in Figure 46. The force versus displacement backbone curve shows the nonlinear behavior of the material. Initially, it starts with a straight, or linear, line. Then, once it reaches a certain capacity, the curve begins to flatten out- creating the nonlinear curve. The stress strain curve can tell a lot of different capacity limits for a material, as discussed in the preceding sections. Significant points are labeled on the curve as well.

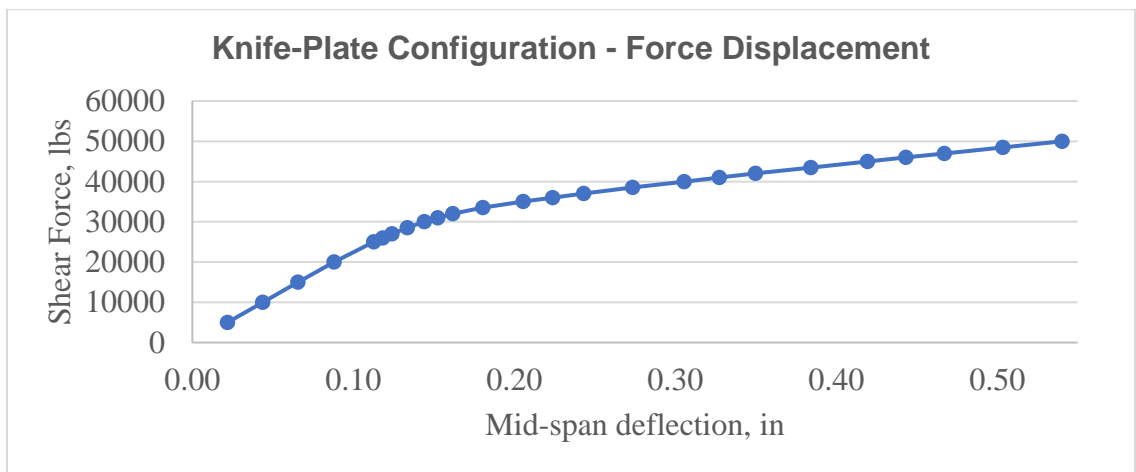


**Figure 45: Force versus Displacement Plot for Knife Plate Connection.**

As seen in Figure 45, the graph begins to show nonlinear behavior around 27 kips. This point is around 5.4 seconds into the 10 second test. At 5.4 seconds, the equivalent stress concentration is 37,412 psi and normal stress is 37,407 psi.

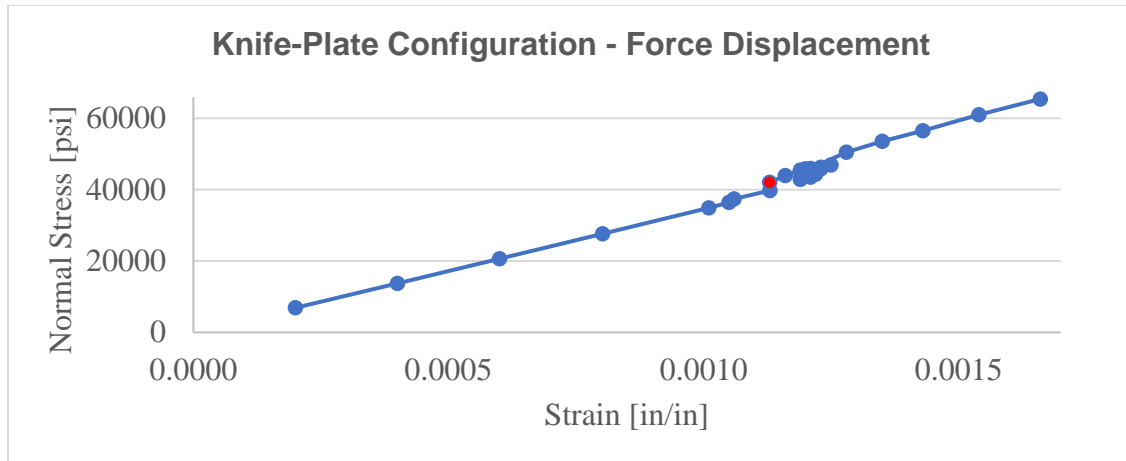


**Figure 46: Stress Strain Curve Knife Plate Connection.**

Figure 46 shows the stress strain curve for the knife plate configuration. As noted by the red marker, the graph first begins to yield at normal stress of 42,000 psi and a strain value of 0.00113.

### 4.3 Knife Plate Connection with Reduced Cross Section (KPRC)

The KPRC connection configuration was analyzed using the exact same process as the knife plate as discussed in §Section 4.2. After calculating the capacity of the connection, the force applied to the model was 30,000 lbs., or 30 kips, to develop an appropriate nonlinear curve. This model, being almost identical in construction as the previously tested knife plate connection, was also small enough to not need to be cut in half along the XZ axis. The following sections of this paper will layout the data gathered from various categories in ANSYS ®: equivalent stress, total and directional deformation, normal stress and strain, and force reaction. See Appendix B for the full report from ANSYS ® on the knife plate with reduced cross section connection.

### 4.3.1 Von Mises Stresses – Equivalent Stress

The von Mises stresses for this connection were concentrated within the steel plate resulting in minimal stresses being present in the CLT member. This is like the previously mentioned knife plate connection configuration. The run was also similar in that it converged after two runs, as shown in Figure 47.

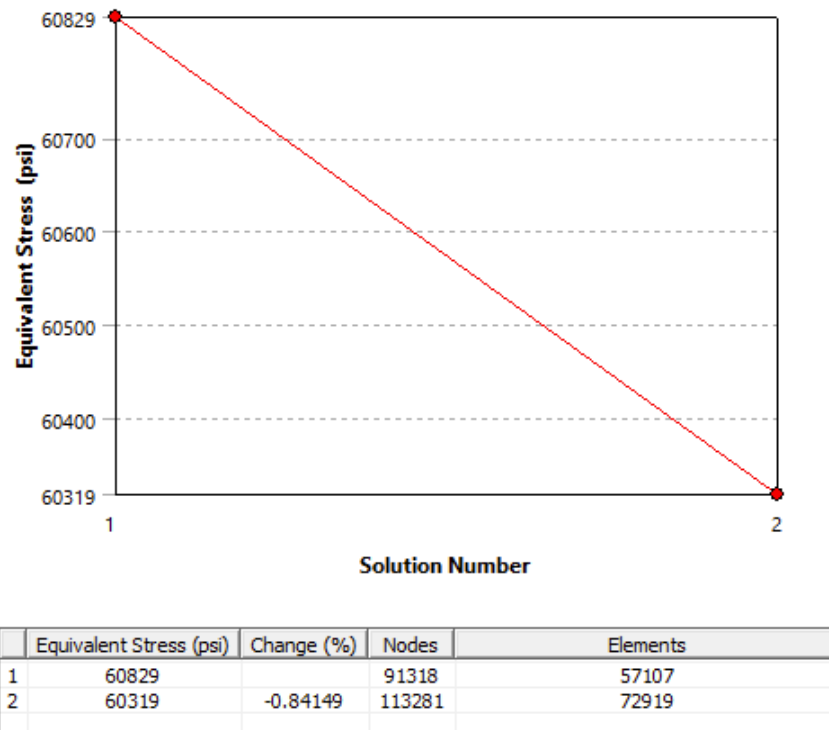


**Figure 47: Convergence Criteria from KPRC Connection Analysis.**

Figure 48 through 51 illustrate the spread of stresses on the geometric body.

Figure 48 shows an overall isometric view of the whole connection. The probe feature was used when creating these figures to show where the maximum and minimum stresses are. Figure 49 shows just the steel component of the KPRC connection to show where the maximum and minimum stresses are located. Figure 50 shows a zoomed view of the maximum stress of 60,319 psi, located at the edge of the plate where the cross section is smallest. Figure 51 shows the minimum stress concentration of 7.7 psi, located at the top

edge of the plate where the cross section is at its largest. It is important to note that a substantial portion of the of the higher stress concentrations are located at near the bolts holes closest to the fixed boundary edge of the connection. This was the goal of this connection type: to have the reduced cross section take on most of the loading and fail first.

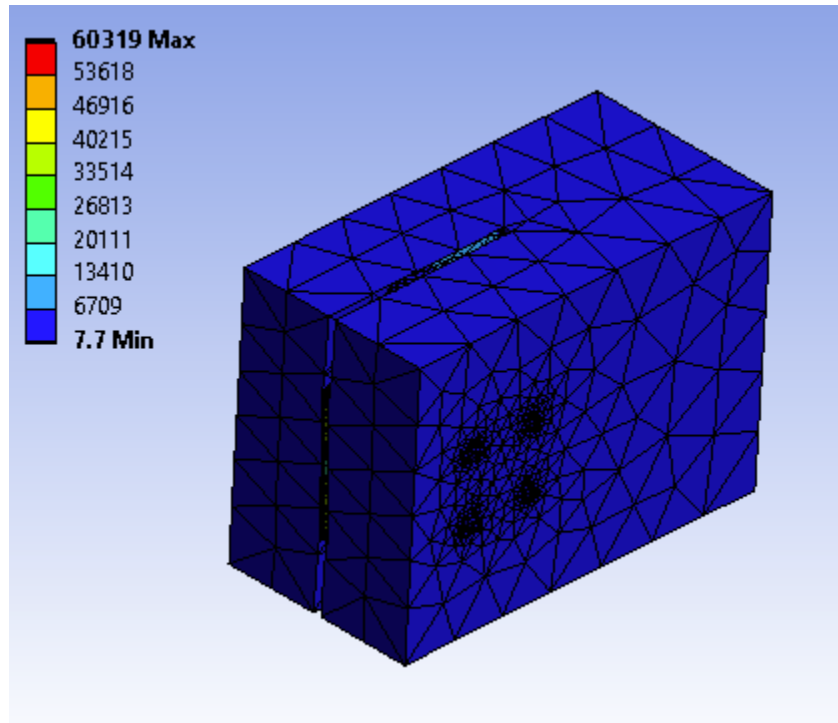


**Figure 48: KPRC von Mises Stress Isometric View, Entire Configuration at 30 kip.**

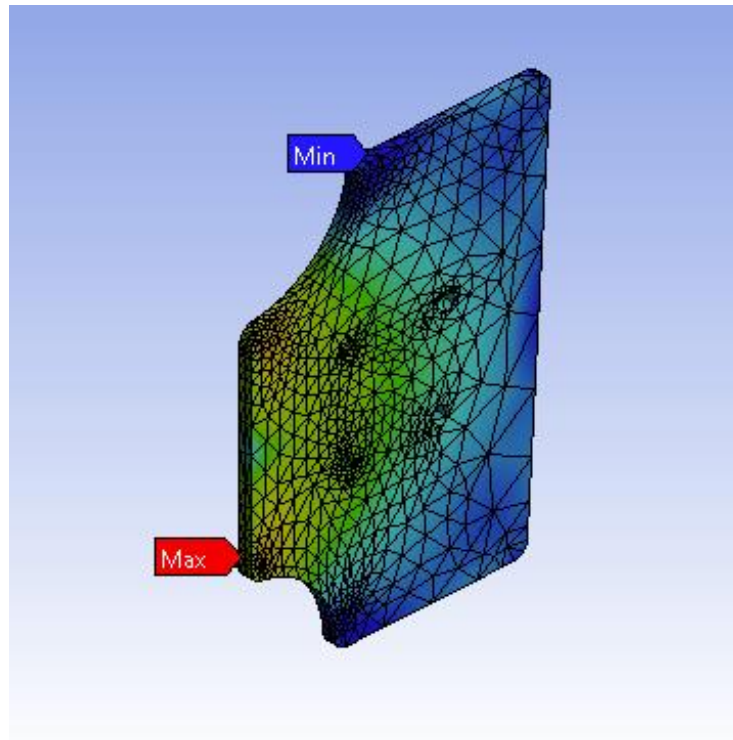


Figure 49: KPRC von Mises Stress Isometric View, Steel Component at 30 kip.

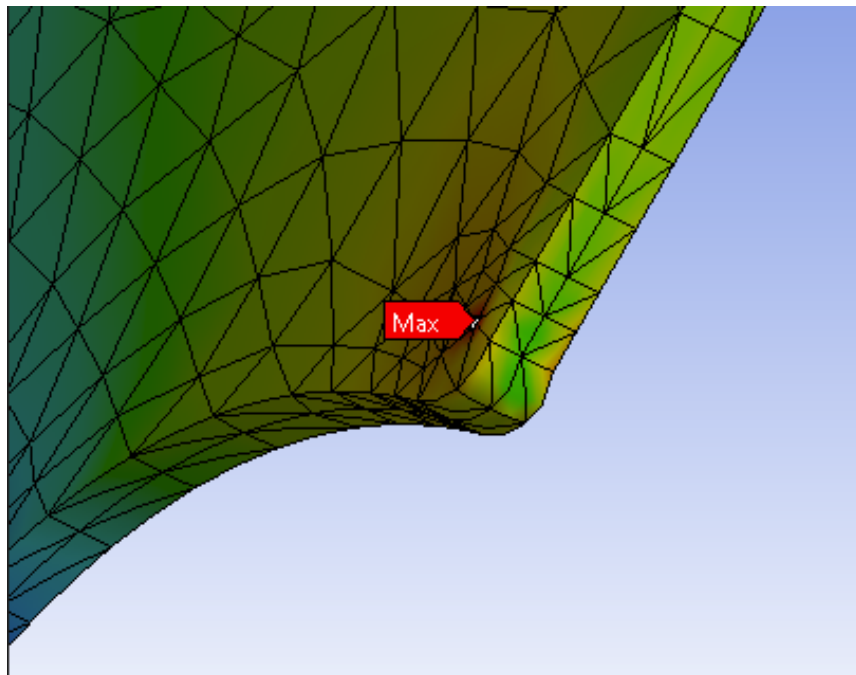
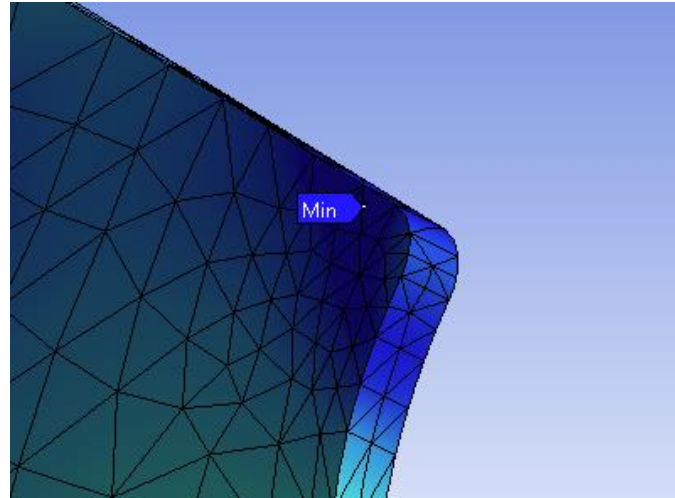


Figure 50: KPRC Maximum Stress at Lowest Cross Section.

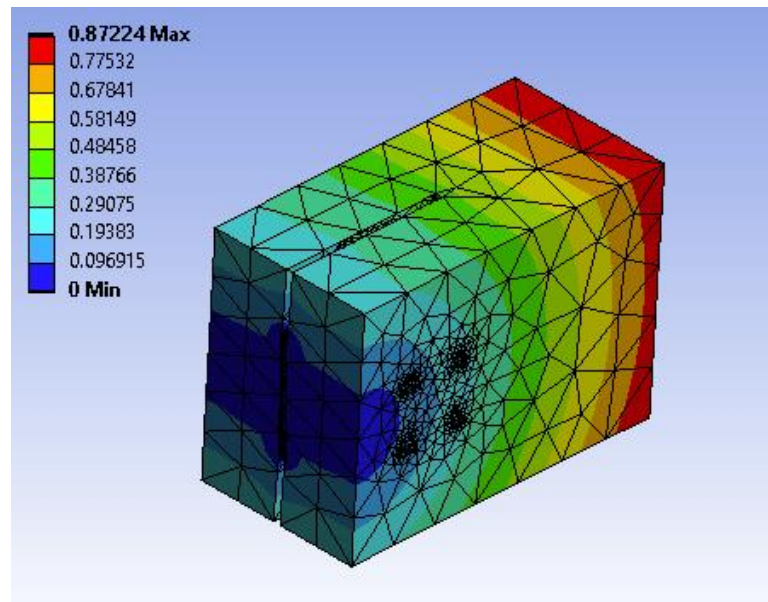




**Figure 51: KPRC Minimum Stress at Largest Cross Section.**

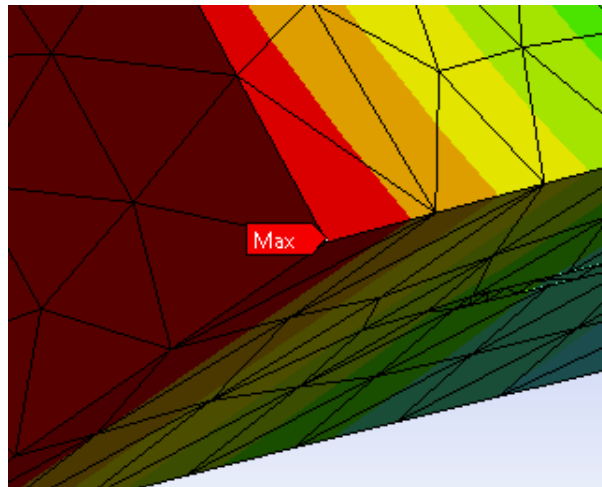
#### ***4.3.2 Total and Directional Deformation***

Total and directional deformation were recorded for the KPRC connection, similarly to the knife plate connection discussed in the previous section. The maximum and minimum total deformation for this connection configuration was 0.872 inches and 0 inches, respectively. Figure 52 shows the overall stress distribution across the entire connection.



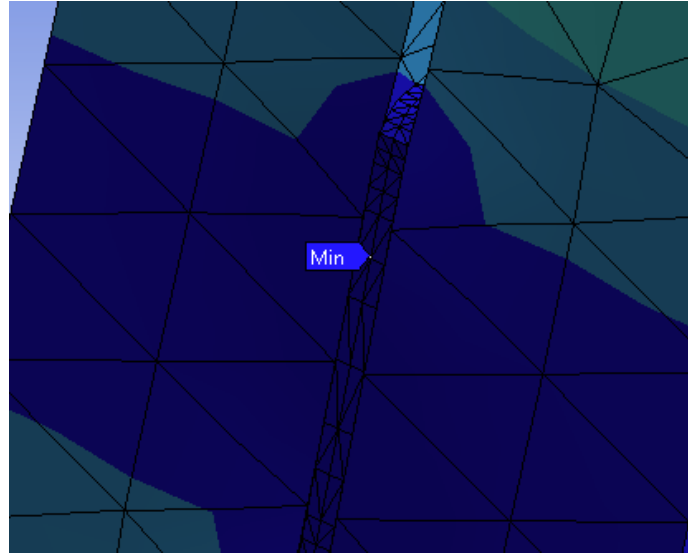
**Figure 52: KPRC Total Deformation Isometric at 30 kip.**

Figure 53 gives a zoomed-in view of where the maximum total deformation is located. The higher deformation values are primarily located along the face of the CLT member where the load is applied, like the knife plate connection discussed previously. This is the location that is not restrained in comparison to the fixed boundary located on the opposite side of the connection. So, when the load is applied here, the deformation should be the largest.



**Figure 53: KPRC Maximum Total Deformation at CLT Face.**

The lower deformation values are located along the opposite edge, at the fixed boundary condition on the steel plate. The minimum value of 0 inches for the total deformation is located along the face of the embedded steel plate, farthest away from where the load is applied, shown in Figure 54. Steel is stronger and can resist a force more efficiently than CLT. So, it is realistic to see the plate maintaining the least amount of deformation while the CLT member experiences a small, but larger amount than the steel.



**Figure 54: KPRC Minimum Total Deformation at Plate Edge.**

Directional deformation, as mentioned earlier, was measured in the Y-direction. Figure 55 shows the overall isometric view of the entire connection. The behavior of the KPRC connection is like that of the knife plate connection particularly when looking at the directional deformation. The face with the applied load sees the absolute maximum value of deformation and face with the fixed support see the local maximum deformation. The minimum value is -0.815 inches. This means that this edge of the configuration is experiencing a downward pull of 0.815 inches. A zoomed-in view of this is in Figure 57. Conversely, the maximum positive deformation of 0.0104 inches. Figure 56 shows a zoomed-in location of where the maximum value is located.

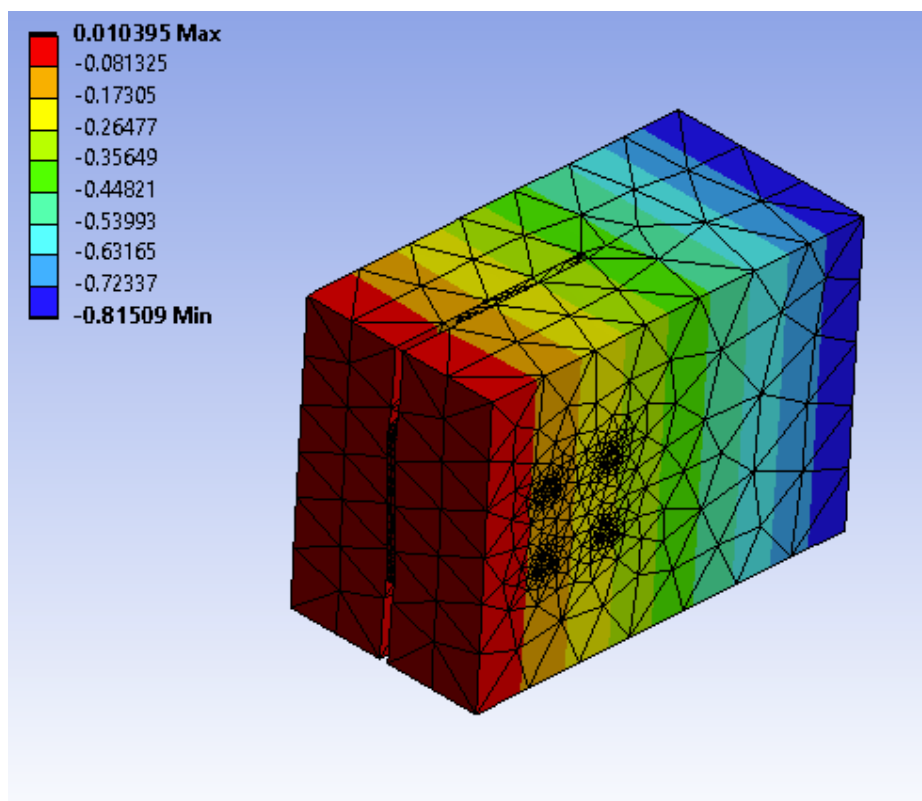


Figure 55: KPRC Directional Deformation Isometric View at 30 kip.

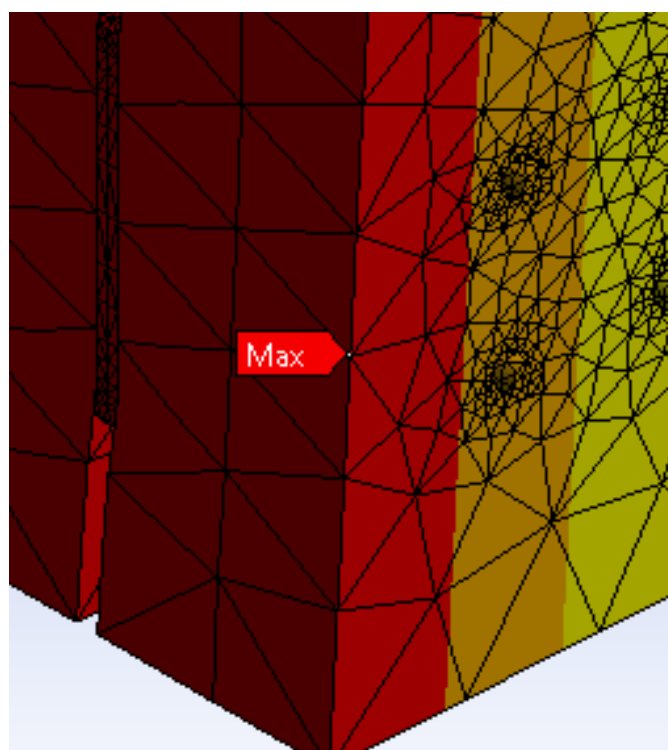
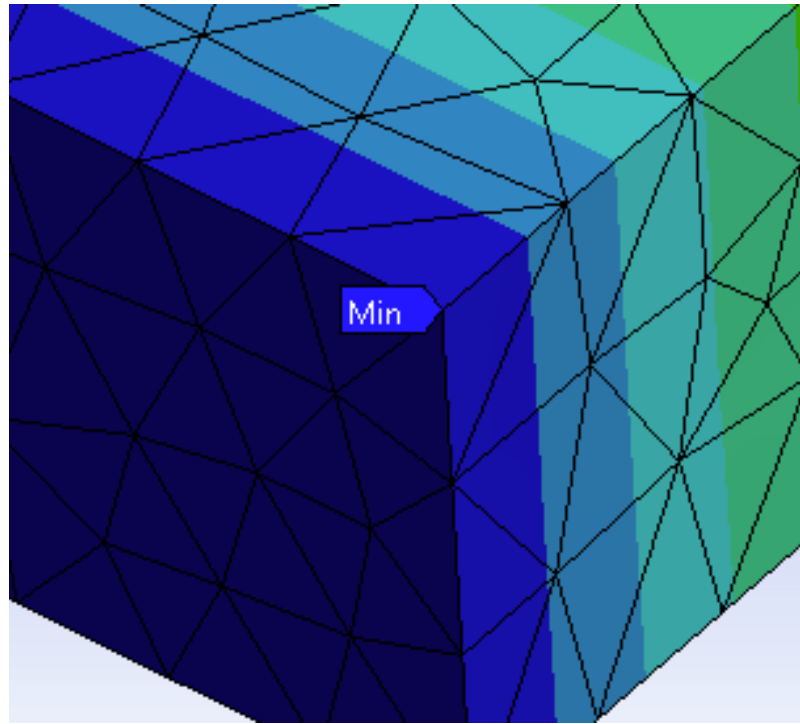


Figure 56: KPRC Maximum Directional Deformation at CLT Beam Edge.



**Figure 57: KPRC Minimum Directional Deformation at CLT Beam Edge.**

### ***4.3.3 Normal Stress and Strain***

Section 4.2.3 gives a more in-depth explanation of normal stress and strain, and why they are important to this research project. The normal stress and strain were recorded during the analysis portion of this project for the KPRC configuration. Several figures below show the distinct locations of the data points. Figure 58 and Figure 59 show the different concentrations of the normal stress. The maximum normal stress is 304,970 psi and the minimum is -261,870 psi. Figure 60 and Figure 61 show the different concentration of the elastic strain on the connection. The maximum elastic strain is 0.00376 and minimum is -0.00312.

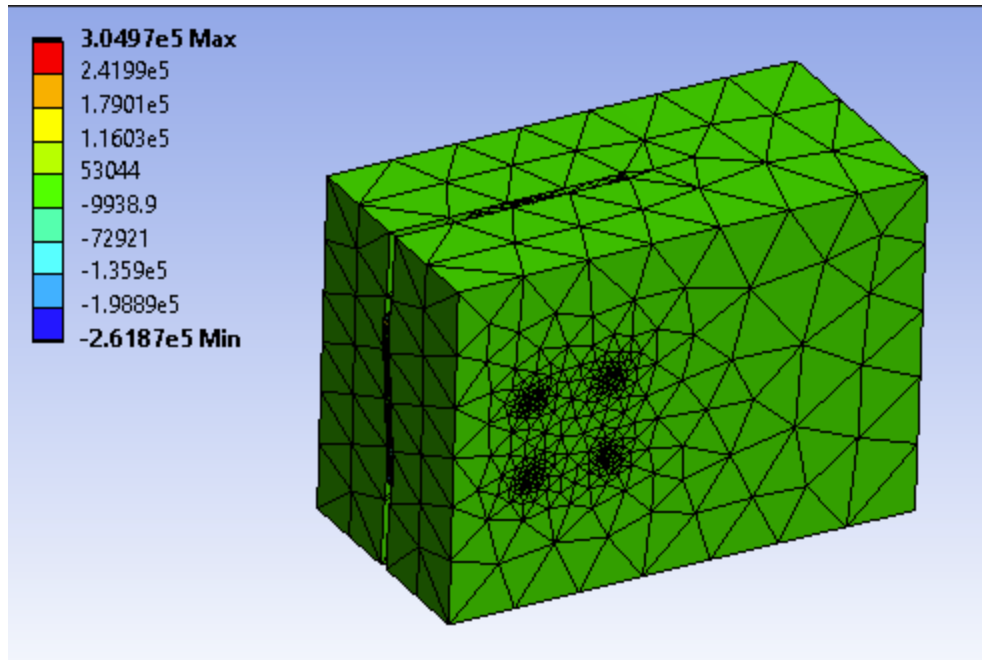


Figure 58: KPRC Normal Stress Concentration Isometric View at 30 kip.

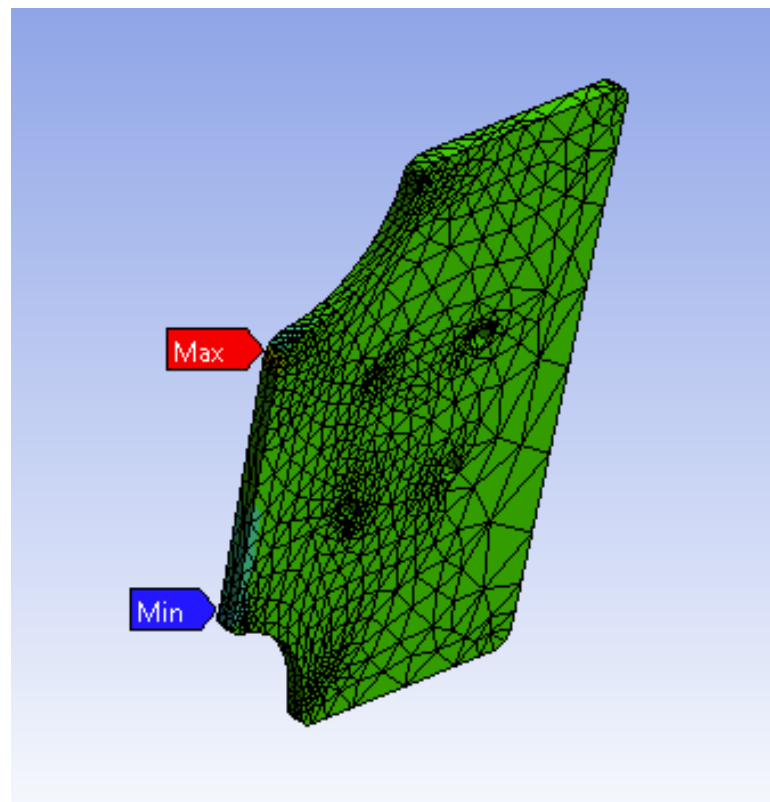


Figure 59: KPRC Steel Component Maximum and Minimum Normal Stress Concentration.

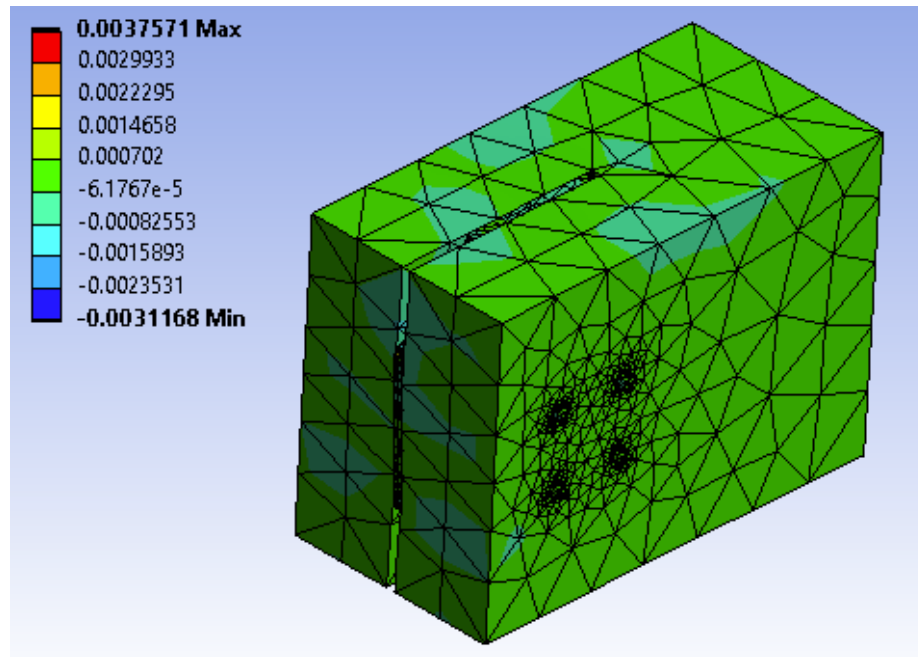


Figure 60: KPRC Strain Concentration Isometric View at 30 kip.

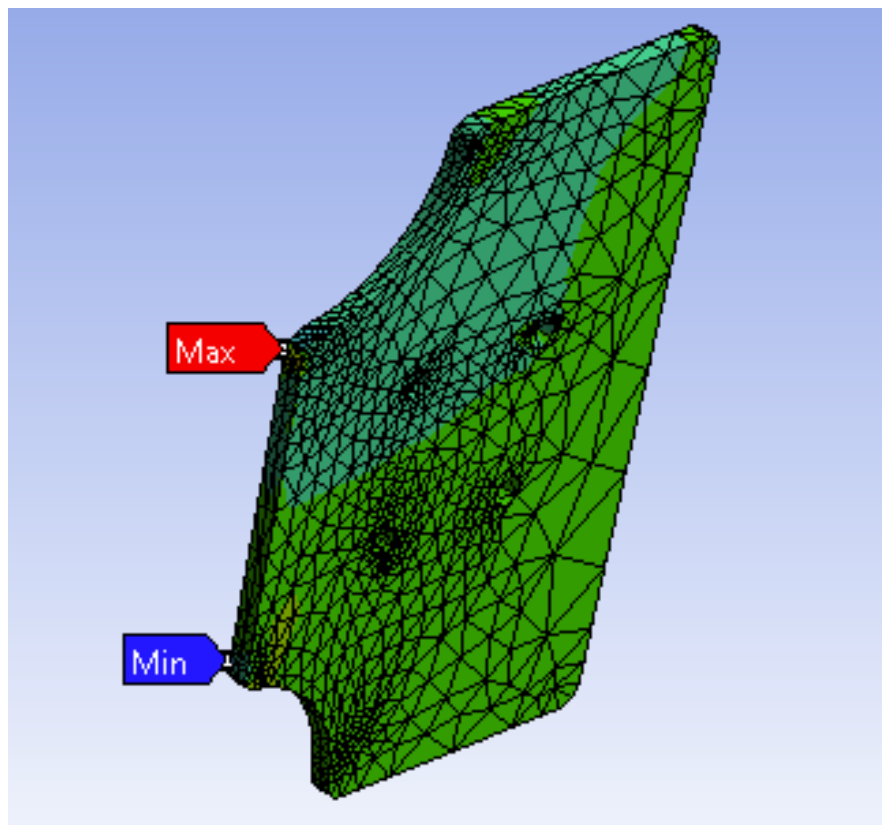
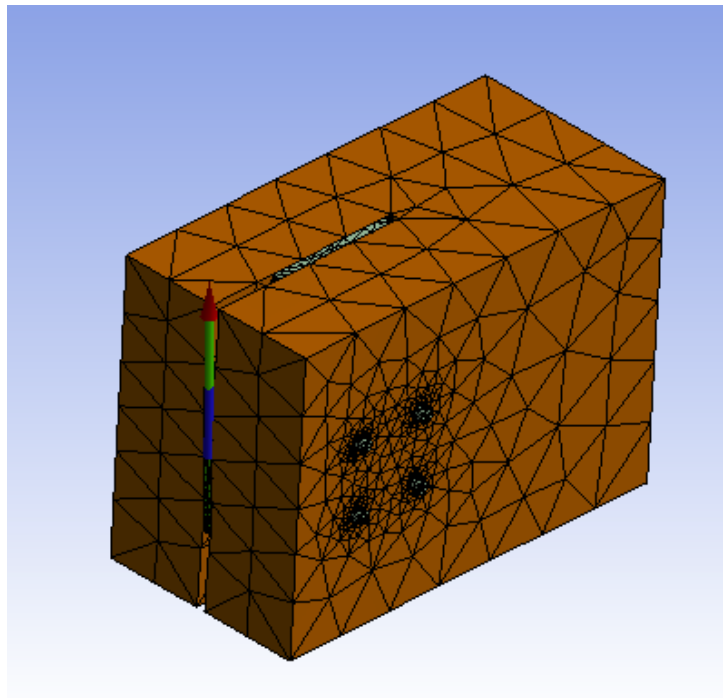


Figure 61: KPRC Steel Component Maximum and Minimum Strain Concentration.

#### 4.3.4 Force Reaction

Figure 62 shows the applied mesh and force reaction direction. The mesh applied to this connection configuration was less refined than that of the previous configurations. The element sizes are slightly larger, which may lead to slightly less accurate results. However, the concentration around the bolt holes and plate edge are higher than the rest of the model, which is where most of the analysis is concentrated on.



**Figure 62: Force Reaction and Applied Mesh for KPRC Connection.**

The results for the force reaction from the KPRC connection analysis are shown in Table 5. This table shows the reaction force present at the fixed boundary condition at each of the time intervals. As mentioned in preceding sections, the fixed boundary condition was placed at the interface between the shear wall and connection, shown in Figure 21. ANSYS ® records the values in all three directions. These data will be used to



create the force versus displacement graph that shows the connection changing from an elastic state to a plastic state.

**Table 5: Force Reaction Results from ANSYS ® Run for the KPRC Connection Configuration.**

Time [sec]	Force Reaction [lbf]			
	X-Dir.	Y-Dir.	Z-Dir.	Total
1	0.0679	3000	-0.01808	3000
2	2.96	6000	-0.0644	6000
3	6.67	9000	5.84	9000
4	11.6	12000	-1.83	12000
5	21.2	14999	6.56	14999
5.2	29.8	15597	2.04	15997
5.4	34.1	16200	0.853	16200
5.7	37.1	17098	-0.832	17098
6	47.9	17998	0.594	17998
6.2	53.8	18588	0.413	18588
6.4	64.0	19200	-0.493	19200
6.7	78.2	20100	-1.28	20100
7	91.2	21000	-0.0905	21000
7.2	99.4	21596	1.01	21596
7.4	107	22200	-0.320	22200
7.7	118	23100	-0.531	23100
8	128	24000	-0.505	24000
8.2	136	24597	1.58	24597
8.4	145	25199	1.32	25199
8.7	158	26100	-0.260	26100
9	171	27000	-0.206	27001
9.2	180	27598	1.39	27598
9.4	190	28199	0.590	28200
9.7	205	29097	1.51	29098
10	219	29998	0.856	29998

*Note.* This table shows force reaction values in the X, Y, and Z-Dir. in pounds force (lbf). The values were recorded for the entirety of the run, seconds 1 through 10, for the KPRC connection configuration with a 30-kip force applied.

#### **4.3.5 Analysis**

The KPRC connection and the knife plate configuration were analyzed in the same way, with the same parameters. The load applied increased every second until it

reached the maximum load of 30 kips. The time steps for this model start at 1 second apart, but after 5 seconds, data are displayed every 0.2 seconds. The force is increased by 3,000 lbs. every second. Table 6 summarizes the data gathered at each time step for force reaction, deformation, stress, and strain for the full 10 seconds of run time.

**Table 6: Results from ANSYS ® Run for the KPRC Connection Configuration up to 10 Seconds.**

<b>Time [sec]</b>	<b>Force Reaction [lbf] Y-Dir.</b>	<b>Displacement [in] Y-Dir.</b>	<b>Normal Stress [psi]</b>	<b>Elastic Strain</b>
1	3000	0.0175	13971	0.000198
2	6000	0.0351	22664	0.000368
3	9000	0.0537	32320	0.000546
4	12000	0.0751	40770	0.000592
5	14999	0.104	50846	0.000687
5.2	15597	0.112	53882	0.000714
5.4	16200	0.122	57294	0.000740
5.7	17098	0.141	63712	0.000779
6	17998	0.170	71148	0.000868
6.2	18588	0.192	75495	0.000949
6.4	19200	0.217	82066	0.00102
6.7	20100	0.259	92862	0.00108
7	21000	0.303	105520	0.00119
7.2	21596	0.335	115020	0.00130
7.4	22200	0.367	125410	0.00143
7.7	23100	0.416	142460	0.00164
8	24000	0.466	160880	0.00187
8.2	24597	0.500	173650	0.00204
8.4	25199	0.534	186860	0.00221
8.7	26100	0.585	207470	0.00248
9	27000	0.638	228830	0.00275
9.2	27598	0.673	243440	0.00295
9.4	28199	0.708	258400	0.00314
9.7	29097	0.761	281390	0.00345
10	29998	0.815	304970	0.00376

*Note.* This table shows deformation, force, stress, and strain values for seconds 1 through 10 from the ANSYS analysis report for the KPRC configuration with a 30-kip force applied.

The data from Table 6 were used to plot the force versus displacement graph in Figure 63 and the stress strain curve in Figure 64. The force versus displacement backbone curve shows the nonlinear behavior of the material. The stress strain curve can tell a lot of different capacity limits for a material, as discussed in the preceding sections. Those points are labeled on the curve as well.

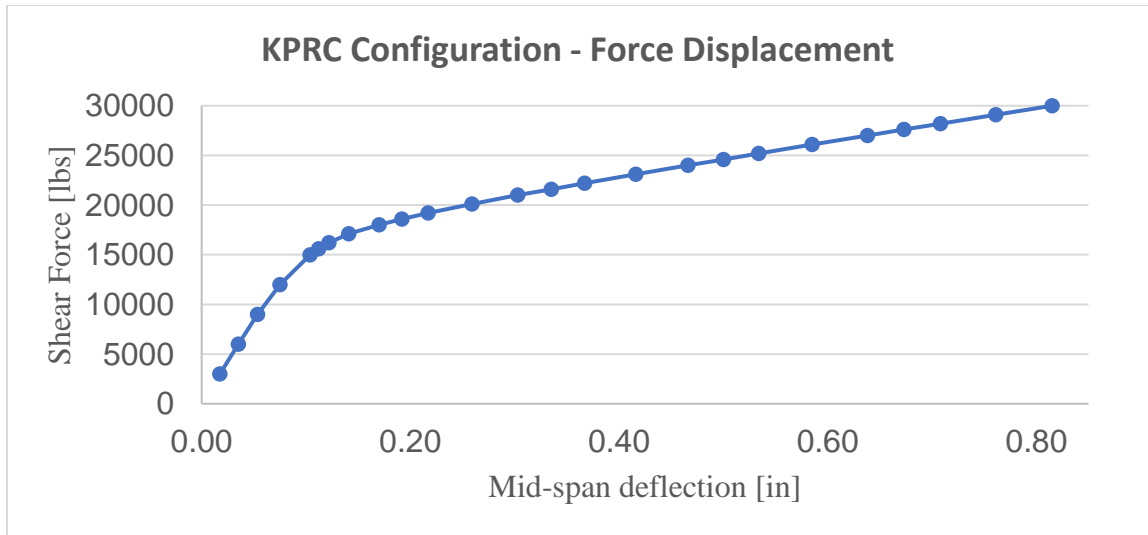


**Figure 63: Force versus Displacement Plot for KPRC Connection.**

As seen in Figure 63, the graph begins to show nonlinear behavior around 16 kips. This point is around 5.2 seconds into the 10 second test.

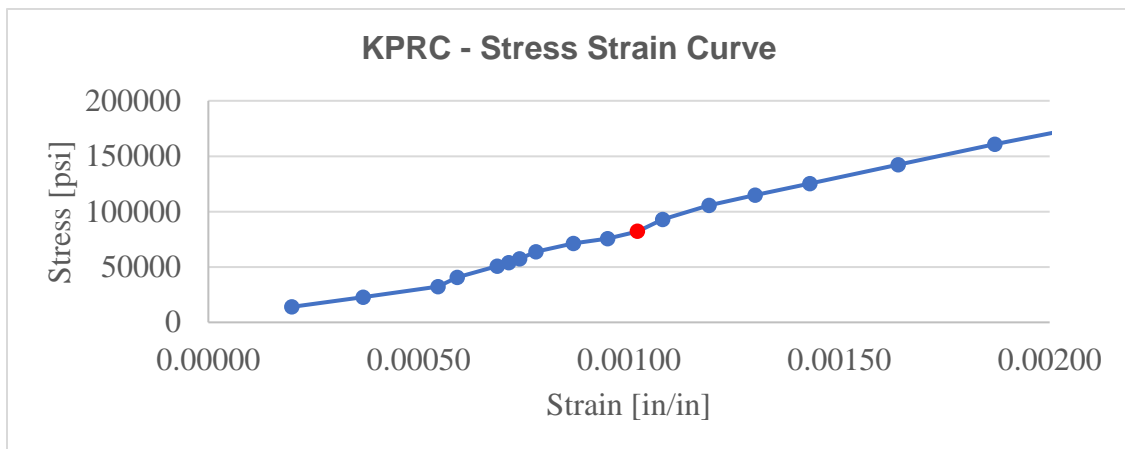


**Figure 64: Stress Strain Curve KPRC Connection.**

Figure 64 shows the stress strain curve for the KPRC configuration. As noted by the red marker, the graph first begins to yield at normal stress of 82,000 psi and a strain value of 0.00102.

#### **4.4 Accuracy**

It is important during any analysis to verify the accuracy of the results. There are several diverse ways to verify the results for this project. A more conceptual approach for verification was to look at how the model deformed and where the stress concentrations were in comparison to how the system was assumed to behave. Preliminary calculations were done to understand basic capacities of the connection but were not adjusted after the simulations had been run. In addition, ANSYS ® provides its own means of proving accuracy by using the convergence criteria after each run. If the numerical values did not converge, the test was re-run for as many iterations as it took to make the model converge. After each run, the solution output creates force convergence graphs, shown in Figure 65 from the I-shape model and Figure 66 from the knife plate model. The plot is complicated to look at and has several different lines and colors within it. A high-level explanation of how to read them is that when the purple line reaches above the teal line, convergence criteria has been met. When this happens, the user can be confident that the results of the test are accurate.

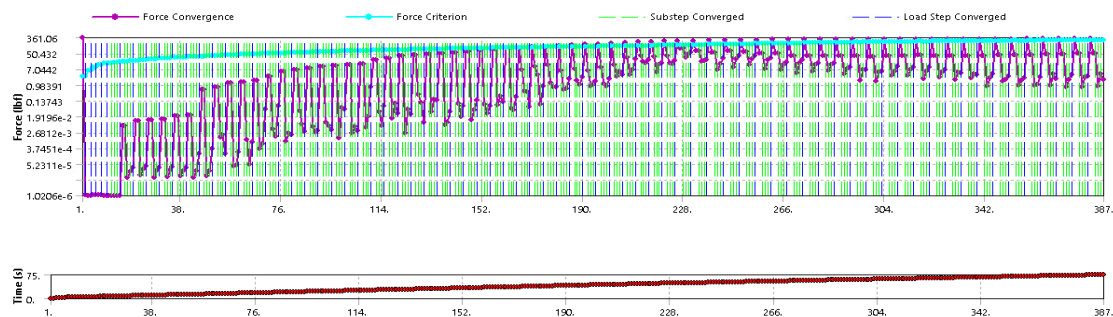


**Figure 65: Force Convergence Plot for I-Shape.**

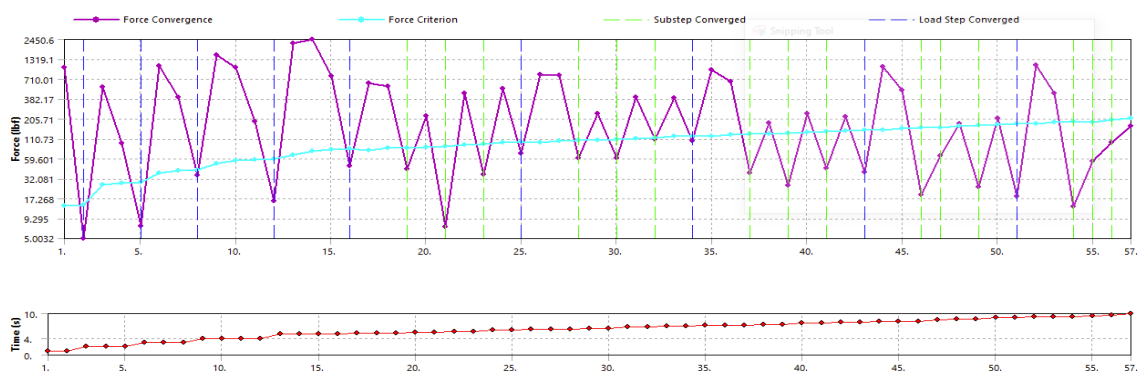


**Figure 66: Force Convergence Plot for Knife Plate.**

## Chapter 5: Conclusions and Recommendations

### 5.1 Summary Values

This portion of the report is for the purpose of summarizing the key values recorded after the simulations of each model was conducted for this project. Table 7 shows the values that were deemed important after testing was completed. There were various parameters being measured and recorded for both connection configurations. The results were plotted on graphs that were used to determine the yield point of the connection and create a nonlinear backbone curve for each connection.

**Table 7: Summary Values from ANSYS ® Runs for Both Knife Plate Connection Configurations.**

Element	Force [kip]	Total Time [sec]	Max Stress [psi]	Values at Yield Point				
				Force [kip]	Time [sec]	Total Def. [in]	Directional Def. [in]	Equivalent Stress [psi]
Knife Plate	50	10	47,854	27	5.4	0.140	0.124	37,412
KPRC	30	10	60,319	15	5.2	0.123	0.112	38,347

*Note.* This table shows force, time, max stress, max deformation, and yield point information for both iterations of the knife plate connection configurations modeled during this capstone project.

### 5.2 Conclusion

The research and testing for this capstone project was conducted for the purpose of bridging the gap of knowledge on how to design a mass timber coupling beam to be used in mid- to high-rise structures. Current practices at the time of this project primarily utilize steel and concrete, or a combination of the two, when designing coupling beams for shear walls. These coupling beams help increase the capacity of shear walls to be able to withstand higher lateral forces, which are seen in taller structures. Mass timber is

becoming increasingly more popular in design. So, conducting more research into potential innovative designs of mass timber coupling beams can aid in the ability to have mid- to high-rises built completely out of mass timber. The proposed materials for this research are nonlinear structural steel and cross-laminated timber.

In addition to the design, analysis was conducted to determine the strength of a hybrid connection element using ANSYS® Workbench 2020 (R2) software. Using this software allowed for a nonlinear finite element analysis to be conducted on three hybrid connection configurations. These three connections were labeled the I-shape connection, knife plate connection, and knife plate with reduced cross section connection as shown in Figure 12, Figure 13, and Figure 14, respectively. There were several criteria recorded from the ANSYS® reports: von Mises stress, total deformation, directional deformation, normal stress, elastic strain, and force reaction. See Appendix B for the connections' complete reports. After obtaining the data from ANSYS®, it was put together in various tables to show the data. These tables were used to plot the force versus deformation and stress strain curves presented in Figure 45 and Figure 63. These graphs were constructed at various forces to create a nonlinear curve. The I-shape connection ended with a force that was a larger capacity than what the mass timber coupling beam could withstand. The knife plate connection and KPRC connection ended with a force of 50,000., and 30,000 lbs., respectively. The summary table, Table 7, shows the various values at the yield point of each connection. The maximum stress at yield point for the knife plate connections is 37,412 psi and knife plate with reduced cross section is 38,347. The forces at yield point, where the curve first showed signs of being nonlinear, are 27,000 lbs., and 15,600 lbs. for the knife plate connection iterations. The maximum deformations for the knife plate

model are 0.140 inches for total deformation and 0.124 inches for Y-directional deformation at yield point. The maximum deformations for the knife plate with reduced cross section model are 0.123 inches for total deformation and 0.112 inches for Y-directional deformation at yield point. These values represent the capacities of each connection under the loading condition where a shear force is applied at the midspan of the CLT beam.

### **5.3 Future Research**

Looking toward what can be done after the completion of this project, there are several options that can be investigated and evaluated moving forward. There are a few other iterations of the hybrid steel-timber connection that were discussed or modeled but not evaluated, due to a lack of time or computing power available. The time it took to run through the iterative process of finding the load that would get the model to produce a nonlinear force versus displacement curve was long, in conjunction with the fact that the ANSYS ® models took hours for each run and multiple runs to reach convergence. Using the computing capacity of ROSIE, MSOE's supercomputer, would significantly decrease the amount of time to finish the simulations of each connection configuration and make future testing more feasible.

An additional future step with the current configurations would be to perform additional hand calculations to verify capacities using the NDS and AISC codes. The end goal of this project is to put together design guide focused on mass timber coupling beams in mid- to high-rise structures. Using the information gathered from this research and future testing of additional configurations can help accomplish that goal, with the hopes of eventually implementing these designs in mass timber construction projects.



## References

- Ansys® Workbench, R2. (2020). ANSYS, Inc.
- Dowden, D. M., & Tatar, A. (2019). Seismically resilient self-centering cross-laminated rocking walls with coupling beams. *Structures Congress 2019*, 151-161.  
<https://doi.org/10.1061/9780784482223.015>
- Falk, M. (2020). Cross laminated timber shear wall connections for seismic applications [Master's thesis, Kansas State University]. K-State Electronic Theses, Dissertations, and Reports: 2004. <https://hdl.handle.net/2097/40569>
- Ghosh, S. (2019). Ductile coupled reinforced concrete shear walls and coupled composite steel plate shear walls as distinct seismic force-resisting the system in ASCE 7. *SEAOC Convention Proceedings*, 339-347.
- Liao, S. & Pimentel, B. (2019, January). Coupling beam types. *Structure Magazine*, 8-13.
- Park, W. & Yun, H. (2005, June). Seismic behavior of steel coupling beams linking reinforced concrete shear walls. *Engineering Structures*, 27 (7), 1024-1039.  
<https://doi.org/10.1016/j.engstruct.2005.02.013>
- Pei, S., Van de Lindt, J., Barbosa, A., Berman, J. Biomgren, Dolan, J., Dolan, J., McDonnell, E., Zimmerman, R., & Fragiaco, M. (2018). Full-scale shake table test of a two-story mass-timber building with resilient rocking walls. *16<sup>th</sup> European Conference on Earthquake Engineering*, 1-10.
- Tassios, T., Moritti, M. & Bezas, A. (1996, November). On the behavior and ductility of reinforced concrete coupling beams of shear walls. *Structural Journal*, 93 (6), 711-720.

## **Appendix A**

### **Reference Tables**

**Table A-1: Mechanical Material Properties for CLT.**

<b>Property</b>	<b>Value</b>	<b>Unit</b>	<b>Source</b>
			<a href="https://forum.ansys.com/discussion/19957/glulam-beam">https://forum.ansys.com/discussion/19957/glulam-beam</a>
Density	0.0191	lb./in <sup>3</sup>	<a href="https://www.glued-laminated-timber.com/glued-laminated-timber/glued-laminated-timber-made-of-beech-and-hybrid-beams-made-of-beech/spruce/strength-classes/mn_44339">https://www.glued-laminated-timber.com/glued-laminated-timber/glued-laminated-timber-made-of-beech-and-hybrid-beams-made-of-beech/spruce/strength-classes/mn_44339</a>
Thermal Expansion	1.47	R-value/in	<a href="https://www.apawood.org/Data/Sites/1/documents/technicalresearch/paper-2017-inter-50-12-1-in-grade-u.s.-glulams.pdf">https://www.apawood.org/Data/Sites/1/documents/technicalresearch/paper-2017-inter-50-12-1-in-grade-u.s.-glulams.pdf</a> <a href="https://www.apawood.org/Data/Sites/1/documents/technicalresearch/paper-2017-inter-50-12-1-in-grade-u.s.-glulams.pdf">https://www.apawood.org/Data/Sites/1/documents/technicalresearch/paper-2017-inter-50-12-1-in-grade-u.s.-glulams.pdf</a>
Modulus of Elasticity	1,508,320	psi	<a href="https://downloads.hindawi.com/journals/ace/2019/9495705.pdf">https://downloads.hindawi.com/journals/ace/2019/9495705.pdf</a> <a href="https://forum.ansys.com/discussion/19957/glulam-beam">https://forum.ansys.com/discussion/19957/glulam-beam</a>
			<a href="https://hal.archives-ouvertes.fr/hal-00599887/document">https://hal.archives-ouvertes.fr/hal-00599887/document</a>
Tensile Yield Strength	2,445	psi	<a href="https://downloads.hindawi.com/journals/ace/2019/9495705.pdf">https://downloads.hindawi.com/journals/ace/2019/9495705.pdf</a> <a href="https://jwoodscience.springeropen.com/articles/10.1007/s10086-010-1127-0">https://jwoodscience.springeropen.com/articles/10.1007/s10086-010-1127-0</a>
Tensile Ultimate Strength	2,445	psi	<a href="https://forum.ansys.com/discussion/19957/glulam-beam">https://forum.ansys.com/discussion/19957/glulam-beam</a>

*Note.* This table shows the different reference values obtained from a combination of outside sources, averaged, and utilized in creating the CLT material type in ANSYS ®.

**Table A-2: Mechanical Material Properties for Bolts.**

<b>Property</b>	<b>Value</b>	<b>Unit</b>	<b>Source</b>
Modulus of Elasticity	29000000	0 psi	AISC Steel Manual <a href="https://www.portlandbolt.com/technical/faqs/a325a490-thread/">https://www.portlandbolt.com/technical/faqs/a325a490-thread/</a>  <a href="https://www.atlrod.com/astm-a325-bolts/">https://www.atlrod.com/astm-a325-bolts/</a>
Tensile Yield Strength	92	psi	<a href="https://www.fastenal.com/en/79/structural-bolts">https://www.fastenal.com/en/79/structural-bolts</a> <a href="https://www.portlandbolt.com/technical/faqs/a325a490-thread/">https://www.portlandbolt.com/technical/faqs/a325a490-thread/</a>  <a href="https://www.atlrod.com/astm-a325-bolts/">https://www.atlrod.com/astm-a325-bolts/</a>
Tensile Ultimate Strength	120	psi	<a href="https://www.fastenal.com/en/79/structural-bolts">https://www.fastenal.com/en/79/structural-bolts</a>

*Note.* This table shows the different reference values obtained from a combination of outside sources, averaged, and utilized in creating the nonlinear stainless steel bolt material type in ANSYS ®.

## **Appendix B**

### **Calculations and ANSYS® Reports**

## Augustine Capstone Steel Connection Design V1

### Givens:

$$V := 10 \text{ kip} \quad \phi := 0.75$$

$$L := 4 \text{ ft}$$

#### *Bolt Information:*

$$\begin{aligned} & \text{A325} \quad l := 1.5 \text{ in} \\ & \text{Type N} \\ & \text{STD} \quad d_b := \frac{3}{4} \text{ in} \end{aligned}$$

#### *Weld Information:*

$$\begin{aligned} & \text{E70} \\ & d_{\text{weld}} := \frac{3}{16} \text{ in} \\ & l_{\text{weld}} := 6 \text{ in} \end{aligned}$$

#### *Plate Information:*

$$\begin{aligned} & l_{\text{SWp}} := 26 \text{ in} \quad w_{\text{plate}} := 12 \text{ in} \\ & l_{\text{CLTp}} := 12 \text{ in} \quad t_{\text{plate}} := \frac{1}{2} \text{ in} \\ & F_u := 58 \text{ ksi} \\ & F_y := 36 \text{ ksi} \end{aligned}$$

### Bolt Spacing and Edge Distance:

$$\begin{aligned} s &:= 2 \text{ in} \\ \frac{8}{3} \cdot d_b &= 2 \cdot \text{in} \quad [AISC, J3.3] \end{aligned}$$

$$12 \cdot t_{\text{plate}} = 6 \cdot \text{in} \quad [AISC, J3.5]$$

$$s_{\min} > \frac{8}{3} d_b \quad OK$$

$$s_{\max} < 12 t_{\text{plate}} \quad OK$$

$$d_{\text{edge}} := 2 \text{ in}$$

$$d_{\text{edge.min}} > 1 \text{ in} \quad OK \quad [AISC, Table J3.4]$$

$$24 t_{\text{plate}} = 12 \cdot \text{in} \quad [AISC, J3.5]$$

$$d_{\text{edge.max}} < 24 t_{\text{plate}} \quad OK$$

### Bolt Strength:

#### *Shear:*

$$\phi F_{nv} := 40.5 \text{ kip} \quad [AISC, Table 7-1]$$

$$\phi r_{nv} := 17.9 \text{ kip} \quad [AISC, Table 7-1]$$

$$\phi R_{n4} := \phi r_{nv} \cdot 4 = 72 \cdot \text{kip}$$

#### *Tension:*

$$\phi F_{nt} := 67.5 \text{ kip} \quad [AISC, Table 7-2]$$

$$\phi r_{nt} := 39.8 \text{ kip} \quad [AISC, Table 7-2]$$

$$\phi R_{n4} := \phi r_{nt} \cdot 4 = 159 \cdot \text{kip}$$

### Bolt Bearing and Tearout

#### *Based on Bolt Spacing:*

$$\phi r_{n1} := 62 \frac{\text{kip}}{\text{in}} \quad [AISC, Table 7-4]$$

$$\phi r_{ns} := \phi r_{n1} \cdot t_{\text{plate}} = 31 \cdot \text{kip}$$

$$\phi R_{n2} := \phi r_{ns} \cdot 2 = 62 \cdot \text{kip}$$

#### *Based on Edge Distance:*

$$\phi r_{n2} := 78.3 \frac{\text{kip}}{\text{in}} \quad [AISC, Table 7-4]$$

$$\phi r_{ne} := \phi r_{n2} \cdot t_{\text{plate}} = 39.1 \cdot \text{kip}$$

$$\phi R_{n2} := \phi r_{ne} \cdot 2 = 78 \cdot \text{kip}$$

### Bolt Shear Yielding and Rupture

#### *Block Shear Shear Yielding:*

$$\phi r_{n11} := 81 \frac{\text{kip}}{\text{in}} \quad [AISC, Table 9-3b, n = 2]$$

$$\phi r_{n21} := \phi r_{n11} \cdot t_{\text{plate}} = 40.5 \cdot \text{kip}$$

$$\phi R_{n2} := \phi r_{n21} \cdot 2 = 81 \cdot \text{kip}$$

#### *Block Shear Shear Rupture*

$$\phi r_{n22} := 96.2 \frac{\text{kip}}{\text{in}} \quad [AISC, Table 9-3c, n = 2]$$

$$\phi r_{n23} := \phi r_{n22} \cdot t_{\text{plate}} = 48.1 \cdot \text{kip}$$

$$\phi R_{n2} := \phi r_{n23} \cdot 2 = 96 \cdot \text{kip}$$

Weld Size and Shear Capacity:

$$s_{w.min} := \frac{3}{16} \text{ in } \quad OK \quad [AISC, Table J2.4]$$

$$F_{exx} := 70 \text{ ksi}$$

$$D := 3 \text{ in}$$

$$\phi r_n := \phi \cdot 0.60 \cdot F_{exx} \cdot \frac{\sqrt{2}}{2} \cdot \frac{D}{16} \cdot l_{weld} = 25.1 \cdot \text{kip} \quad [AISC, Eq. J8-1]$$

Rupture at Welds:

$$t_{min} := \frac{0.6 \cdot F_{exx} \cdot \left( \frac{\sqrt{2}}{2} \right) \cdot \left( \frac{D}{16} \right)}{0.6 \cdot F_u} = 0.16 \cdot \text{in} \quad [AISC, Eq. J9-2]$$

$$t_{plate} > t_{min} \quad OK$$

Summary:

Number of Bolts	Limit State	Strength [kip]
2	Shear Strength	72
	Tensile Strength	159
	Bearing (space)	62
	Bearing (edge)	78
	Shear Yielding	81
	Shear Rupture	96
Weld	Shear	25

## Augustine Capstone Calculations Connection Configurations

### 1. Bending and Shear Capacity of Steel

$$F_y := 36 \text{ ksi}$$

$$L_{CLT} := 4 \text{ ft}$$

*I-shape*

$$t_{IS} := 0.5 \text{ in}$$

$$h_{IS} := 18 \text{ in}$$

$$A_{IS} := t_{IS} \cdot h_{IS} = 9 \text{ in}^2$$

$$Z_{IS} := \frac{t_{IS} \cdot h_{IS}^2}{4} = 40.5 \text{ in}^3$$

$$V_{maxIS} := 0.6 \cdot F_y \cdot A_{IS} = 194 \text{ kip}$$

$$M_{pIS} := Z_{IS} \cdot F_y = 122 \text{ kip} \cdot \text{ft}$$

$$V_{pIS} := \frac{M_{pIS} \cdot 2}{L_{CLT}} = 60.8 \text{ kip}$$

*Knife Plate*

$$t_{KP} := 0.25 \text{ in} \quad d_b := \frac{3}{4} \text{ in}$$

$$h_{KP} := 17 \text{ in} - (2 \cdot d_b) = 15.5 \text{ in}$$

$$l_{KP} := 12 \text{ in}$$

$$A_{KP} := t_{KP} \cdot h_{KP} = 3.875 \text{ in}^2$$

$$Z_{KP} := \frac{t_{KP} \cdot h_{KP}^2}{4} = 15 \text{ in}^3$$

$$V_{maxKP} := 0.6 \cdot F_y \cdot A_{KP} = 84 \text{ kip}$$

$$M_{pKP} := Z_{KP} \cdot F_y = 45 \text{ kip} \cdot \text{ft}$$

$$V_{pKP} := \frac{M_{pKP} \cdot 2}{L_{CLT}} = 22.5 \text{ kip}$$

*Knife Plate - Reduced Cross Section*

$$t_{KPRC} := 0.5 \text{ in}$$

$$h_{KPRC} := 8 \text{ in}$$

$$l_{KPRC} := 12 \text{ in}$$

$$A_{KPRC} := t_{KPRC} \cdot h_{KPRC} = 4 \text{ in}^2$$

$$Z_{KPRC} := \frac{t_{KPRC} \cdot h_{KPRC}^2}{4} = 8 \text{ in}^3$$

$$V_{maxKPRC} := 0.6 \cdot F_y \cdot A_{KPRC} = 86 \text{ kip}$$

$$M_{KPRC} := Z_{KPRC} \cdot F_y = 24 \text{ kip} \cdot \text{ft}$$

$$V_{KPRC} := \frac{M_{KPRC} \cdot 2}{L_{CLT}} = 12 \text{ kip}$$



## 2. Bending and Shear Capacity of CLT

Table 6.1. Estimated mean shear stress at failure (shear mode III) and evaluation of Equation (11a).

	$t_{0,k}/n_{CA,k} = t_{net,0}/n_{CA} = 30 \text{ mm}$			$t_{0,k}/n_{CA,k} = 40 \text{ mm}$		
	$\tau_{xz}$	$\tau_{xy}$	Interaction	$\tau_{xz}$	$\tau_{xy}$	Interaction
	(7) [MPa]	(10) [MPa]	(11a) [-]	(12) [MPa]	(13) [MPa]	(11a) [-]
Test series C	0.60	1.49	0.83	0.79	1.99	1.10
Test series E	0.78	1.95	1.08	1.04	2.60	1.44

[Taken from In-place loaded CLT beams - Test and analysis of element lay-up, Table 6-1]

$$W := 12 \text{ in}$$

$$H := 17 \text{ in}$$

$$L := 4 \text{ ft}$$

$$\sigma := \frac{0.79 \text{ MPa} + 1.04 \text{ MPa}}{2} = 0.133 \text{ ksi}$$

$$V_{CLT} := \sigma \cdot (W - t_{KP}) \cdot H = 26.5 \text{ kip}$$

$$M_{CLT} := V_{CLT} \cdot \frac{L}{2} = 53 \text{ kip} \cdot \text{ft}$$

CLT shear capacity is greater than the capacity of the knife plate with and without the reduced cross section, but less than the capacity of the I-shape. The goal of these connections are to have the steel yield prior to the CLT. Therefore, the I-Shape values are NG and the KP and KPRC values are OK.

## 3. Shear Capacity of Bolts

$$d_b := \frac{3}{4} \text{ in}$$

A325, Type N, STD Bolts

4 - Bolts

$$\phi r_{nv} := 17.9 \text{ kip} \quad [\text{AISC, Table 7-1}]$$

$$n := 4$$

$$\phi R_{nv} := \phi r_{nv} \cdot n = 71.6 \text{ kip}$$

6 - Bolts

$$\phi r_{nv} := 17.9 \text{ kip}$$

$$n := 6$$

$$\phi R_{nv} := \phi r_{nv} \cdot n = 107 \text{ kip}$$

Bolt shear capacity is greater than the capacity of the knife plate and CLT. Therefore, the values are OK.

#### 4. Bearing Capacity of CLT at Bolt Interface

4 - Bolts

$$n := 4$$

$$V := V_{CLT} = 26.5 \text{ kip}$$

$$F := \frac{6 \cdot V}{\sqrt{2}} = 112 \text{ kip}$$

$$A_{hole} := \frac{W - t_{KP}}{2} \cdot d_b = 4.41 \text{ in}^2$$

$$V_{hole} := \frac{V}{2n} + \frac{F}{2} = 59.5 \text{ kip}$$

$$\sigma_{bearing} := \frac{V_{hole}}{A_{hole}} = 13.5 \text{ ksi}$$

6 - Bolts

$$n := 6$$

$$V := V_{CLT} = 26.5 \text{ kip}$$

$$F := \frac{6 \cdot V}{\sqrt{2}} = 112 \text{ kip}$$

$$A_{hole} := \frac{W - t_{KP}}{2} \cdot d_b = 4.41 \text{ in}^2$$

$$V_{hole} := \frac{V}{2n} + \frac{F}{2} = 58.4 \text{ kip}$$

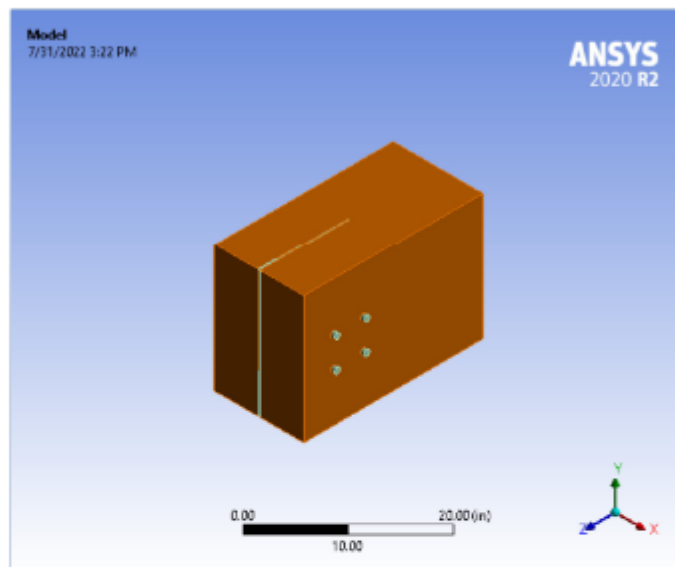
$$\sigma_{bearing} := \frac{V_{hole}}{A_{hole}} = 13.3 \text{ ksi}$$

Bearing capacity at bolt interface is greater than the capacity CLT. Therefore, the values are OK.



## Project

First Saved	Thursday, January 20, 2022
Last Saved	Sunday, July 31, 2022
Product Version	2020 R2
Save Project Before Solution	No
Save Project After Solution	No



## Contents

- [Units](#)
- [Model \(A4\)](#)
  - [Geometry](#)
    - [Parts](#)
  - [Materials](#)
  - [Coordinate Systems](#)
  - [Connections](#)
    - [Contacts](#)
    - [Contact Regions](#)
  - [Mesh](#)
    - [Mesh Controls](#)
  - [Static Structural \(A6\)](#)
    - [Analysis Settings](#)
    - [Loads](#)
    - [Solution \(A6\)](#)
      - [Solution Information](#)
      - [Results](#)
        - [Convergence](#)
      - [Force Reaction](#)
- [Material Data](#)
  - [C/T](#)
  - [Structural Steel NL - I-Shape](#)
  - [Structural Steel NL - Bolts](#)

## Units

TABLE 1

Unit System	U.S. Customary (in, lbm, lbf, s, V, A) Degrees rad/s Fahrenheit
Angle	Degrees
Rotational Velocity	rad/s
Temperature	Fahrenheit

## Model (A4)

### Geometry

TABLE 2  
Model (A4) > Geometry

Object Name	Geometry
State	Fully Defined
<b>Definition</b>	
Source	C:\Users\krysczlopi\z\Desktop\KJA - Capstone\KPI\Knife Plate Converged 30KIP_files\dp0\SYS\DM\SYS.scdoc
Type	SpaceClaim
Length Unit	Meters
Element Control	Program Controlled
Display Style	Material
<b>Bounding Box</b>	
Length X	13. in
Length Y	17. in
Length Z	24. in
<b>Properties</b>	
Volume	4897.8 in <sup>3</sup>
Mass	113.11 lbm
Scale Factor Value	1.
<b>Statistics</b>	
Bodies	6
Active Bodies	6
Nodes	101123
Elements	63428
Mesh Metric	None
<b>Update Options</b>	
Assign Default Material	No
<b>Basic Geometry Options</b>	
Solid Bodies	Yes
Surface Bodies	Yes
Line Bodies	Yes
Parameters	Independent
Parameter Key	
Attributes	Yes
Attribute Key	
Named Selections	Yes
Named Selection Key	
Material Properties	Yes
<b>Advanced Geometry Options</b>	
Use Associativity	Yes
Coordinate Systems	Yes
Coordinate System Key	

Reader Mode Saves Updated File	No
Use Instances	Yes
Smart CAD Update	Yes
Compare Parts On Update	No
Analysis Type	3-D
Mixed Import Resolution	None
Clean Bodies On Import	No
Stitch Surfaces On Import	None
Decompose Disjoint Geometry	Yes
Enclosure and Symmetry Processing	Yes

**TABLE 3**  
**Model (A4) > Geometry > Parts**

Object Name	2 Foot CLT Solid	Knife Plate Solid	Bolt_Horiz_Left 2 1 Bolt_Horiz_Left 2	Bolt_Horiz_Left 2 1 Bolt_Horiz_Left 1	Bolt_Horiz_Right 2 1 Bolt_Horiz_Right 2	Bolt_Horiz_Right 2 1 Bolt_Horiz_Right 1
State	Meshed					
Graphics Properties						
Visible	Yes					
Transparency	1					
Definition						
Suppressed	No					
Stiffness Behavior	Flexible					
Coordinate System	Default Coordinate System					
Reference Temperature	By Environment					
Treatment	None					
Material						
Assignment	CLT	Structural Steel NL - I-Shape	Structural Steel NL - Bolts			
Nonlinear Effects	Yes					
Thermal Strain Effects	Yes					
Bounding Box						
Length X	12. in	0.25 in	13. in			
Length Y	17. in		0.75 in			
Length Z	24. in	12. in	0.75 in			
Properties						
Volume	4824.2 in³	50.558 in³	5.7432 in³			
Mass	92.255 lbm	14.338 lbm	1.6288 lbm			
Centroid X	6. in					
Centroid Y	8.4996 in	8.4992 in	10.59 in	6.5901 in	10.59 in	6.5901 in
Centroid Z	-8.9104e-002 in	6. in	7.9959 in	3.9959 in		
Moment of Inertia Ip1	6660.5 lbm-in²	520.89 lbm-in²	0.11337 lbm-in²			
Moment of Inertia Ip2	5549.4 lbm-in²	173.13 lbm-in²	22.879 lbm-in²			
Moment of Inertia Ip3	3348.4 lbm-in²	347.9 lbm-in²	22.879 lbm-in²			
Statistics						
Nodes	92043	1216	1966			
Elements	61833	155	360			
Mesh Metric	None					
CAD Attributes						
PartTolerance:	0.00000001					
Color:143,175,143						

**FIGURE 1**  
**Model (A4) > Geometry > Model Isometric**

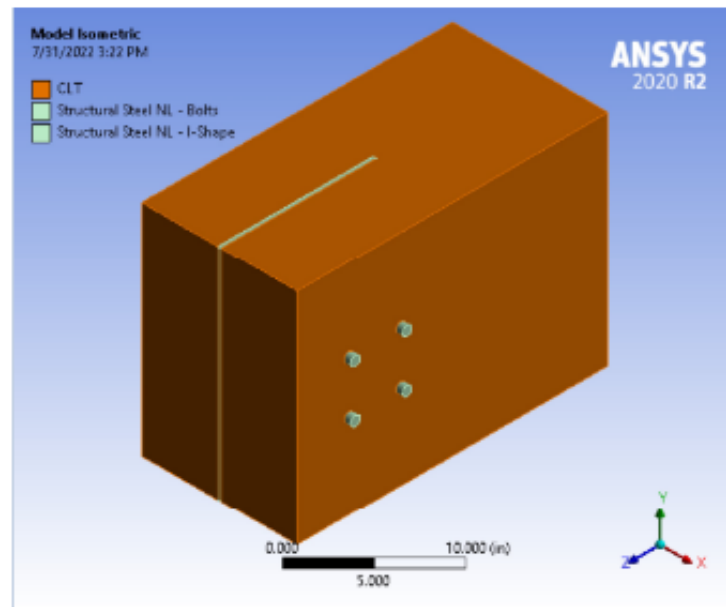


**FIGURE 2**  
Model (A4) > Geometry > ZY Face Elevation

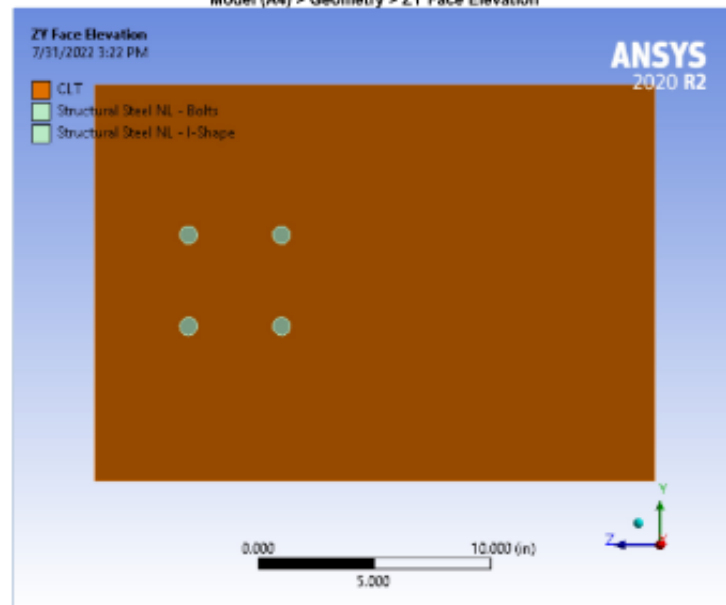


**FIGURE 3**  
Model (A4) > Geometry > XY Face Elevation

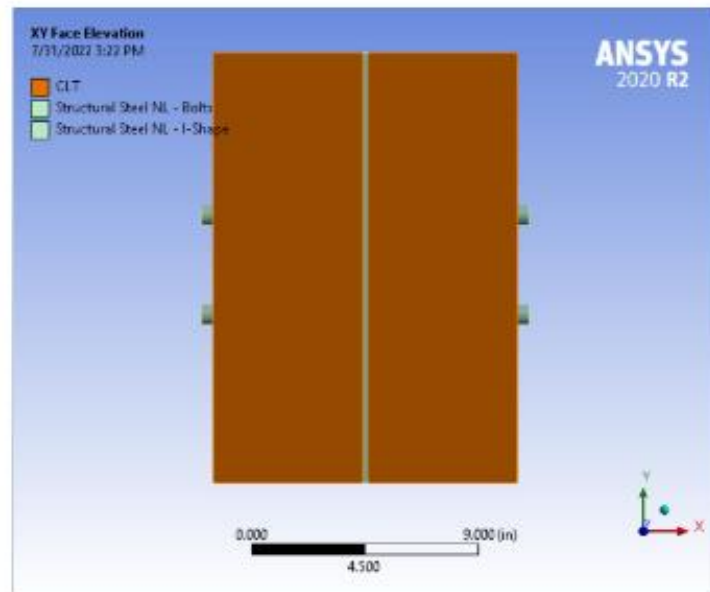


FIGURE 4  
Model (A4) > Geometry > XZ Face Elevation

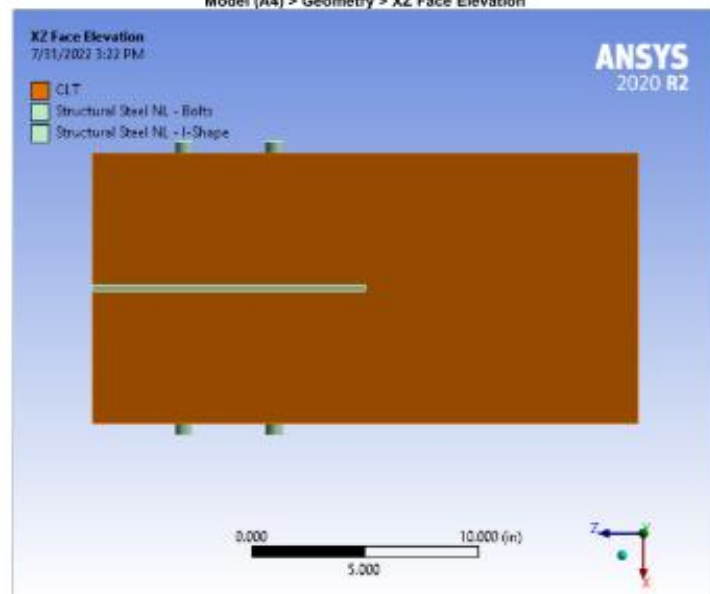


FIGURE 5  
Model (A4) > Geometry > Steel Isometric

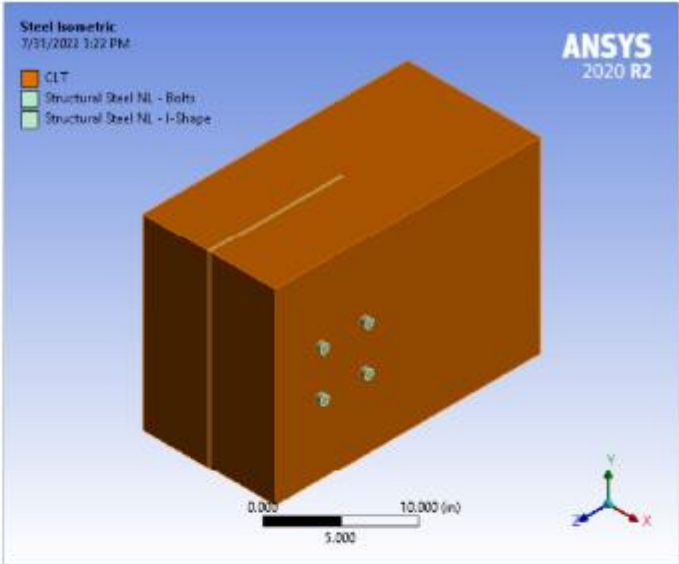


FIGURE 6  
Model (A4) > Geometry > CLT Isometric

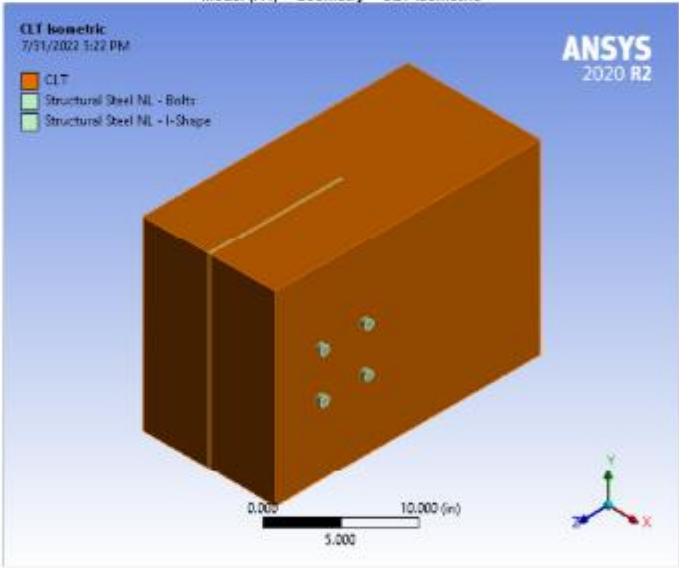


TABLE 4  
Model (A4) > Materials

Object Name	Materials
State	Fully Defined
Statistics	
Materials	5
Material Assignments	0

Coordinate Systems

TABLE 5  
Model (A4) > Coordinate Systems > Coordinate System

Object Name	Global Coordinate System
State	Fully Defined
Definition	
Type	Cartesian
Coordinate System ID	0.
Origin	
Origin X	0. in
Origin Y	0. in
Origin Z	0. in





Contact Geometry Correction	None
Target Geometry Correction	None

### Mesh

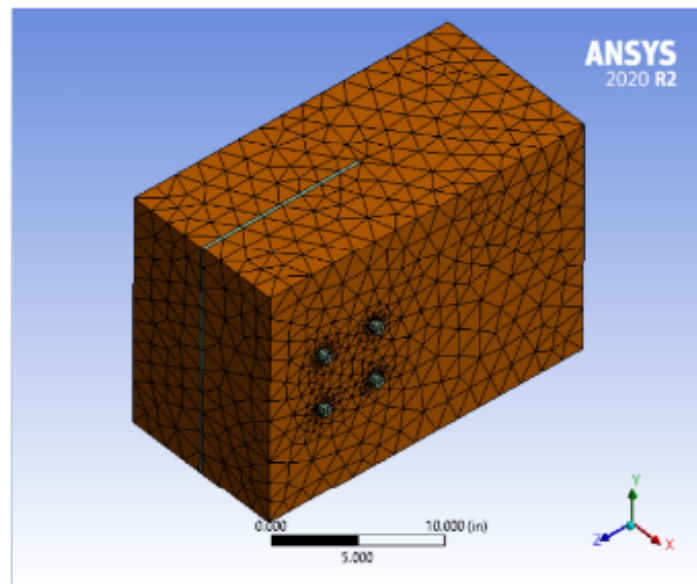
**TABLE 9**  
**Model (A4) > Mesh**

Object Name	Mesh
State	Solved
<b>Display</b>	
Display Style	Use Geometry Setting
<b>Defaults</b>	
Physics Preference	Nonlinear Mechanical
Element Order	Program Controlled
Element Size	Default (1.6078 in)
<b>Sizing</b>	
Growth Rate	1.6
Max Size	4.0 in
Mesh Defeaturing	Yes
Defeature Size	Default (8.039e-003 in)
Capture Curvature	Yes
Curvature Min Size	Default (1.6078e-002 in)
Curvature Normal Angle	Default (60.0°)
Capture Proximity	No
Bounding Box Diagonal	32.166 in
Average Surface Area	71.32 in²
Minimum Edge Length	0.25 in
<b>Quality</b>	
Check Mesh Quality	Yes, Errors
Target Skewness	Default (0.900000)
Target Jacobian Ratio (Corner Nodes)	Default (0.040000)
Mesh Metric	None
<b>Inflation</b>	
Use Automatic Inflation	None
Inflation Option	Smooth Transition
Transition Ratio	0.272
Maximum Layers	5
Growth Rate	1.2
Inflation Algorithm	Pre
View Advanced Options	No
<b>Advanced</b>	
Number of CPUs for Parallel Part Meshing	Program Controlled
Straight Sided Elements	No
Rigid Body Behavior	Dimensionally Reduced
Triangle Surface Mesher	Program Controlled
Topology Checking	Yes
Pinch Tolerance	Default (1.447e-002 in)
Generate Pinch on Refresh	No
<b>Statistics</b>	
Nodes	101123
Elements	63428

**TABLE 10**  
**Model (A4) > Mesh > Mesh Controls**

Object Name	Refinement_Bolts	Refinement_CLT	Refinement_I-Shape	Body Sizing_Bolts	Face Sizing_Bolt holes in I-Shape	Face Sizing_Bolt holes in CLT
State		Suppressed		Fully Defined	Suppressed	Fully Defined
<b>Scope</b>						
Scoping Method	Geometry Selection					
Geometry	4 Faces		No Selection	4 Bodies	No Selection	6 Faces
<b>Definition</b>						
Suppressed	Yes			No	Yes	No
Active	No, Suppressed				No, Suppressed	
Refinement	1					
Type					Element Size	
Element Size				0.3 in		0.2 in
<b>Advanced</b>						
Defeature Size					Default (8.039e-003 in)	
Behavior					Soft	
Growth Rate					Default (1.6)	
Capture Curvature					No	
Capture Proximity					No	
Influence Volume						No

**FIGURE 7**  
**Model (A4) > Mesh > Mesh Isometric**



### Static Structural (A5)

**TABLE 11**  
Model (A4) > Analysis

Object Name	Static Structural (A5)
State	Solved
<b>Definition</b>	
Physics Type	Structural
Analysis Type	Static Structural
Solver Target	Mechanical APDL
<b>Options</b>	
Environment Temperature	71.6 °F
Generate Input Only	No

**TABLE 12**  
Model (A4) > Static Structural (A5) > Analysis Settings

Object Name	Analysis Settings
State	Fully Defined
<b>Step Controls</b>	
Number Of Steps	10
Current Step Number	10
Step End Time	10. s
Auto Time Stepping	Program Controlled
<b>Solver Controls</b>	
Solver Type	Direct
Weak Springs	Off
Solver Pivot Checking	Program Controlled
Large Deflection	Off
Inertia Relief	Off
Quasi-Static Solution	Off
<b>Rotordynamics Controls</b>	
Coriolis Effect	Off
<b>Restart Controls</b>	
Generate Restart Points	Program Controlled
Retain Files After Full Solve	No
Combine Restart Files	Program Controlled
<b>Nonlinear Controls</b>	
Newton-Raphson Option	Program Controlled
Force Convergence	Program Controlled
Moment Convergence	Program Controlled
Displacement Convergence	Program Controlled
Rotation Convergence	Program Controlled
Line Search	Program Controlled
Stabilization	Program Controlled
<b>Advanced</b>	
Inverse Option	No
Contact Split (DMP)	Off
<b>Output Controls</b>	
Stress	Yes
Surface Stress	No
Back Stress	No
Strain	Yes
Contact Data	Yes

Nonlinear Data	No
Nodal Forces	No
Volume and Energy	Yes
Euler Angles	Yes
General Miscellaneous	No
Contact Miscellaneous	No
Store Results At	All Time Points
Result File Compression	Program Controlled
<b>Analysis Data Management</b>	
Solver Files Directory	C:\Users\krystopikz\Desktop\KJA - Capstone\Appendix\Knife Plate Converged 50KIP_files\dp0\SYSMECH\
Future Analysis	None
Scratch Solver Files Directory	
Save MAPDL db	No
Contact Summary	Program Controlled
Delete Unneeded Files	Yes
Nonlinear Solution	Yes
Solver Units	Active System
Solver Unit System	Bin

**TABLE 13**  
Model (A4) > Static Structural (A5) > Analysis Settings  
Step-Specific "Step Controls"

Step	Step End Time	Auto Time Stepping	Define By	Initial Substeps	Minimum Substeps	Maximum Substeps	Carry Over Time Step
1	1. s	On	Substeps	1.	1.	10.	Off
2	2. s						
3	3. s						
4	4. s						
5	5. s						
6	6. s	Program Controlled					
7	7. s						
8	8. s						
9	9. s						
10	10. s						

**TABLE 14**  
Model (A4) > Static Structural (A5) > Loads

Model (A4) > Static Structural (A5) > Loads			
Object Name	Fixed Support i-Shape	Force	Displacement
State	Fully Defined		
Scope			
Scoping Method	Geometry Selection		
Geometry	1 Face		8 Faces
Definition			
Type	Fixed Support	Force	Displacement
Suppressed	No		
Define By	Components		
Applied By	Surface Effect		
Coordinate System	Global Coordinate System		
X Component	0. lbf (ramped)		0. in (ramped)
Y Component	Tabular Data		Free
Z Component	0. lbf (ramped)		Free
Tabular Data			
Independent Variable	Time		

**FIGURE 8**  
Model (A4) > Static Structural (A5) > Force

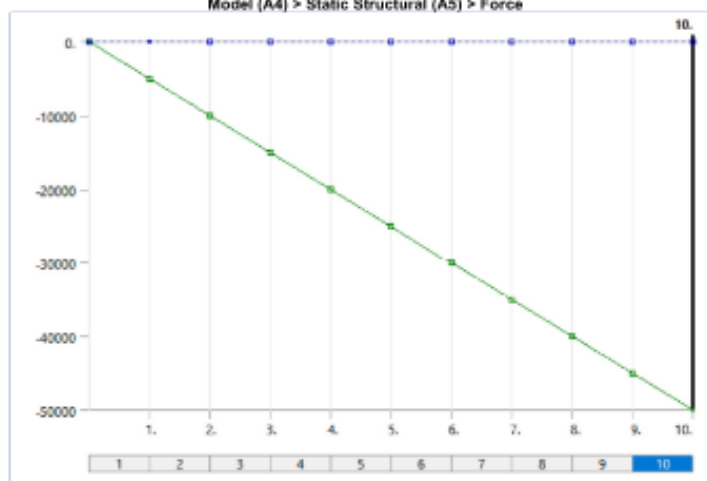


**TABLE 15**  
Model (A4) > Static Structural (A5) > Force

Steps	Time (s)	X (lbf)	Y (lbf)	Z (lbf)
1	0.	= 0.	0.	= 0.
	1.	0.	= -5000.	0.

2	2.	= -10000
3	3.	= -15000
4	4.	= -20000
5	5.	= -25000
6	6.	= -30000
7	7.	= -35000
8	8.	= -40000
9	9.	= -45000
10	10.	= -50000

FIGURE 9

Model (A4) &gt; Static Structural (A5) &gt; Force &gt; Applied Force Isometric

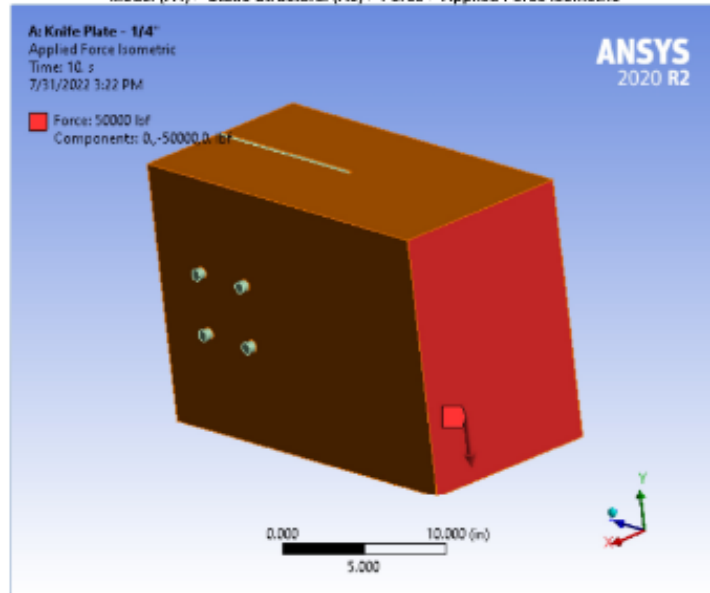


FIGURE 10

Model (A4) &gt; Static Structural (A5) &gt; Displacement

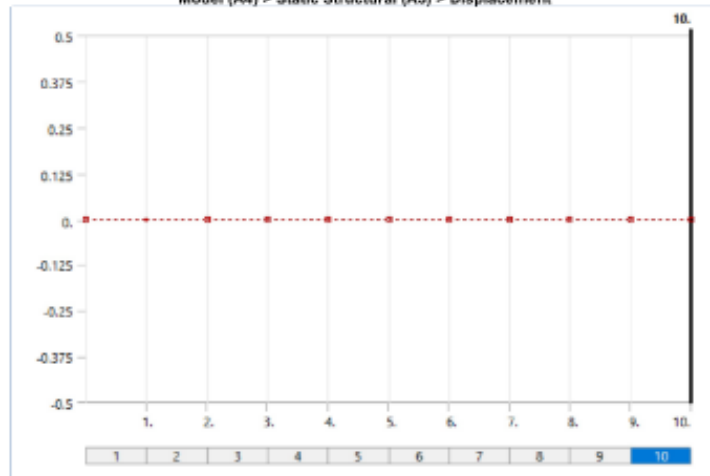
**Solution (A6)**

TABLE 16

Model (A4) &gt; Static Structural (A5) &gt; Solution

Object Name	Solution (A6)
State	Solved
<b>Adaptive Mesh Refinement</b>	
Max Refinement Loops	1.
Refinement Depth	2.
<b>Information</b>	
Status	Done
MAPDL Elapsed Time	17 m 4 s
MAPDL Memory Used	4.8184 GB
MAPDL Result File Size	818.06 MB
<b>Post Processing</b>	

Beam Section Results	No
On Demand Stress/Strain	No

**TABLE 17**  
Model (A4) > Static Structural (A5) > Solution (A6) > Solution Information

Object Name	Solution Information
State	Solved
<b>Solution Information</b>	
Solution Output	Force Convergence
Newton-Raphson Residuals	0
Identify Element Violations	0
Update Interval	2.5 s
Display Points	All
<b>FE Connection Visibility</b>	
Activate Visibility	Yes
Display	All FE Connectors
Draw Connections Attached To	All Nodes
Line Color	Connection Type
Visible on Results	No
Line Thickness	Single
Display Type	Lines

**FIGURE 11**  
Model (A4) > Static Structural (A5) > Solution (A6) > Solution Information

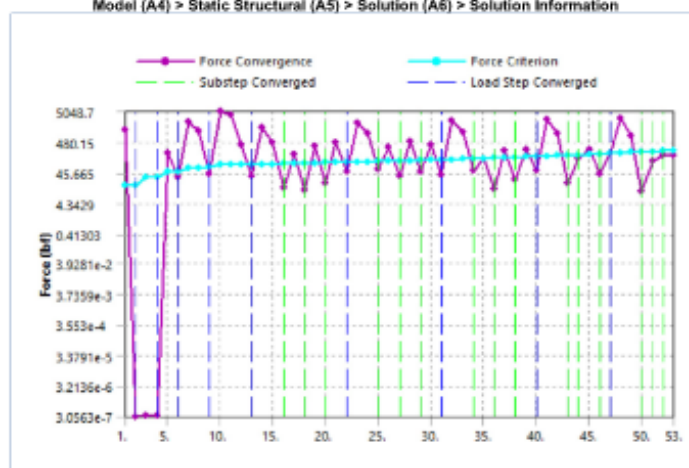


**FIGURE 12**  
Model (A4) > Static Structural (A5) > Solution (A6) > Solution Information

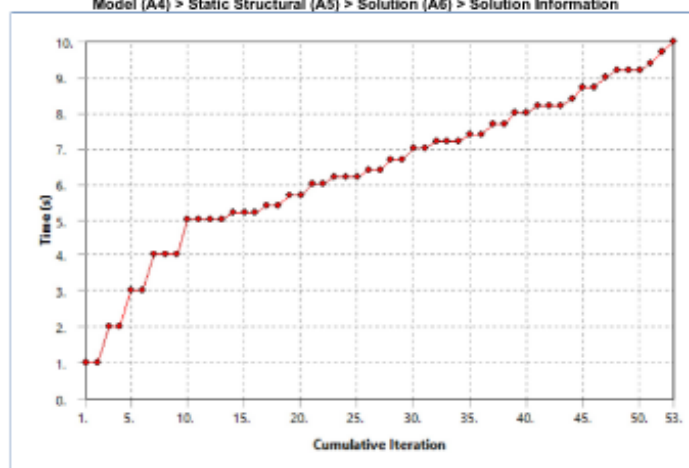


**TABLE 18**  
Model (A4) > Static Structural (A5) > Solution (A6) > Results

Model (A4) > Static Structural (A5) > Solution (A6) > Results					
Object Name	Equivalent Stress	Total Deformation	Directional Deformation	Normal Stress	Normal Elastic Strain
State	Solved				
Scope					
Scoping Method	Geometry Selection				
Geometry	All Bodies				
Definition					
Type	Equivalent (von-Mises) Stress	Total Deformation	Directional Deformation	Normal Stress	Normal Elastic Strain

By	Time				
Display Time	Last				
Calculate Time History	Yes				
Identifier					
Suppressed	No				
Orientation	Y Axis		X Axis		
Coordinate System	Global Coordinate System				
Integration Point Results					
Display Option	Averaged		Averaged		
Average Across Bodies	No		No		
Results					
Minimum	11.446 psi	0. in	-0.54049 in	-56667 psi	-2.0643e-003 in/in
Maximum	47085 psi	0.58643 in	1.0973e-002 in	65405 psi	1.6622e-003 in/in
Average	4522.4 psi	0.11914 in	-0.1087 in	40.938 psi	-1.5359e-006 in/in
Minimum Occurs On	2 Foot CLT/Solid	Knife Plate/Solid	2 Foot CLT/Solid	Knife Plate/Solid	2 Foot CLT/Solid
Maximum Occurs On	Knife Plate/Solid	2 Foot CLT/Solid	Knife Plate/Solid	2 Foot CLT/Solid	2 Foot CLT/Solid
Minimum Value Over Time					
Minimum	0.80294 psi	0. in	-0.54049 in	-56667 psi	-2.0643e-003 in/in
Maximum	11.446 psi	0. in	-2.1881e-002 in	-7241.1 psi	-1.7833e-004 in/in
Maximum Value Over Time					
Minimum	11971 psi	2.4747e-002 in	1.2509e-003 in	6885.9 psi	1.9998e-004 in/in
Maximum	47085 psi	0.58643 in	1.0973e-002 in	65405 psi	1.6622e-003 in/in
Information					
Time	10. s				
Load Step	10				
Substep	4				
Iteration Number	53				

**FIGURE 13**  
Model (A4) > Static Structural (A5) > Solution (A6) > Equivalent Stress

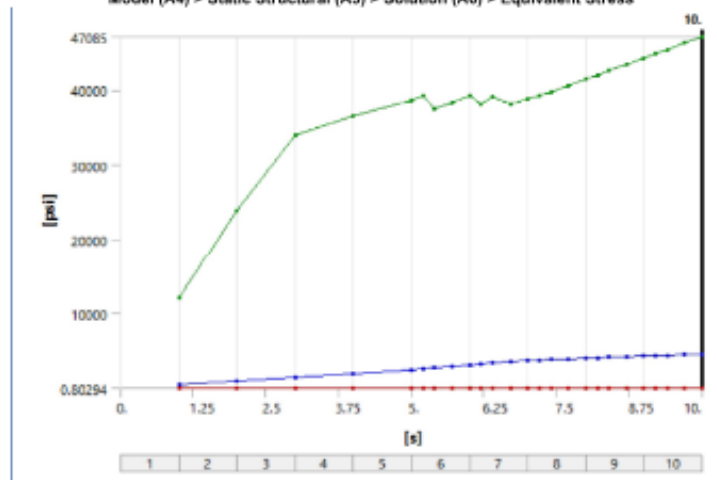


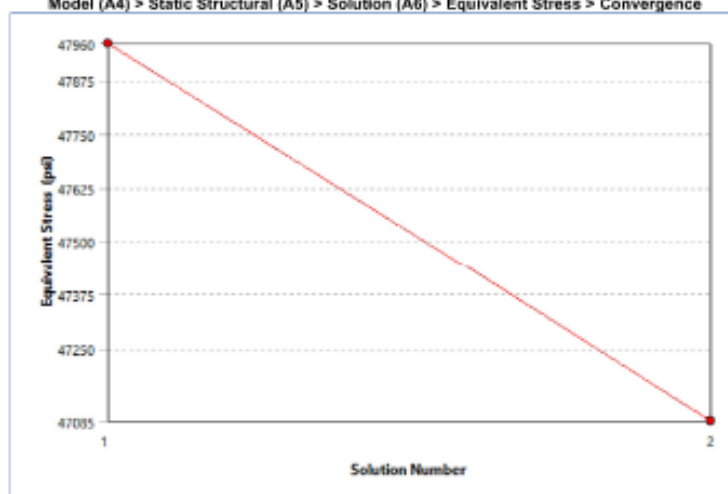
**TABLE 19**  
Model (A4) > Static Structural (A5) > Solution (A6) > Equivalent Stress

Time [s]	Minimum [psi]	Maximum [psi]	Average [psi]
1.	0.80294	11971	474.82
2.	1.6059	23942	949.64
3.	2.4023	33997	1424.8
4.	3.2513	36462	1916.9
5.	4.9485	38673	2463.
5.2	5.3433	39178	2581.2
5.4	5.5084	37412	2703.1
5.7	5.7142	38231	2895.3
6.	5.8646	39306	3093.9
6.2	5.9397	38107	3225.9
6.4	5.9993	39020	3351.9
6.7	6.1242	38054	3512.3
7.	6.296	38772	3643.6
7.2	6.4224	39277	3724.4
7.4	6.6074	39792	3798.2
7.7	7.042	40572	3893.5
8.	5.5256	41401	3981.
8.2	4.3723	41963	4038.
8.4	3.3082	42529	4094.9
8.7	3.2136	43379	4179.5
9.	5.7573	44231	4262.2
9.2	7.3378	44800	4317.1
9.4	10.887	45370	4370.3
9.7	7.3796	46226	4447.3
10.	11.446	47085	4522.4

**TABLE 20**  
Model (A4) > Static Structural (A5) > Solution (A6) > Equivalent Stress > Convergences

Object Name	Convergence
State	Solved
<b>Definition</b>	
Type	Maximum
Allowable Change	2. %
<b>Results</b>	
Last Change	-1.8396 %
Converged	Yes

**FIGURE 14**  
Model (A4) > Static Structural (A5) > Solution (A6) > Equivalent Stress > Convergence



Model (A4) > Static Structural (A5) > Solution (A6) > Equivalent Stress > Convergence

	Equivalent Stress (psi)	Change (%)	Nodes	Elements
1	47960		101123	63428
2	47085	-1.8396	118373	76251

**FIGURE 15**  
Model (A4) > Static Structural (A5) > Solution (A6) > Equivalent Stress > Stress Isometric

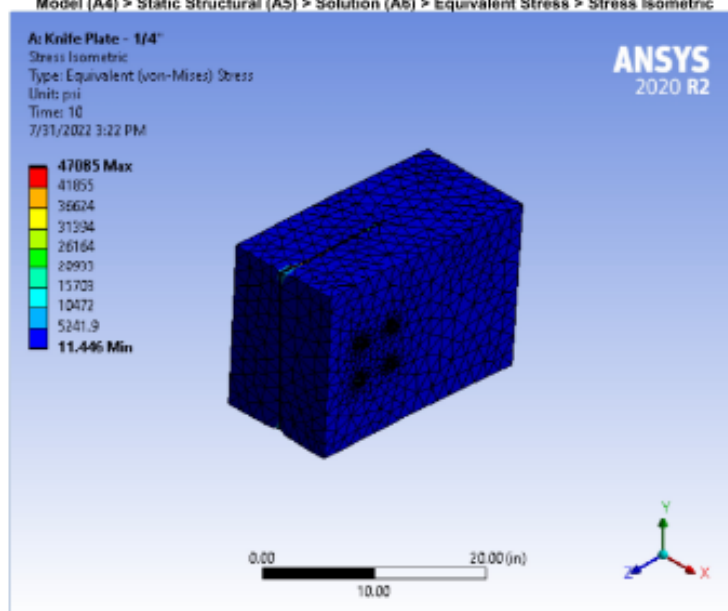


**FIGURE 16**  
Model (A4) > Static Structural (A5) > Solution (A6) > Equivalent Stress > Stress w/ Max and Min



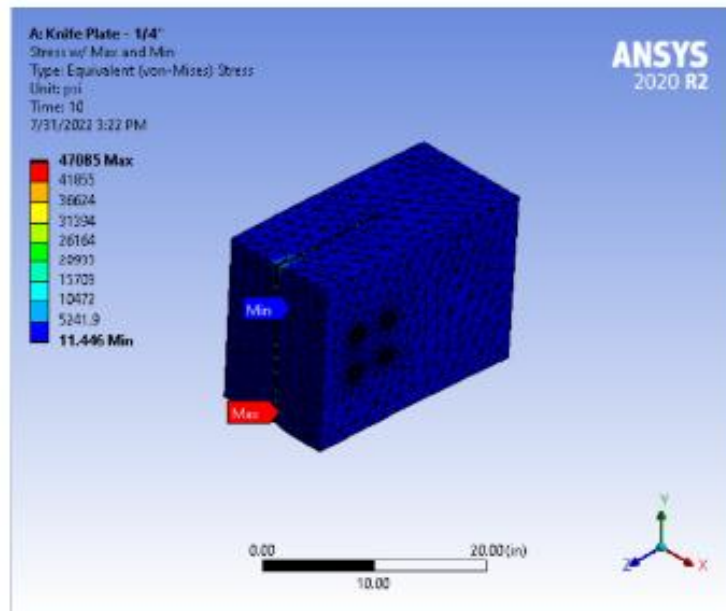


FIGURE 17  
Model (A4) > Static Structural (A5) > Solution (A6) > Total Deformation

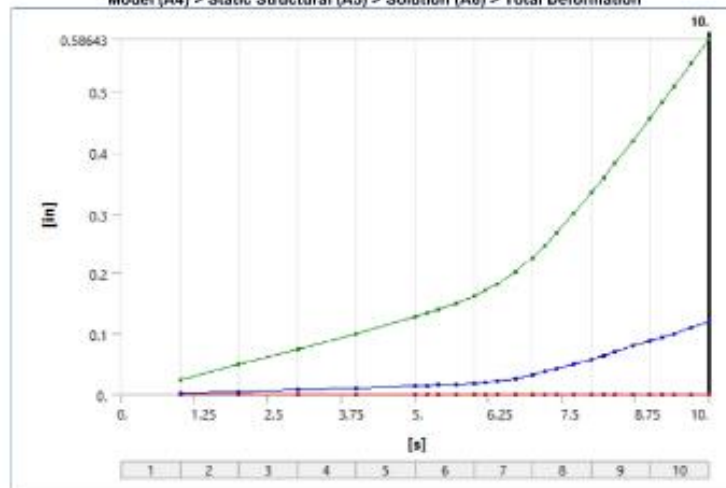


TABLE 21  
Model (A4) > Static Structural (A5) > Solution (A6) > Total Deformation

Time [s]	Minimum [in]	Maximum [in]	Average [in]
1.		2.4747e-002	2.4881e-003
2.		4.9495e-002	4.9763e-003
3.		7.4259e-002	7.4699e-003
4.		9.957e-002	1.0127e-002
5.		0.12725	1.3439e-002
5.2		0.13335	1.425e-002
5.4		0.13977	1.5148e-002
5.7		0.1503	1.6731e-002
6.		0.16208	1.8644e-002
6.2		0.17105	2.0229e-002
6.4		0.18137	2.2189e-002
6.7		0.20147	2.6501e-002
7.	0.	0.22826	3.2854e-002
7.2		0.24773	3.7544e-002
7.4		0.26832	4.2535e-002
7.7		0.30089	5.0438e-002
8.		0.33503	5.8715e-002
8.2		0.35849	6.4395e-002
8.4		0.38249	7.0199e-002
8.7		0.41937	7.9098e-002
9.		0.45697	8.8146e-002
9.2		0.48244	9.426e-002
9.4		0.50812	0.10042
9.7		0.54706	0.10974

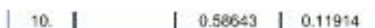


FIGURE 18

Model (A4) &gt; Static Structural (A5) &gt; Solution (A6) &gt; Total Deformation &gt; Total Deformation w/ Max and Min

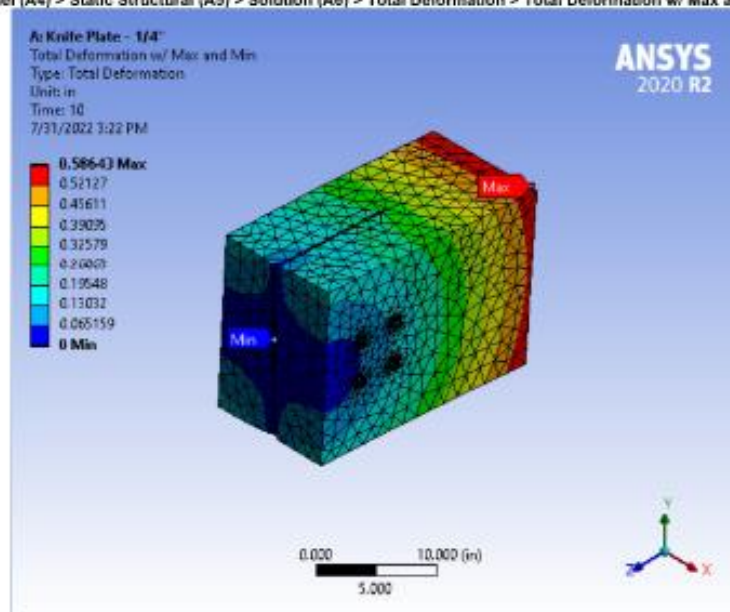


FIGURE 19

Model (A4) &gt; Static Structural (A5) &gt; Solution (A6) &gt; Total Deformation &gt; Total Deformation Isometric

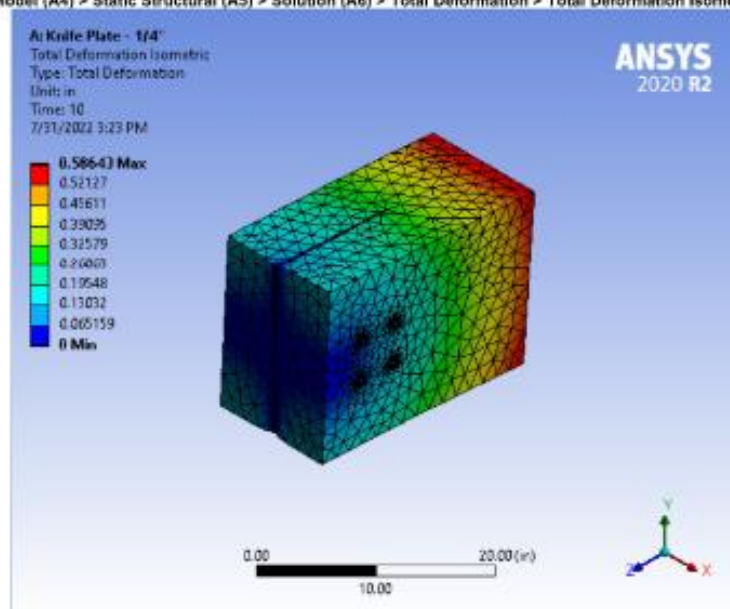


FIGURE 20

Model (A4) &gt; Static Structural (A5) &gt; Solution (A6) &gt; Directional Deformation

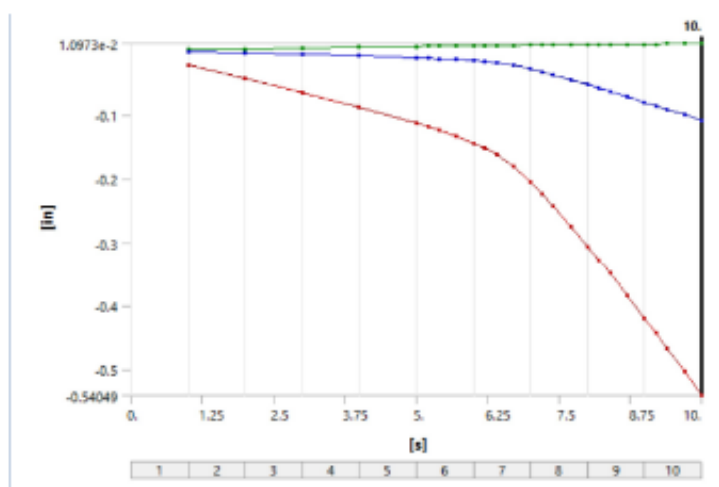


TABLE 22  
Model (A4) > Static Structural (A5) > Solution (A6) > Directional Deformation

Time (s)	Minimum (in)	Maximum (in)	Average (in)
1.	-2.1881e-002	1.2509e-003	-2.0403e-003
2.	-4.3763e-002	2.5018e-003	-4.0807e-003
3.	-6.566e-002	3.7506e-003	-6.1268e-003
4.	-8.8066e-002	4.9758e-003	-8.3389e-003
5.	-0.11278	6.1738e-003	-1.119e-002
5.2	-0.11825	6.4156e-003	-1.1902e-002
5.4	-0.12403	6.6586e-003	-1.2695e-002
5.7	-0.13356	7.0254e-003	-1.4109e-002
6.	-0.14426	7.3999e-003	-1.583e-002
6.2	-0.15247	7.6444e-003	-1.7269e-002
6.4	-0.16195	7.8801e-003	-1.908e-002
6.7	-0.18061	8.1312e-003	-2.3049e-002
7.	-0.20564	8.1776e-003	-2.899e-002
7.2	-0.22385	8.2048e-003	-3.3363e-002
7.4	-0.24312	8.245e-003	-3.8007e-002
7.7	-0.27358	8.3589e-003	-4.5338e-002
8.	-0.30562	8.5303e-003	-5.3004e-002
8.2	-0.32746	8.6773e-003	-5.8256e-002
8.4	-0.3499	8.8487e-003	-6.3619e-002
8.7	-0.38438	9.156e-003	-7.1832e-002
9.	-0.41953	9.5097e-003	-8.0175e-002
9.2	-0.44332	9.7721e-003	-8.5808e-002
9.4	-0.46733	1.0048e-002	-9.1481e-002
9.7	-0.50371	1.0495e-002	-0.10006
10.	-0.54049	1.0973e-002	-0.1087

FIGURE 21  
Model (A4) > Static Structural (A5) > Solution (A6) > Directional Deformation > Directional Deformation w/ Max and Min

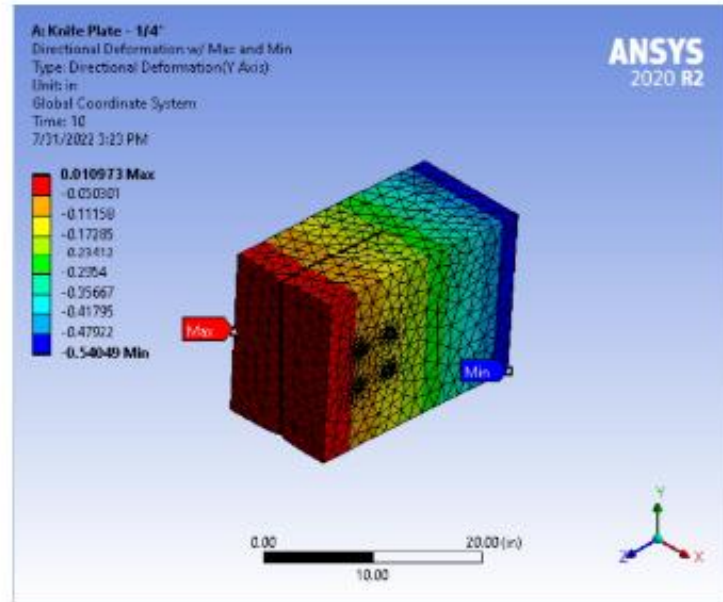


FIGURE 22

Model (A4) &gt; Static Structural (A5) &gt; Solution (A6) &gt; Directional Deformation &gt; Directional Deformation Isometric

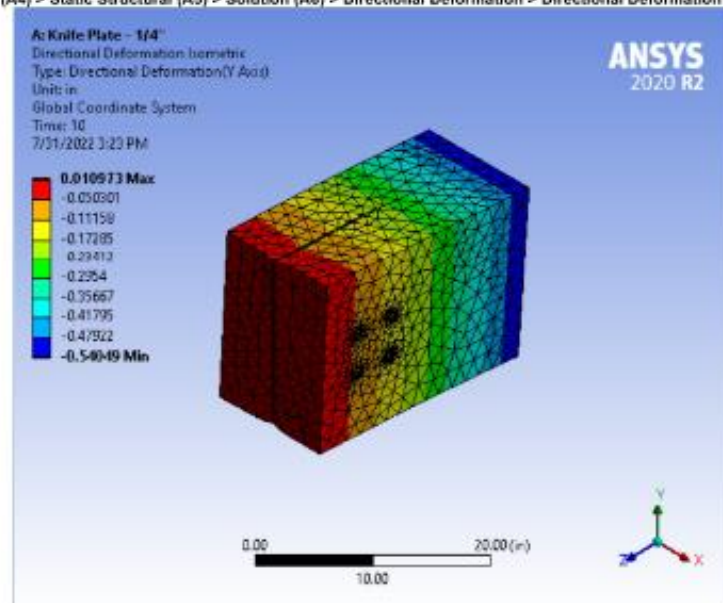
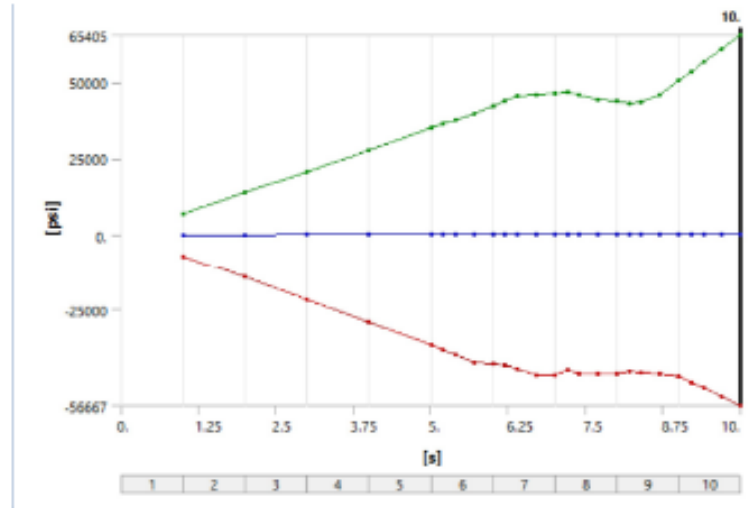


FIGURE 23

Model (A4) &gt; Static Structural (A5) &gt; Solution (A6) &gt; Normal Stress



**TABLE 23**  
**Model (A4) > Static Structural (A5) > Solution (A6) > Normal Stress**

Time [s]	Minimum [psi]	Maximum [psi]	Average [psi]
1.	-7241.1	6865.9	3.5173
2.	-14482	13772	7.0346
3.	-21725	20659	10.577
4.	-29056	27620	13.852
5.	-36769	34890	17.417
5.2	-38376	36402	18.218
5.4	-40003	37407	19.003
5.7	-42479	39764	20.237
6.	-43089	42067	21.302
6.2	-43311	43927	22.129
6.4	-44743	45430	22.815
6.7	-46761	45848	23.76
7.	-46633	46279	25.145
7.2	-45149	46891	26.371
7.4	-46198	45811	27.5
7.7	-46092	44328	29.274
8.	-46227	43982	30.575
8.2	-45414	42849	31.723
8.4	-45816	43536	32.807
8.7	-46247	45933	34.63
9.	-47209	50495	36.379
9.2	-49051	53517	37.403
9.4	-50915	56519	38.392
9.7	-53766	60980	39.71
10.	-56667	65405	40.938

**FIGURE 24**  
**Model (A4) > Static Structural (A5) > Solution (A6) > Normal Stress > Figure**

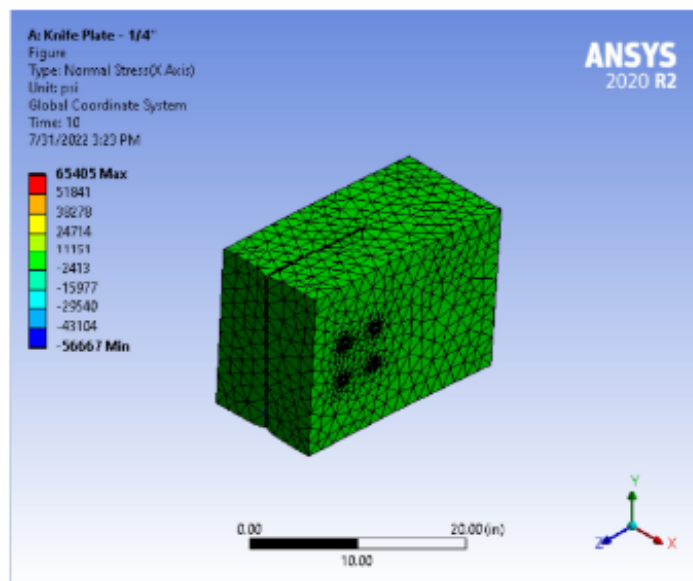


FIGURE 25  
 Model (A4) > Static Structural (A5) > Solution (A6) > Normal Elastic Strain

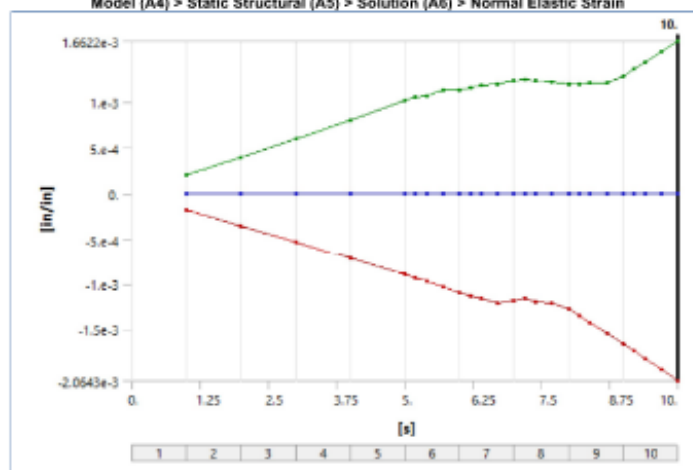


TABLE 24  
 Model (A4) > Static Structural (A5) > Solution (A6) > Normal Elastic Strain

Time [s]	Minimum [in/in]	Maximum [in/in]	Average [in/in]
1.	-1.7833e-004	1.9988e-004	-1.26e-007
2.	-3.5867e-004	3.9995e-004	-2.52e-007
3.	-5.3503e-004	5.9987e-004	-3.7757e-007
4.	-7.1519e-004	8.0179e-004	-5.2581e-007
5.	-9.0213e-004	1.0111e-003	-6.8303e-007
5.2	-9.4061e-004	1.0543e-003	-7.1547e-007
5.4	-9.7947e-004	1.0806e-003	-7.5047e-007
5.7	-1.0377e-003	1.1259e-003	-8.1452e-007
6.	-1.0956e-003	1.1254e-003	-8.9225e-007
6.2	-1.133e-003	1.1565e-003	-9.5059e-007
6.4	-1.1684e-003	1.1862e-003	-1.0343e-006
6.7	-1.2185e-003	1.1974e-003	-1.2024e-006
7.	-1.1919e-003	1.2266e-003	-1.3044e-006
7.2	-1.1695e-003	1.2482e-003	-1.3612e-006
7.4	-1.1971e-003	1.2263e-003	-1.3997e-006
7.7	-1.216e-003	1.2198e-003	-1.4233e-006
8.	-1.2769e-003	1.1954e-003	-1.4558e-006
8.2	-1.3521e-003	1.1914e-003	-1.467e-006
8.4	-1.4279e-003	1.206e-003	-1.4797e-006
8.7	-1.5431e-003	1.212e-003	-1.4906e-006
9.	-1.6601e-003	1.2803e-003	-1.4963e-006
9.2	-1.7394e-003	1.354e-003	-1.5052e-006
9.4	-1.8194e-003	1.429e-003	-1.5157e-006
9.7	-1.941e-003	1.5442e-003	-1.525e-006

10.	-2.0843e-003	1.8622e-003	-1.5359e-008
-----	--------------	-------------	--------------

FIGURE 26

Model (A4) &gt; Static Structural (A5) &gt; Solution (A6) &gt; Normal Elastic Strain &gt; Figure

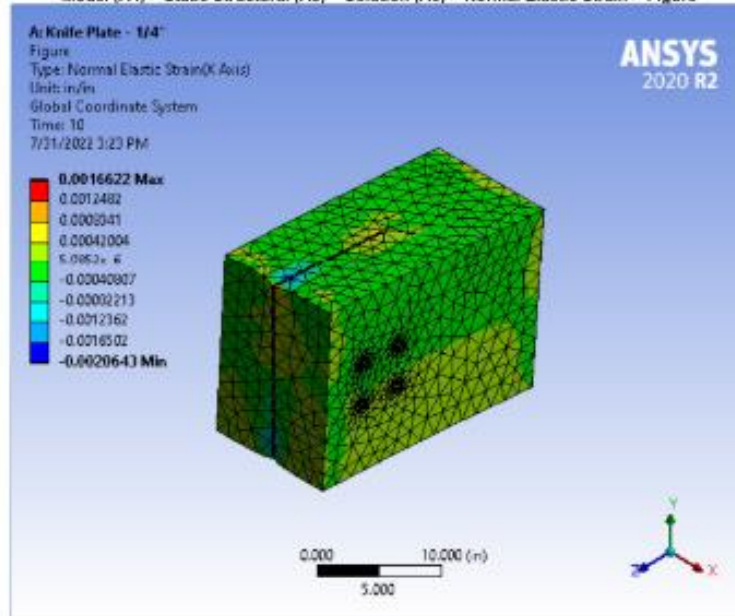


TABLE 25

Model (A4) &gt; Static Structural (A5) &gt; Solution (A6) &gt; Probes

Object Name	Force Reaction
State	Solved
<b>Definition</b>	
Type	Force Reaction
Location Method	Boundary Condition
Boundary Condition	Fixed Support, I-Shape
Orientation	Global Coordinate System
Suppressed	No
<b>Options</b>	
Result Selection	All
Display Time	End Time
<b>Results</b>	
X Axis	242.77 lbf
Y Axis	4999.7 lbf
Z Axis	5.0421e-002 lbf
Total	4999.8 lbf
<b>Maximum Value Over Time</b>	
X Axis	242.77 lbf
Y Axis	4999.7 lbf
Z Axis	2.1757 lbf
Total	4999.8 lbf
<b>Minimum Value Over Time</b>	
X Axis	1.7064 lbf
Y Axis	5000. lbf
Z Axis	-7.5391 lbf
Total	5000. lbf
<b>Information</b>	
Time	10. s
Load Step	10
Substep	4
Iteration Number	53

FIGURE 27

Model (A4) &gt; Static Structural (A5) &gt; Solution (A6) &gt; Force Reaction



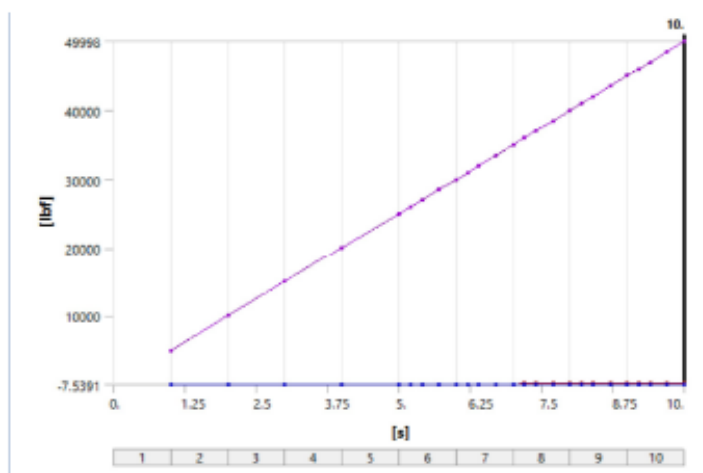
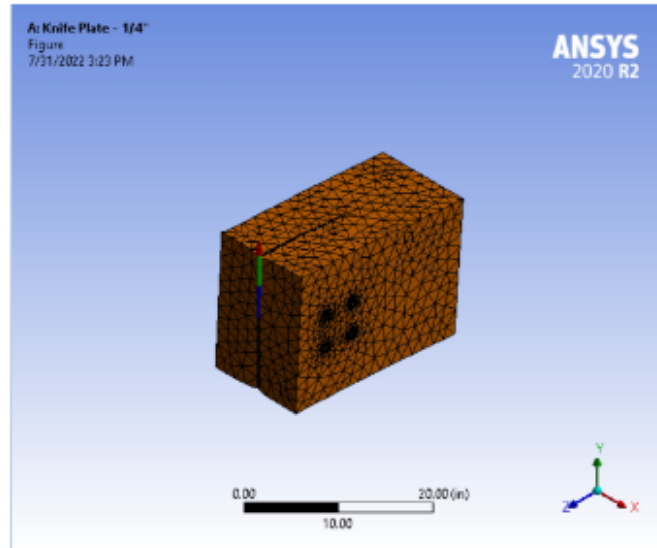


TABLE 26  
Model (A4) > Static Structural (A5) > Solution (A6) > Force Reaction

Time (s)	Force Reaction (X) (lb)	Force Reaction (Y) (lb)	Force Reaction (Z) (lb)	Force Reaction (Total) (lb)
1.	1.7064	5000.	2.766e-010	5000.
2.	3.4129	10000	-1.4541e-010	10000
3.	5.5611	15000	0.10411	15000
4.	9.5789	20000	2.1757	20000
5.	21.257	25001	0.69018	25001
5.2	22.905	26000	-0.38958	26000
5.4	24.253	27000	-0.3308	27000
5.7	28.105	28500	-3.3999e-003	28500
6.	37.807	30000	-0.42872	30000
6.2	41.416	30998	-7.5391	30998
6.4	40.855	32000	-0.49947	32000
6.7	57.805	33498	-1.8999	33498
7.	69.152	35000	2.7297e-002	35000
7.2	80.951	35994	-3.3727	35994
7.4	92.749	37000	7.6086e-003	37000
7.7	110.11	38500	-2.7966e-003	38500
8.	127.37	40000	7.0066e-003	40000
8.2	139.4	40998	0.81047	40998
8.4	151.79	41997	-1.3226	41998
8.7	171.01	43500	-9.807e-002	43500
9.	187.58	44994	0.17202	44994
9.2	199.87	45998	0.51064	45999
9.4	211.01	46999	6.4651e-002	47000
9.7	226.92	48497	2.7796e-002	48498
10.	242.77	49997	5.0421e-002	49998

FIGURE 28  
Model (A4) > Static Structural (A5) > Solution (A6) > Force Reaction > Figure





## Material Data

### CLT

TABLE 27

CLT > Constants

Density	1.9123e-002 lbm in <sup>-3</sup>
Tensile Yield Strength	2445 psi
Tensile Ultimate Strength	2445 psi
Coefficient of Thermal Expansion	5.75e-002 F <sup>-1</sup>
Thermal Conductivity	2.3927e-006 BTU s <sup>-1</sup> in <sup>-1</sup> F <sup>-1</sup>
Specific Heat	0.40245 BTU lbm <sup>-1</sup> F <sup>-1</sup>
Resistivity	5.4901e+013 ohm cmil in <sup>-1</sup>

TABLE 28

CLT > Opacity

Red	Green	Blue
224	112	0
Opacity		
1		
Metallic Finish		
0		

TABLE 29

CLT > Orthotropic Elasticity

Young's Modulus X direction psi	Young's Modulus Y direction psi	Young's Modulus Z direction psi	Poisson's Ratio XY	Poisson's Ratio YZ	Poisson's Ratio XZ	Shear Modulus XY psi	Shear Modulus YZ psi	Shear Modulus XZ psi	Temperature F
1.6969e+006	1.3053e+006	1.4504e+005	0.35	7.e-002	0.35	81656	1.0602e+005	14504	

TABLE 30

CLT > Isotropic Secant Coefficient of Thermal Expansion

Zero-Thermal-Strain Reference Temperature F
73.4

### Structural Steel NL - I-Shape

TABLE 31

Structural Steel NL - I-Shape > Constants

Density	0.2836 lbm in <sup>-3</sup>
Specific Heat	0.10366 BTU lbm <sup>-1</sup> F <sup>-1</sup>

TABLE 32

Structural Steel NL - I-Shape > Isotropic Elasticity

Young's Modulus psi	Poisson's Ratio	Bulk Modulus psi	Shear Modulus psi	Temperature F
2.9008e+007	0.3	2.4173e+007	1.1157e+007	

TABLE 33

Structural Steel NL - I-Shape > Bilinear Isotropic Hardening

Yield Strength psi	Tangent Modulus psi	Temperature F
36259	2.103e+005	

TABLE 34

Structural Steel NL - I-Shape > Color

Red	Green	Blue
184	235	197

### Structural Steel NL - Bolts

**TABLE 35**  
**Structural Steel NL - Bolts > Constants**

Density	0.2836 lbm in <sup>-3</sup>
Specific Heat	0.10366 BTU lbm <sup>-1</sup> F <sup>-1</sup>

**TABLE 36**  
**Structural Steel NL - Bolts > Isotropic Elasticity**

Young's Modulus psi	Poisson's Ratio	Bulk Modulus psi	Shear Modulus psi	Temperature F
2.9008e+007	0.3	2.4173e+007	1.1157e+007	

**TABLE 37**  
**Structural Steel NL - Bolts > Bilinear Isotropic Hardening**

Yield Strength psi	Tangent Modulus psi	Temperature F
36259	2.103e+005	

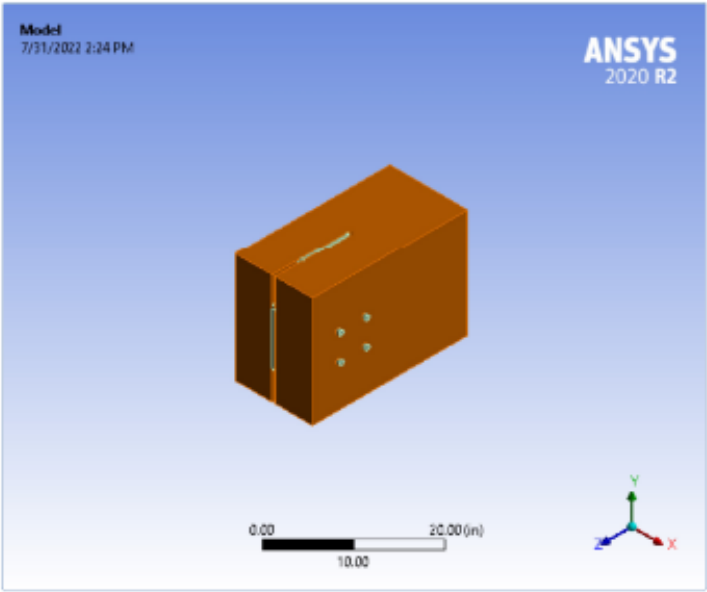
**TABLE 38**  
**Structural Steel NL - Bolts > Color**

Red	Green	Blue
184	235	197



Project

First Saved	Thursday, January 20, 2022
Last Saved	Sunday, July 31, 2022
Product Version	2020 R2
Save Project Before Solution	No
Save Project After Solution	No



## Contents

- [Units](#)
- [Model \(A4\)](#)
  - [Geometry](#)
    - [Parts](#)
  - [Materials](#)
  - [Coordinate Systems](#)
  - [Connections](#)
    - [Contacts](#)
      - [Contact Regions](#)
  - [Mesh](#)
    - [Mesh Controls](#)
  - [Static Structural \(A5\)](#)
    - [Analysis Settings](#)
    - [Loads](#)
    - [Solution \(A6\)](#)
      - [Solution Information](#)
      - [Results](#)
        - [Convergence](#)
      - [Force Reaction](#)
- [Material Data](#)
  - [C3.T](#)
  - [Structural Steel NI - I-Shape](#)
  - [Structural Steel NI - Bolts](#)

## Units

TABLE 1

Unit System:	U.S. Customary (in, lbm, lbf, s, V, A) Degrees rad/s Fahrenheit
Angle	Degrees
Rotational Velocity	rad/s
Temperature	Fahrenheit

## Model (A4)

### Geometry

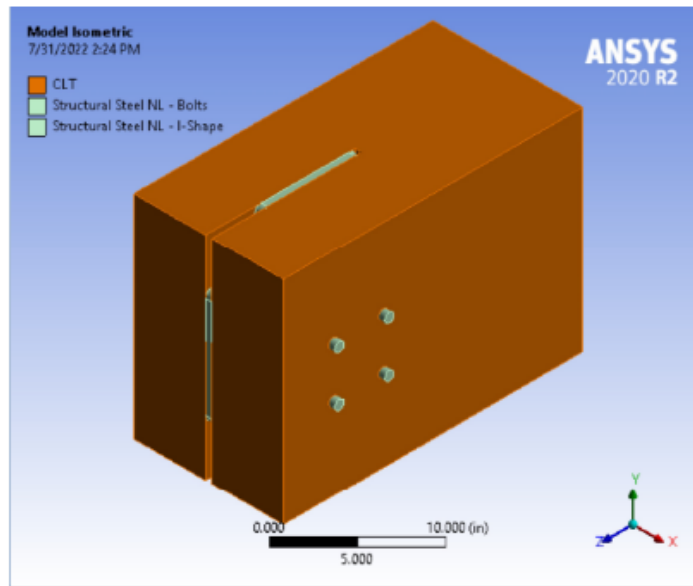
TABLE 2  
Model (A4) > Geometry

Object Name	Geometry
State	Fully Defined
<b>Definition</b>	
Source	C:\Users\krysztopikz\Desktop\KJA - Capstone\KPRC\KPRC - Converged 30 KIP_files\ldp01\SYS\DM\SYS.scdoc
Type	SpaceClaim
Length Unit	Meters
Element Control	Program Controlled
Display Style	Material
<b>Bounding Box</b>	
Length X	13. in
Length Y	17. in
Length Z	24. in
<b>Properties</b>	
Volume	4885.1 in <sup>3</sup>
Mass	122.87 lbm
Scale Factor Value	1.
<b>Statistics</b>	
Bodies	6
Active Bodies	6
Nodes	91316
Elements	57107
Mesh Metric	None
<b>Update Options</b>	
Assign Default Material	No
<b>Basic Geometry Options</b>	
Solid Bodies	Yes
Surface Bodies	Yes
Line Bodies	Yes
Parameters	Independent
Parameter Key	
Attributes	Yes
Attribute Key	
Named Selections	Yes
Named Selection Key	
Material Properties	Yes
<b>Advanced Geometry Options</b>	
Use Associativity	Yes
Coordinate Systems	Yes
Coordinate System Key	

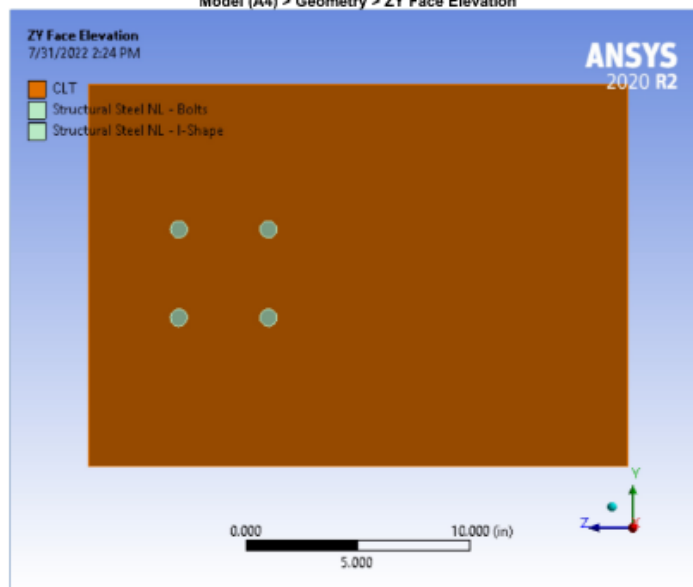
Reader Mode Saves Updated File	No
Use Instances	Yes
Smart CAD Update	Yes
Compare Parts On Update	No
Analysis Type	3-D
Mixed Import Resolution	None
Clean Bodies On Import	No
Stitch Surfaces On Import	None
Decompose Disjoint Geometry	Yes
Enclosure and Symmetry Processing	Yes

TABLE 3 Model (A4) > Geometry > Parts						
Object Name	2 Foot CLT\Solid	Knife Plate\Solid	Bolt_Horiz_Left.2 \Bolt_Horiz_Left 2	Bolt_Horiz_Left.2 \Bolt_Horiz_Left 1	Bolt_Horiz_Right.2 \Bolt_Horiz_Right 2	Bolt_Horiz_Right.2 \Bolt_Horiz_Right 1
State	Meshed					
Graphics Properties						
Visible	Yes					
Transparency	1					
Definition						
Suppressed	No					
Stiffness Behavior	Flexible					
Coordinate System	Default Coordinate System					
Reference Temperature	By Environment					
Treatment	None					
Material						
Assignment	CLT	Structural Steel NL - I-Shape	Structural Steel NL - Bolts			
Nonlinear Effects	Yes					
Thermal Strain Effects	Yes					
Bounding Box						
Length X	12. in	0.5 in	13. in			
Length Y	17. in		0.75 in			
Length Z	24. in	12. in	0.75 in			
Properties						
Volume	4773.7 in³	88.407 in³	5.7432 in³			
Mass	91.288 lbm	25.072 lbm	1.6288 lbm			
Centroid X	6. in					
Centroid Y	8.4996 in	8.4991 in	10.59 in	6.5901 in	10.59 in	6.5901 in
Centroid Z	-0.1536 in	5.3889 in	7.9959 in	3.9959 in		
Moment of Inertia Ip1	6589.2 lbm-in²	790.51 lbm-in²	0.11337 lbm-in²			
Moment of Inertia Ip2	5501.5 lbm-in²	266.35 lbm-in²	22.879 lbm-in²			
Moment of Inertia Ip3	3325. lbm-in²	525.2 lbm-in²	22.879 lbm-in²			
Statistics						
Nodes	82133	1321	1966			
Elements	55502	165	360			
Mesh Metric	None					
CAD Attributes						
PartTolerance:	0.00000001					
Color:143.175.143						

FIGURE 1  
Model (A4) > Geometry > Model Isometric



**FIGURE 2**  
Model (A4) > Geometry > ZY Face Elevation



**FIGURE 3**  
Model (A4) > Geometry > XY Face Elevation

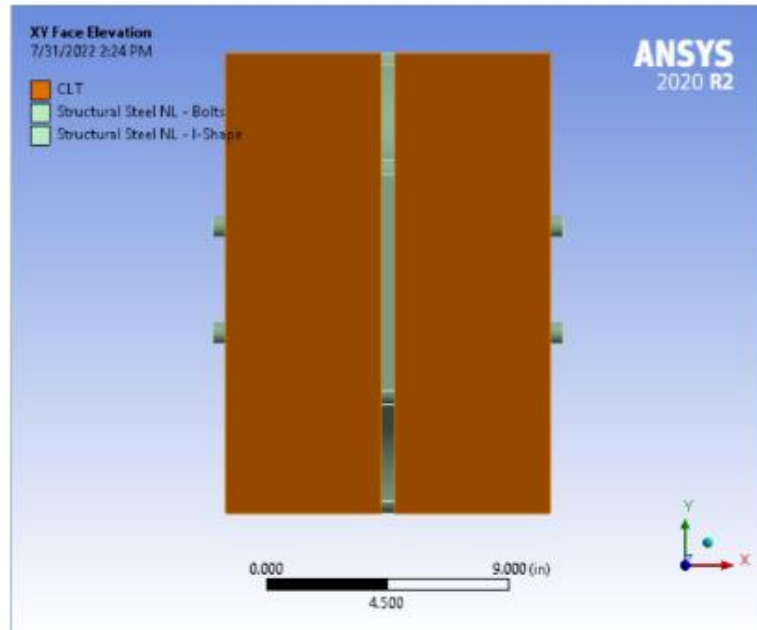


**FIGURE 4**  
Model (A4) > Geometry > XZ Face Elevation

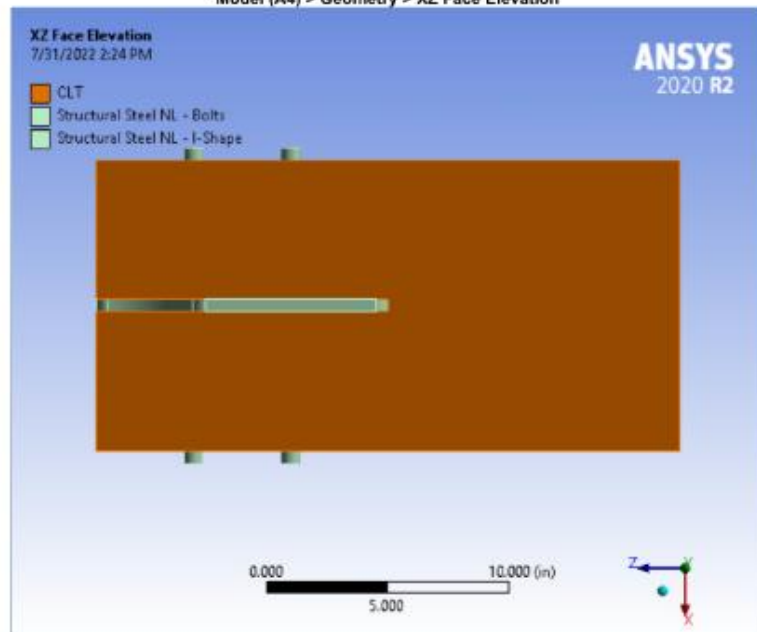


**FIGURE 5**  
Model (A4) > Geometry > Steel Isometric

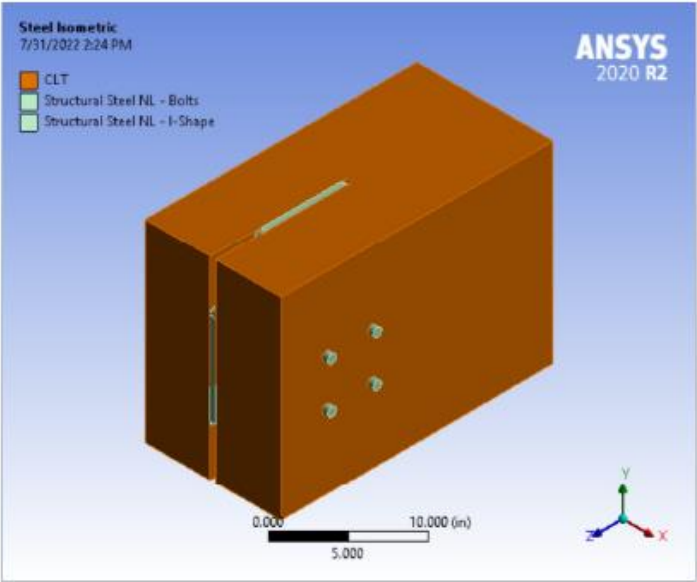


FIGURE 6  
Model (A4) > Geometry > CLT Isometric

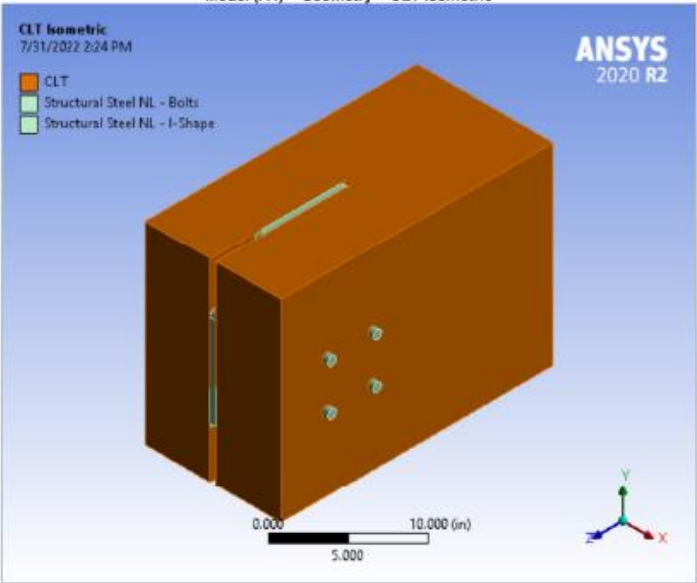


TABLE 4  
Model (A4) > Materials

Object Name	Materials
State	Fully Defined
Statistics	
Materials	5
Material Assignments	0

Coordinate Systems

TABLE 5  
Model (A4) > Coordinate Systems > Coordinate System

Object Name	Global Coordinate System
State	Fully Defined
Definition	
Type	Cartesian
Coordinate System ID	0
Origin	
Origin X	0. in
Origin Y	0. in
Origin Z	0. in





Contact Geometry Correction	None
Target Geometry Correction	None

### Mesh

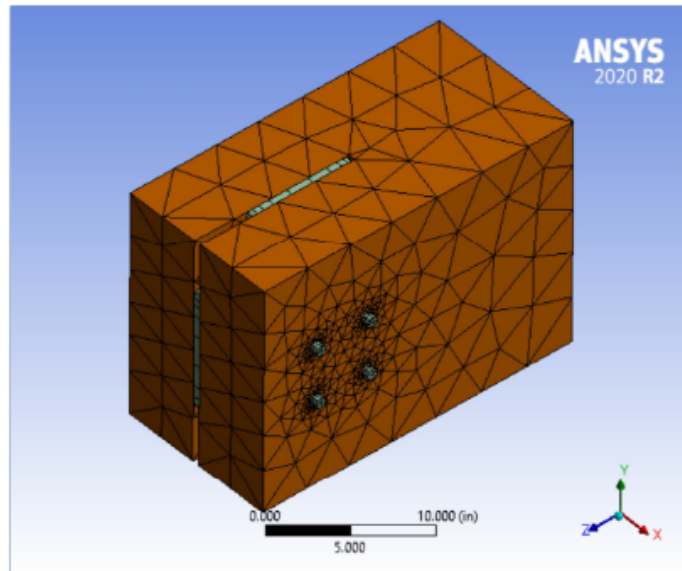
**TABLE 9**  
**Model (A4) > Mesh**

Object Name	Mesh
State	Solved
<b>Display</b>	
Display Style	Use Geometry Setting
<b>Defaults</b>	
Physics Preference	Nonlinear Mechanical
Element Order	Program Controlled
Element Size	3.5 in
<b>Sizing</b>	
Growth Rate	1.6
Max Size	4.0 in
Mesh Defeaturing	Yes
Defeature Size	Default (1.75e-002 in)
Capture Curvature	Yes
Curvature Min Size	Default (3.5e-002 in)
Curvature Normal Angle	Default (60.0°)
Capture Proximity	No
Bounding Box Diagonal	32.156 in
Average Surface Area	58.504 in²
Minimum Edge Length	0.5 in
<b>Quality</b>	
Check Mesh Quality	Yes, Errors
Target Skewness	Default (0.900000)
Target Jacobian Ratio (Corner Nodes)	Default (0.040000)
Mesh Metric	None
<b>Inflation</b>	
Use Automatic Inflation	None
Inflation Option	Smooth Transition
Transition Ratio	0.272
Maximum Layers	5
Growth Rate	1.2
Inflation Algorithm	Pre
View Advanced Options	No
<b>Advanced</b>	
Number of CPUs for Parallel Part Meshing	Program Controlled
Straight Sided Elements	No
Rigid Body Behavior	Dimensionally Reduced
Triangle Surface Mesher	Program Controlled
Topology Checking	Yes
Pinch Tolerance	Default (3.15e-002 in)
Generate Pinch on Refresh	No
<b>Statistics</b>	
Nodes	91318
Elements	57107

**TABLE 10**  
**Model (A4) > Mesh > Mesh Controls**

Object Name	Refinement_Bolts	Refinement_CLT	Refinement_I-Shape	Body Sizing_Bolts	Face Sizing_Bolt holes in I-Shape	Face Sizing_Bolt holes in CLT
State	Suppressed			Fully Defined	Suppressed	Fully Defined
<b>Scope</b>						
Scoping Method	Geometry Selection					
Geometry	4 Faces	No Selection	4 Bodies	No Selection	8 Faces	
<b>Definition</b>						
Suppressed	Yes		No	Yes	No	
Active	No, Suppressed			No, Suppressed		
Refinement	1					
Type	Element Size					
Element Size			0.3 in		0.2 in	
<b>Advanced</b>						
Defeature Size	Default (1.75e-002 in)					
Behavior	Soft					
Growth Rate	Default (1.6)					
Capture Curvature	No					
Capture Proximity	No					
Influence Volume	No					

**FIGURE 7**  
**Model (A4) > Mesh > Mesh Isometric**



### Static Structural (A5)

**TABLE 11**  
**Model (A4) > Analysis**

Object Name	Static Structural (A5)
State	Solved
<b>Definition</b>	
Physics Type	Structural
Analysis Type	Static Structural
Solver Target	Mechanical APDL
<b>Options</b>	
Environment Temperature	71.6 °F
Generate Input Only	No

**TABLE 12**  
**Model (A4) > Static Structural (A5) > Analysis Settings**

Object Name	Analysis Settings
State	Fully Defined
<b>Step Controls</b>	
Number Of Steps	10.
Current Step Number	10.
Step End Time	10. s
Auto Time Stepping	Program Controlled
<b>Solver Controls</b>	
Solver Type	Direct
Weak Springs	Off
Solver Pivot Checking	Program Controlled
Large Deflection	Off
Inertia Relief	Off
Quasi-Static Solution	Off
<b>Rotordynamics Controls</b>	
Coriolis Effect	Off
<b>Restart Controls</b>	
Generate Restart Points	Program Controlled
Retain Files After Full Solve	No
Combine Restart Files	Program Controlled
<b>Nonlinear Controls</b>	
Newton-Raphson Option	Program Controlled
Force Convergence	Program Controlled
Moment Convergence	Program Controlled
Displacement Convergence	Program Controlled
Rotation Convergence	Program Controlled
Line Search	Program Controlled
Stabilization	Program Controlled
<b>Advanced</b>	
Inverse Option	No
Contact Split (DMP)	Off
<b>Output Controls</b>	
Stress	Yes
Surface Stress	No
Back Stress	No
Strain	Yes
Contact Data	Yes

Nonlinear Data	No
Nodal Forces	No
Volume and Energy	Yes
Euler Angles	Yes
General Miscellaneous	No
Contact Miscellaneous	No
Store Results At	All Time Points
Result File Compression	Program Controlled
<b>Analysis Data Management</b>	
Solver Files Directory	C:\Users\krysztopikz\Desktop\KJA - Capstone\KPRC\KPRC - Converged 30 KIP_files\dp0\SYS\MECH\
Future Analysis	None
Scratch Solver Files Directory	
Save MAPDL db	No
Contact Summary	Program Controlled
Delete Unneeded Files	Yes
Nonlinear Solution	Yes
Solver Units	Active System
Solver Unit System	Bin

**TABLE 13**  
**Model (A4) > Static Structural (A5) > Analysis Settings**  
**Step-Specific "Step Controls"**

Step	Step End Time	Auto Time Stepping	Define By	Initial Substeps	Minimum Substeps	Maximum Substeps	Carry Over Time Step
1	1. s	On	Substeps	1.	1.	10.	Off
2	2. s						
3	3. s						
4	4. s						
5	5. s						
6	6. s	Program Controlled					
7	7. s						
8	8. s						
9	9. s						
10	10. s						

**TABLE 14**  
**Model (A4) > Static Structural (A5) > Loads**

Model (A4) > Static Structural (A5) > Loads			
Object Name	Fixed Support - I-Shape	Force	Displacement
State	Fully Defined		
Scope			
Scoping Method	Geometry Selection		
Geometry	1 Face	8 Faces	
Definition			
Type	Fixed Support	Force	Displacement
Suppressed	No		
Define By	Components		
Applied By	Surface Effect		
Coordinate System	Global Coordinate System		
X Component	0. lbf (ramped)	0. in (ramped)	
Y Component	Tabular Data		Free
Z Component	0. lbf (ramped)	Free	
Tabular Data			
Independent Variable	Time		

**FIGURE 8**  
**Model (A4) > Static Structural (A5) > Force**

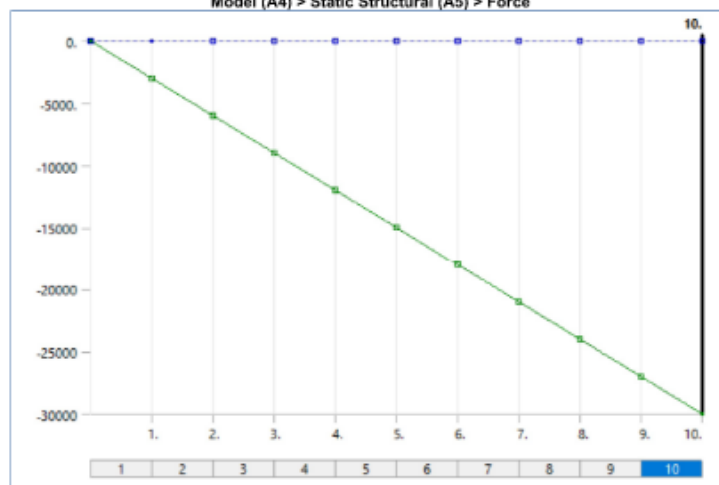


**TABLE 15**  
**Model (A4) > Static Structural (A5) > Force**

Steps	Time [s]	X [lbf]	Y [lbf]	Z [lbf]
1	0.	= 0.	0.	= 0.
	1.	0.	= -3000.	0.

2	2.	= -6000.
3	3.	= -9000.
4	4.	= -12000
5	5.	= -15000
6	6.	= -18000
7	7.	= -21000
8	8.	= -24000
9	9.	= -27000
10	10.	= -30000

FIGURE 9

Model (A4) &gt; Static Structural (A5) &gt; Force &gt; Applied Force Isometric

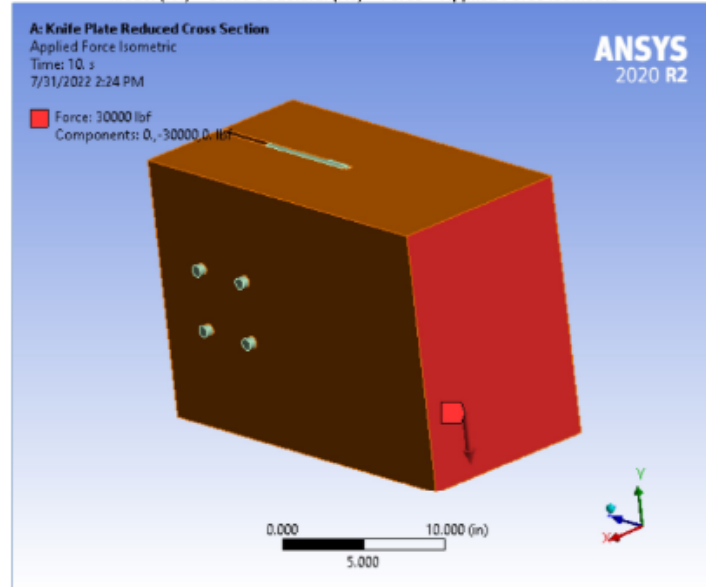
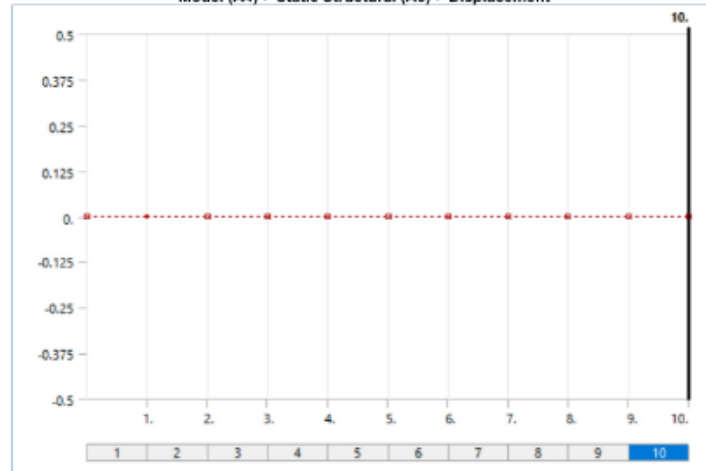


FIGURE 10

Model (A4) &gt; Static Structural (A5) &gt; Displacement



Solution (A6)

TABLE 16

Model (A4) &gt; Static Structural (A5) &gt; Solution

Object Name	Solution (A6)
State	Solved
<b>Adaptive Mesh Refinement</b>	
Max Refinement Loops	1.
Refinement Depth	2.
<b>Information</b>	
Status	Done
MAPDL Elapsed Time	13 m 29 s
MAPDL Memory Used	4.3701 GB
MAPDL Result File Size	787.19 MB
<b>Post Processing</b>	

Beam Section Results	No
On Demand Stress/Strain	No

**TABLE 17**  
**Model (A4) > Static Structural (A5) > Solution (A6) > Solution Information**

Object Name	<i>Solution Information</i>
State	Solved
<b>Solution Information</b>	
Solution Output	Solver Output
Newton-Raphson Residuals	0
Identify Element Violations	0
Update Interval	2.5 s
Display Points	All
<b>FE Connection Visibility</b>	
Activate Visibility	Yes
Display	All FE Connectors
Draw Connections Attached To	All Nodes
Line Color	Connection Type
Visible on Results	No
Line Thickness	Single
Display Type	Lines

**TABLE 18**  
**Model (A4) > Static Structural (A5) > Solution (A6) > Results**

Object Name	Equivalent Stress	Total Deformation	Directional Deformation	Normal Stress	Normal Elastic Strain
State	Solved				
Scope					
Scoping Method	Geometry Selection				
Geometry	All Bodies				
Definition					
Type	Equivalent (von-Mises) Stress	Total Deformation	Directional Deformation	Normal Stress	Normal Elastic Strain
By	Time				
Display Time	Last				
Calculate Time History	Yes				
Identifier					
Suppressed	No				
Orientation			Y Axis	X Axis	
Coordinate System			Global Coordinate System		
Integration Point Results					
Display Option	Averaged			Averaged	
Average Across Bodies	No			No	
Results					
Minimum	7.7 psi	0. in	-0.81509 in	-2.6187e+005 psi	-3.1168e-003 in/in
Maximum	60319 psi	0.87224 in	1.0395e-002 in	3.0497e+005 psi	3.7571e-003 in/in
Average	4224.7 psi	0.19775 in	-0.18126 in	9.328 psi	-6.8077e-007 in/in
Minimum Occurs On	2 Foot CLT\Solid	Knife Plate\Solid	2 Foot CLT\Solid	Knife Plate\Solid	
Maximum Occurs On	Knife Plate\Solid	2 Foot CLT\Solid		Knife Plate\Solid	
Minimum Value Over Time					
Minimum	1.0896 psi	0. in	-0.81509 in	-2.6187e+005 psi	-3.1168e-003 in/in
Maximum	7.7 psi	0. in	-1.7481e-002 in	-10890 psi	-2.0144e-004 in/in
Maximum Value Over Time					
Minimum	31354 psi	1.9416e-002 in	9.2213e-004 in	13971 psi	1.9834e-004 in/in
Maximum	60319 psi	0.87224 in	1.0395e-002 in	3.0497e+005 psi	3.7571e-003 in/in
Information					
Time	10. s				
Load Step	10				
Substep	4				
Iteration Number	57				

**FIGURE 11**  
**Model (A4) > Static Structural (A5) > Solution (A6) > Equivalent Stress**

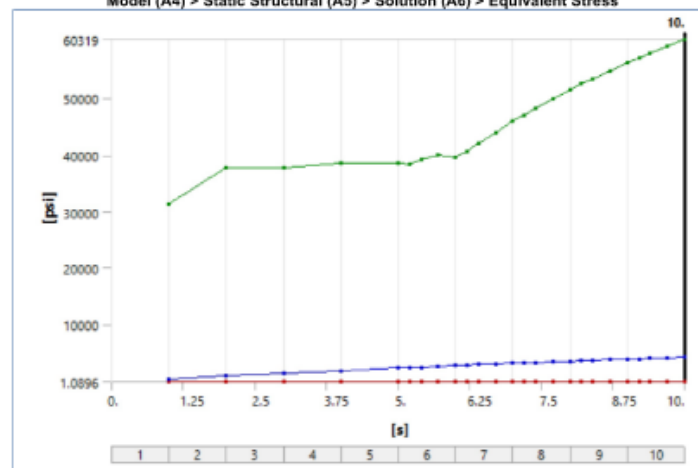


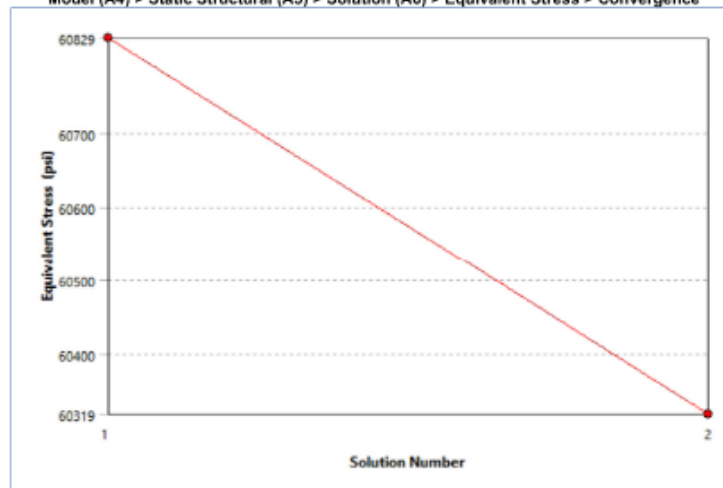
**TABLE 19**  
Model (A4) > Static Structural (A5) > Solution (A6) > Equivalent Stress

Time [s]	Minimum [psi]	Maximum [psi]	Average [psi]
1.	1.0896	31354	476.99
2.	2.1041	37655	950.8
3.	2.9585	37756	1422.3
4.	3.5317	38607	1894.5
5.	3.9624	38514	2369.
5.2	4.0392	38347	2460.8
5.4	4.1128	39288	2549.9
5.7	3.7549	39937	2678.9
6.	2.5505	39669	2810.5
6.2	2.3787	40666	2897.5
6.4	3.099	41984	2982.6
6.7	1.7851	43968	3102.9
7.	5.1511	45862	3216.7
7.2	7.1389	47067	3290.8
7.4	7.1327	48225	3362.4
7.7	7.1062	49870	3465.8
8.	7.0756	51448	3567.5
8.2	7.0559	52464	3634.7
8.4	4.8924	53432	3700.9
8.7	7.0428	54819	3800.2
9.	7.0845	56151	3899.5
9.2	7.1421	57011	3966.5
9.4	7.2291	57855	4033.
9.7	7.4239	59102	4130.9
10.	7.7	60319	4224.7

**TABLE 20**  
Model (A4) > Static Structural (A5) > Solution (A6) > Equivalent Stress > Convergences

Object Name	Convergence
State	Solved
<b>Definition</b>	
Type	Maximum
Allowable Change	2. %
<b>Results</b>	
Last Change	-0.84149 %
Converged	Yes

**FIGURE 12**  
Model (A4) > Static Structural (A5) > Solution (A6) > Equivalent Stress > Convergence



Model (A4) > Static Structural (A5) > Solution (A6) > Equivalent Stress > Convergence

	Equivalent Stress (psi)	Change (%)	Nodes	Elements
1	60829		91318	57107
2	60319	-0.84149	113281	72919

**FIGURE 13**  
Model (A4) > Static Structural (A5) > Solution (A6) > Equivalent Stress > Stress Isometric

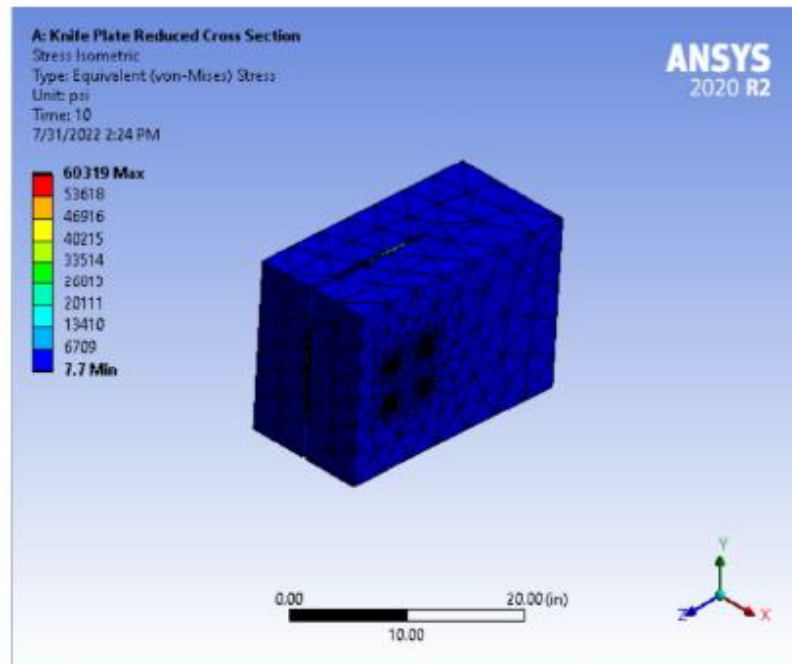


FIGURE 14

Model (A4) &gt; Static Structural (A5) &gt; Solution (A6) &gt; Equivalent Stress &gt; Stress w/ Max and Min

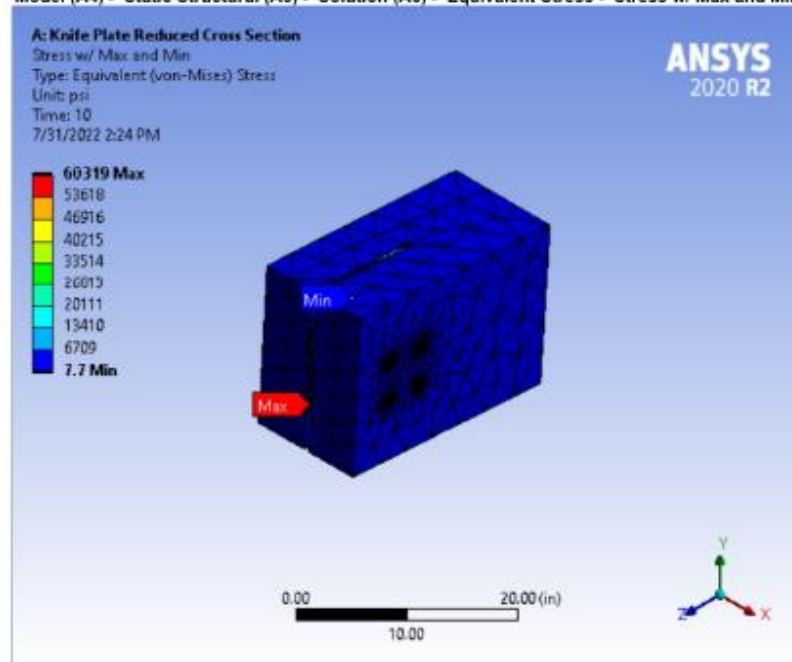
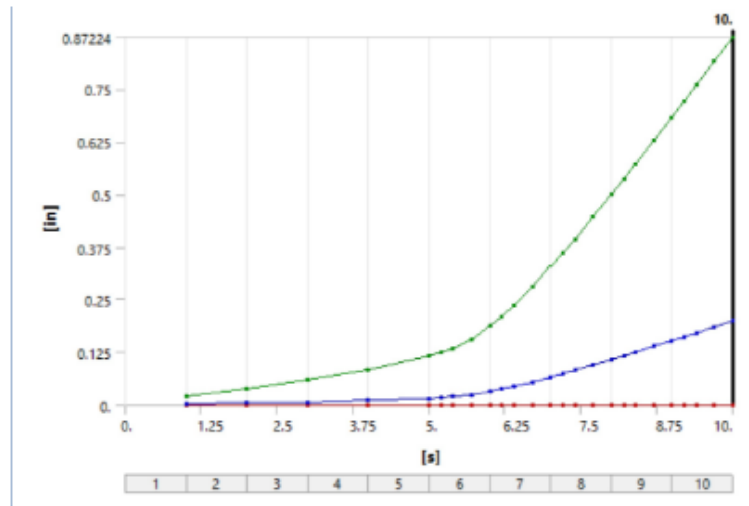


FIGURE 15

Model (A4) &gt; Static Structural (A5) &gt; Solution (A6) &gt; Total Deformation





**TABLE 21**  
**Model (A4) > Static Structural (A5) > Solution (A6) > Total Deformation**

Time [s]	Minimum [in]	Maximum [in]	Average [in]
1.		1.9416e-002	2.3196e-003
2.		3.8987e-002	4.6815e-003
3.		5.956e-002	7.3052e-003
4.		8.316e-002	1.0697e-002
5.		0.11494	1.6136e-002
5.2		0.12344	1.7761e-002
5.4		0.13358	1.9803e-002
5.7		0.15481	2.4485e-002
6.		0.18566	3.1803e-002
6.2		0.20886	3.7359e-002
6.4		0.23504	4.3672e-002
6.7		0.27963	5.4497e-002
7.	0.	0.32793	6.6247e-002
7.2		0.36114	7.432e-002
7.4		0.3952	8.2595e-002
7.7		0.44734	9.5243e-002
8.		0.50047	0.10811
8.2		0.53626	0.11676
8.4		0.57247	0.12551
8.7		0.6275	0.1388
9.		0.68316	0.15223
9.2		0.72052	0.16123
9.4		0.75817	0.1703
9.7		0.81499	0.18397
10.		0.87224	0.19775

**FIGURE 16**  
**Model (A4) > Static Structural (A5) > Solution (A6) > Total Deformation > Total Deformation w/ Max and Min**

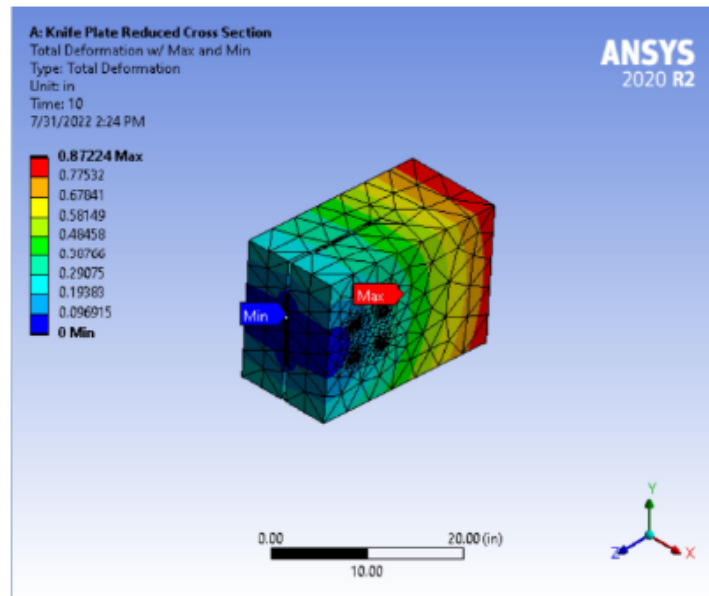


**FIGURE 17**  
 Model (A4) > Static Structural (A5) > Solution (A6) > Directional Deformation

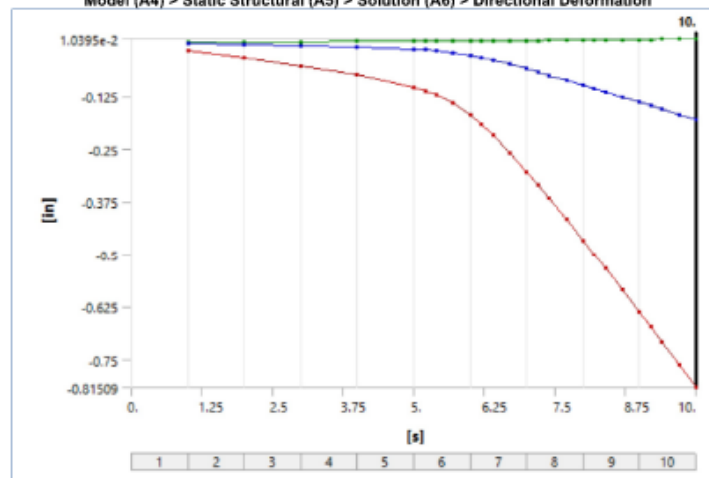


**TABLE 22**  
 Model (A4) > Static Structural (A5) > Solution (A6) > Directional Deformation

Time [s]	Minimum [in]	Maximum [in]	Average [in]
1.	-1.7481e-002	9.2213e-004	-2.0153e-003
2.	-3.5111e-002	1.845e-003	-4.0707e-003
3.	-5.3692e-002	2.7618e-003	-6.3711e-003
4.	-7.5139e-002	3.6861e-003	-9.3827e-003
5.	-0.10432	4.6817e-003	-1.4275e-002
5.2	-0.11219	4.9022e-003	-1.5746e-002
5.4	-0.1216	5.1299e-003	-1.76e-002
5.7	-0.14143	5.383e-003	-2.1896e-002
6.	-0.17037	5.4336e-003	-2.8666e-002
6.2	-0.19215	5.4745e-003	-3.38e-002
6.4	-0.21673	5.534e-003	-3.9627e-002
6.7	-0.25861	5.6631e-003	-4.9612e-002
7.	-0.30398	5.8517e-003	-6.0439e-002
7.2	-0.33517	6.009e-003	-6.7875e-002
7.4	-0.36717	6.1962e-003	-7.5492e-002
7.7	-0.41614	6.5303e-003	-8.7127e-002
8.	-0.46604	6.9191e-003	-9.8957e-002
8.2	-0.49964	7.2062e-003	-0.10691
8.4	-0.53364	7.5102e-003	-0.11495
8.7	-0.58531	7.9965e-003	-0.12715
9.	-0.63757	8.514e-003	-0.13948
9.2	-0.67265	8.8739e-003	-0.14774
9.4	-0.70799	9.243e-003	-0.15607
9.7	-0.76134	9.8101e-003	-0.16862

10.	-0.81509	1.0395e-002	-0.18126
-----	----------	-------------	----------

FIGURE 18

Model (A4) &gt; Static Structural (A5) &gt; Solution (A6) &gt; Directional Deformation &gt; Directional Deformation w/ Max and Min

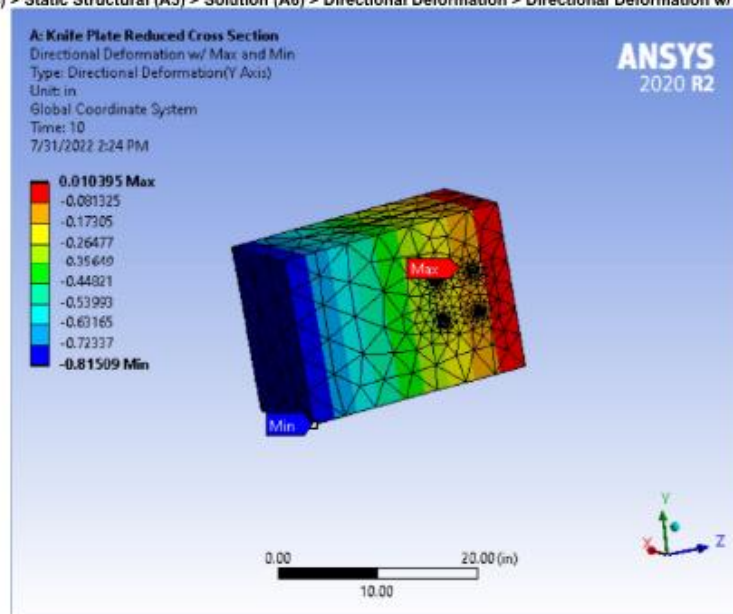


FIGURE 19

Model (A4) &gt; Static Structural (A5) &gt; Solution (A6) &gt; Directional Deformation &gt; Directional Deformation Isometric

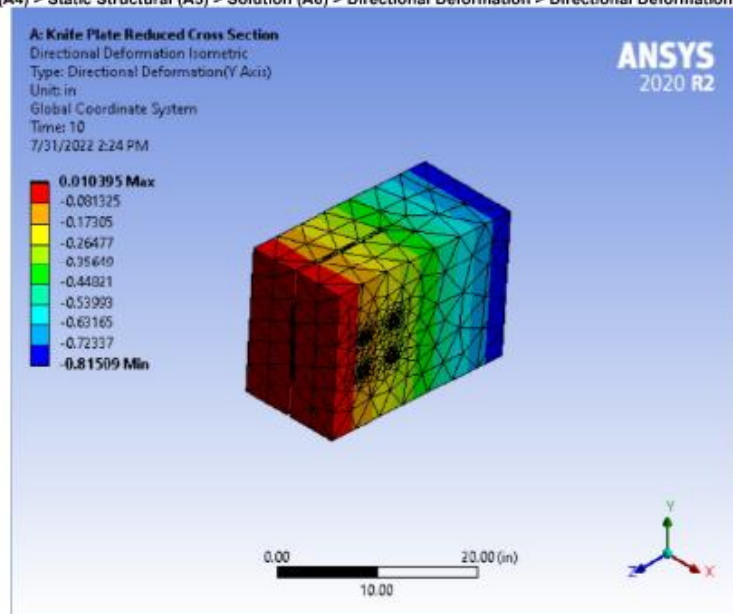
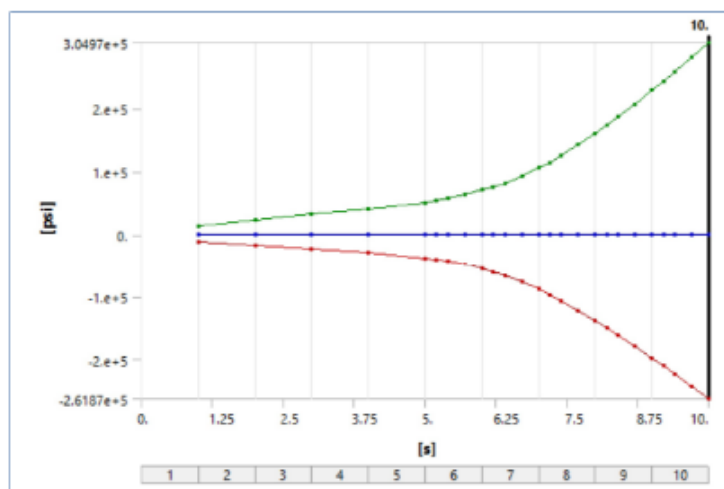


FIGURE 20

Model (A4) &gt; Static Structural (A5) &gt; Solution (A6) &gt; Normal Stress



**TABLE 23**  
**Model (A4) > Static Structural (A5) > Solution (A6) > Normal Stress**

Time [s]	Minimum [psi]	Maximum [psi]	Average [psi]
1.	-10890	13971	2.5594
2.	-17522	22664	5.1821
3.	-23084	32320	7.2866
4.	-28729	40770	9.1195
5.	-37420	50846	10.222
5.2	-39724	53882	10.257
5.4	-42290	57294	10.141
5.7	-47689	63712	9.5927
6.	-55639	71148	8.3564
6.2	-61438	75495	7.6337
6.4	-67464	82066	7.0308
6.7	-77492	92862	7.1991
7.	-89045	1.0552e+005	7.5848
7.2	-97621	1.1502e+005	7.9274
7.4	-1.0697e+005	1.2541e+005	8.1968
7.7	-1.2214e+005	1.4246e+005	8.2543
8.	-1.3836e+005	1.6088e+005	8.1168
8.2	-1.4965e+005	1.7365e+005	8.1159
8.4	-1.6127e+005	1.8686e+005	8.0359
8.7	-1.792e+005	2.0747e+005	7.8838
9.	-1.9754e+005	2.2883e+005	8.0167
9.2	-2.0998e+005	2.4344e+005	8.178
9.4	-2.2266e+005	2.584e+005	8.4654
9.7	-2.4203e+005	2.8139e+005	8.9084
10.	-2.6187e+005	3.0497e+005	9.328

**FIGURE 21**  
**Model (A4) > Static Structural (A5) > Solution (A6) > Normal Stress > Figure**

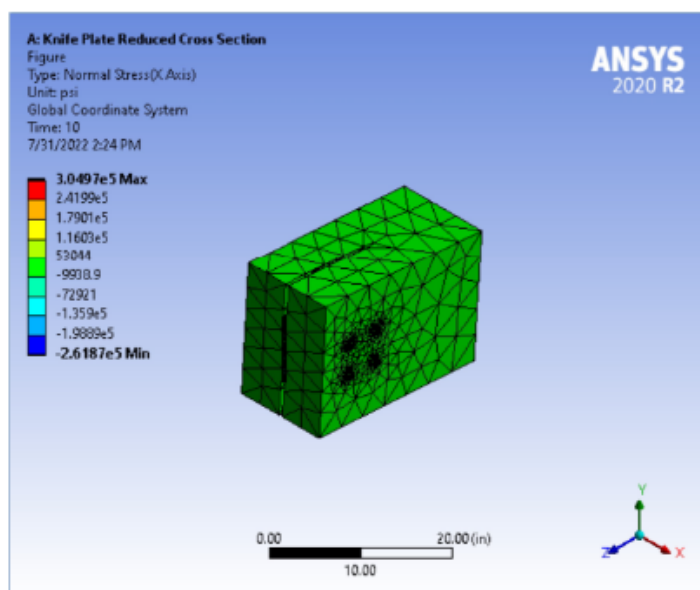


**FIGURE 22**  
 Model (A4) > Static Structural (A5) > Solution (A6) > Normal Elastic Strain

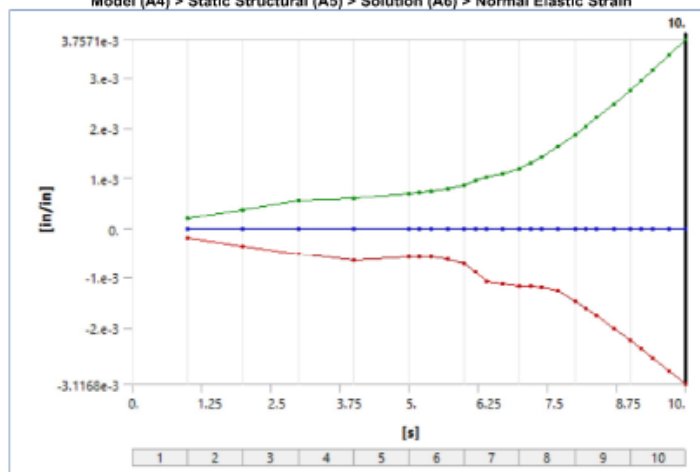


**TABLE 24**  
 Model (A4) > Static Structural (A5) > Solution (A6) > Normal Elastic Strain

Time [s]	Minimum [in/in]	Maximum [in/in]	Average [in/in]
1.	-2.0144e-004	1.9834e-004	7.8089e-008
2.	-3.5919e-004	3.6812e-004	1.7661e-007
3.	-5.1431e-004	5.4648e-004	2.3526e-007
4.	-6.5451e-004	5.9183e-004	2.2027e-007
5.	-5.8478e-004	6.8696e-004	1.5361e-007
5.2	-5.9115e-004	7.1419e-004	1.2928e-007
5.4	-5.9592e-004	7.4026e-004	9.1487e-008
5.7	-6.3054e-004	7.7873e-004	1.7832e-009
6.	-7.3137e-004	8.6819e-004	-1.2021e-007
6.2	-8.9243e-004	9.4875e-004	-1.9947e-007
6.4	-1.0768e-003	1.0153e-003	-2.6664e-007
6.7	-1.1399e-003	1.0847e-003	-3.1308e-007
7.	-1.1648e-003	1.1884e-003	-3.4807e-007
7.2	-1.182e-003	1.3015e-003	-3.5957e-007
7.4	-1.1952e-003	1.4275e-003	-3.6924e-007
7.7	-1.2639e-003	1.6399e-003	-3.8706e-007
8.	-1.4718e-003	1.8737e-003	-4.0836e-007
8.2	-1.6185e-003	2.037e-003	-4.2558e-007
8.4	-1.7717e-003	2.2074e-003	-4.5114e-007
8.7	-2.01e-003	2.4755e-003	-4.9513e-007
9.	-2.2549e-003	2.7543e-003	-5.5307e-007
9.2	-2.4212e-003	2.9455e-003	-5.8989e-007
9.4	-2.5909e-003	3.142e-003	-6.2044e-007
9.7	-2.8508e-003	3.4453e-003	-6.5971e-007

10.	-3.1168e-003	3.7571e-003	-6.8077e-007
-----	--------------	-------------	--------------

FIGURE 23

Model (A4) &gt; Static Structural (A5) &gt; Solution (A6) &gt; Normal Elastic Strain &gt; Figure

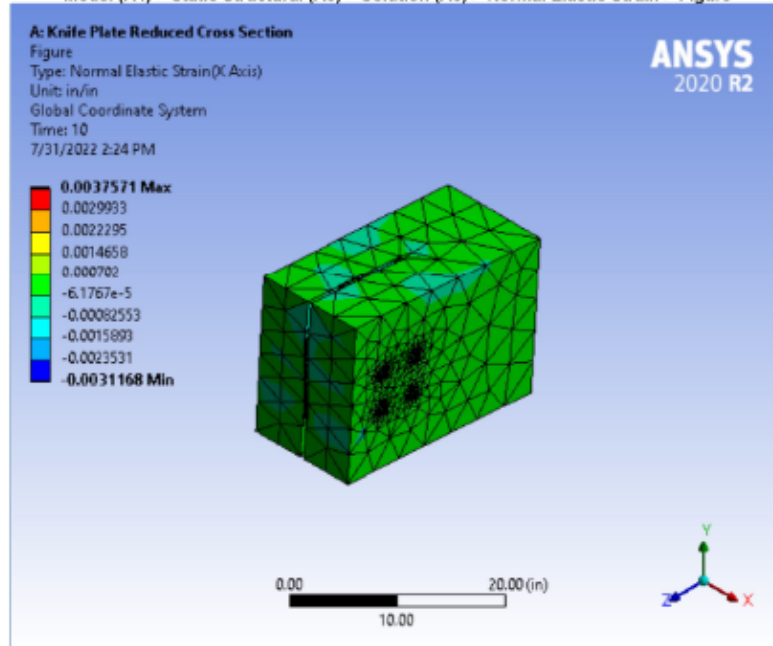


TABLE 25

Model (A4) &gt; Static Structural (A5) &gt; Solution (A6) &gt; Probes

Object Name	Force Reaction
State	Solved
<b>Definition</b>	
Type	Force Reaction
Location Method	Boundary Condition
Boundary Condition	Fixed Support I-Shape
Orientation	Global Coordinate System
Suppressed	No
<b>Options</b>	
Result Selection	All
Display Time	End Time
<b>Results</b>	
X Axis	219.39 lbf
Y Axis	29998 lbf
Z Axis	0.85587 lbf
Total	29998 lbf
<b>Maximum Value Over Time</b>	
X Axis	219.39 lbf
Y Axis	29998 lbf
Z Axis	6.5635 lbf
Total	29998 lbf
<b>Minimum Value Over Time</b>	
X Axis	0.6793 lbf
Y Axis	3000. lbf
Z Axis	-1.8282 lbf
Total	3000. lbf
<b>Information</b>	
Time	10. s
Load Step	10
Substep	4
Iteration Number	57

FIGURE 24

Model (A4) &gt; Static Structural (A5) &gt; Solution (A6) &gt; Force Reaction

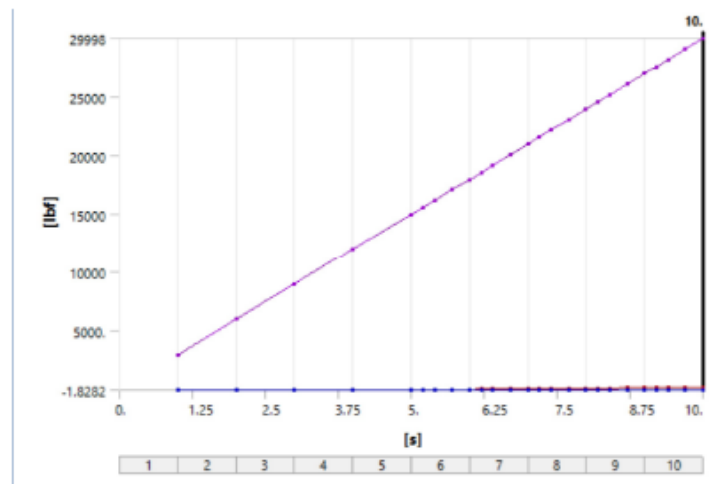
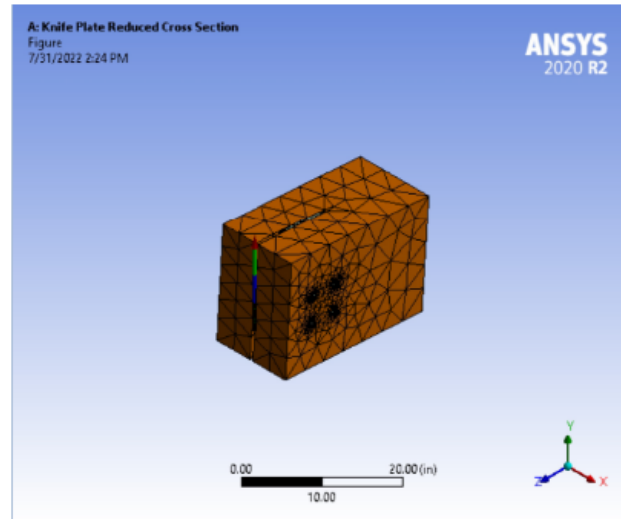


**TABLE 26**  
**Model (A4) > Static Structural (A5) > Solution (A6) > Force Reaction**

Time [s]	Force Reaction (X) [lb]	Force Reaction (Y) [lb]	Force Reaction (Z) [lb]	Force Reaction (Total) [lb]
1.	0.6793	3000.	-1.8078e-002	3000.
2.	2.9551	5999.8	-6.4394e-002	5999.8
3.	6.6687	8999.2	5.8369	8999.2
4.	11.601	12000	-1.8282	12000
5.	21.198	14999	6.5635	14999
5.2	29.791	15597	2.0434	15597
5.4	34.058	16200	0.85348	16200
5.7	37.095	17098	-0.83255	17098
6.	47.887	17998	0.5941	17998
6.2	53.807	18588	0.41346	18588
6.4	63.985	19200	-0.49373	19200
6.7	78.153	20100	-1.2808	20100
7.	91.215	21000	-9.0482e-002	21000
7.2	99.404	21596	1.0136	21596
7.4	107.41	22200	-0.3198	22200
7.7	118.24	23100	-0.53124	23100
8.	128.47	24000	-0.50542	24000
8.2	135.74	24597	1.5791	24597
8.4	144.52	25199	1.3178	25199
8.7	157.97	26100	-0.26	26100
9.	170.77	27000	-0.20612	27001
9.2	180.3	27598	1.3869	27598
9.4	190.39	28199	0.59004	28200
9.7	205.02	29097	1.506	29098
10.	219.39	29998	0.85587	29998

**FIGURE 25**  
**Model (A4) > Static Structural (A5) > Solution (A6) > Force Reaction > Figure**



## Material Data

### CLT

**TABLE 27**  
**CLT > Constants**

Density	1.9123e-002 lbm in <sup>-3</sup>
Tensile Yield Strength	2445 psi
Tensile Ultimate Strength	2445 psi
Coefficient of Thermal Expansion	5.75e-002 F <sup>-1</sup>
Thermal Conductivity	2.3927e-006 BTU s <sup>-1</sup> in <sup>-1</sup> F <sup>-1</sup>
Specific Heat	0.40245 BTU lbm <sup>-1</sup> F <sup>-1</sup>
Resistivity	5.4901e+013 ohm cmil in <sup>-1</sup>

**TABLE 28**  
**CLT > Opacity**

Red	Green	Blue
224	112	0
Opacity		
1		
Metallic Finish		
0		

**TABLE 29**  
**CLT > Orthotropic Elasticity**

Young's Modulus X direction psi	Young's Modulus Y direction psi	Young's Modulus Z direction psi	Poisson's Ratio XY	Poisson's Ratio YZ	Poisson's Ratio XZ	Shear Modulus XY psi	Shear Modulus YZ psi	Shear Modulus XZ psi	Temperature F
1.6969e+006	1.3053e+006	1.4504e+005	0.35	7.e-002	0.35	81656	1.0602e+005	14504	

**TABLE 30**  
**CLT > Isotropic Secant Coefficient of Thermal Expansion**

Zero-Thermal-Strain Reference Temperature F
73.4

### Structural Steel NL - I-Shape

**TABLE 31**  
**Structural Steel NL - I-Shape > Constants**

Density	0.2836 lbm in <sup>-3</sup>
Specific Heat	0.10366 BTU lbm <sup>-1</sup> F <sup>-1</sup>

**TABLE 32**  
**Structural Steel NL - I-Shape > Isotropic Elasticity**

Young's Modulus psi	Poisson's Ratio	Bulk Modulus psi	Shear Modulus psi	Temperature F
2.9008e+007	0.3	2.4173e+007	1.1157e+007	

**TABLE 33**  
**Structural Steel NL - I-Shape > Bilinear Isotropic Hardening**

Yield Strength psi	Tangent Modulus psi	Temperature F
36259	2.103e+005	

**TABLE 34**  
**Structural Steel NL - I-Shape > Color**



Red	Green	Blue
184	235	197

**Structural Steel NL - Bolts**

**TABLE 35**  
**Structural Steel NL - Bolts > Constants**

Density	0.2836 lbm in <sup>-3</sup>
Specific Heat	0.10366 BTU lbm <sup>-1</sup> F <sup>-1</sup>

**TABLE 36**  
**Structural Steel NL - Bolts > Isotropic Elasticity**

Young's Modulus psi	Poisson's Ratio	Bulk Modulus psi	Shear Modulus psi	Temperature F
2.9008e+007	0.3	2.4173e+007	1.1157e+007	

**TABLE 37**  
**Structural Steel NL - Bolts > Bilinear Isotropic Hardening**

Yield Strength psi	Tangent Modulus psi	Temperature F
36259	2.103e+005	

**TABLE 38**  
**Structural Steel NL - Bolts > Color**

Red	Green	Blue
184	235	197

**Structural Engineering****Capstone Report Approval Form****Master of Science in Architectural Engineering****Milwaukee School of Engineering**


This capstone report, entitled "Analysis and Design of Shear Wall Coupling Beams in Mid- to High-rise Timber Buildings," submitted by the student Katherine J Augustine, has been approved by the following committee:

Faculty Advisor:  Date: 8/3/2022

Dr. Pouria Bahmani, Ph.D., PE

Faculty Member:  Date: 8/3/2022

Dr. Christopher Raebel, Ph.D., PE, SE

Faculty Member:  Date: 8/4/2022

Dr. Todd Davis, Ph.D., PE